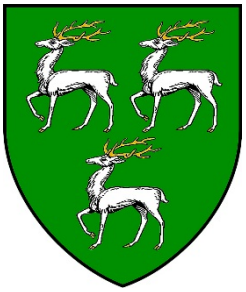
THE ROLE OF MACROPHAGES IN THE HOST RESPONSE TO RADIATION

Dr Keaton Jones

Jesus College



A thesis submitted to the Medical Sciences Division of the University of Oxford in partial fulfilment of the requirements for the degree of Doctor of Philosophy



Cancer Research UK Oxford Institute for Radiation Oncology

Department of Oncology

University of Oxford

Michaelmas 2018

Word count: 33,295

Abstract

Emerging pre-clinical data suggests a role for radiation in eliciting antitumor immunity. Effective anti-tumour responses can be hindered by highly immunosuppressive tumour microenvironments. We aimed to investigate the role of macrophages in the immune response to radiation.

We used the murine colorectal cancer cell line MC38 and the pancreatic cell line KPC for in vitro and in vivo work. To examine the immune response following irradiation, subcutaneous xenografts were analysed by flow cytometry. Further characterisation of macrophages was carried out by gene expression analyses of RNA from isolated cells, along with ex-vivo functional assays. To determine the effect of macrophage depletion, we used an antibody targeting macrophage colony stimulating factor (CSF-1).

Single dose 10Gy irradiation to murine tumors, generated from colorectal (MC38) and pancreatic (KPC) cell lines induced Colony Stimulating Factor 1 (CSF-1). Coincident with the elevation in CSF1, CD11b+ F480+ macrophages increased in the tumors, peaking five days following irradiation. These tumor-associated macrophages (TAMs) from irradiated tumors were skewed toward an immunosuppressive phenotpye ($CD206^{hi}$ $iNOS^{lo}$) and were more effective in suppressing CD8 T cell expansion ex vivo.

Macrophage depletion via anti-CSF (aCSF) reduced macrophage numbers yet only achieved tumor growth delay when combined with radiation. The tumor growth delay from aCSF after radiation was abrogated by depletion of CD8 T cells. There was enhanced recognition of tumor cell antigens by T cells isolated from irradiated tumors, consistent with increased antigen priming. Radiation stimulated increased expression of PD-L1 on tumor cells, limiting antitumor responses. The addition of anti-PD-L1 resulted in improved tumor suppression and even regression in the highly resistant murine pancreatic cancer model.

In summary we show that adaptive immunity induced by radiation is limited by the recruitment of highly M2 polarised immunosuppressive macrophages. Macrophage depletion with aCSF partly reduced the immunosuppression after radiation, but additional treatment with anti-PD-L1 was required to achieve tumor regression.

Acknowledgements

Firstly, I wish to thank my supervisor Professor Ruth Muschel. Professor Muschel has provided guidance during my time as an academic clinical fellow as well as throughout my DPhil. Drawing on a wealth of experience and knowledge, Ruth has helped me to navigate my way through a stimulating and challenging project. Her enthusiasm for the subject matter is inspiring, and much of what I have learnt will stay with me in my future scientific and clinical career.

I wish to also acknowledge two members of the lab team who have helped me enormously during my research. Firstly, Alex Gordon-Weeks for supervising my initial forays into lab work nearly five years ago. I have learnt a great deal from working with Alex, in particular he taught me the fundamental principles of developing research questions and designing the right experiment to answer them. Arseniy Yuzhalin is a scholar in the truest sense of the word. Close friends both in and outside the lab, he has provided a tremendous amount of practical help, and is always the first I approach to discuss a new hypothesis.

There are many other members of the lab as well as the wider scientific community who are too numerous in number to list here, but have also provided support and guidance throughout.

I would also like to thank Jiske Tiersma, whom I supervised during her time completing a research Master's project in Oxford.

The work could not have taken place without funding from Cancer Research UK and the Medical Research Council.

Finally, my wife Lauren has never once faltered in her constant support during my time in the lab. Lauren now has a very good understanding of what it is to have an experiment 'succeed', and has tolerated many evenings and weekends alone whilst I have been busy in the animal unit.

Specific acknowledgements

Figure 3.3.1 – Jiske Tiersma conducted some of the experiments presented under supervision by myself.

Figure 3.3.1 – Flow cytometry experiments were performed with help from Dr Alex Gordon-Weeks

Figure 3.3.3 – Flow assisted cell sorting was performed with help from Dr Andrew Worth

Figure 4.3.4 – Animal experiments were performed with help from Dr Arseniy Yuzhalin

Figure 4.3.5 - Jiske Tiersma conducted the experiments presented under supervision by myself.

Figure 4.3.6 – Experiments performed with help from Bostjan Markelc and Jakob Kaeppler

Abbreviations

αSMA	alpha smooth muscle actin
ANOVA	Analysis Of Variance
ATP	Adenosine TriPhosphate
ATCC	American Type Tissue Culture
BED	Biologically Effective Dose
BMDMs	Bone marrow-derived macrophages
BMI	Body Mass Index
CCL	Chemokine (C-C motif) ligand
CCR	Chemokine (C-C motif) receptor
CD	Cluster differentiation
cGAS	cyclic guanosine monophosphate adenosine synthase
CFSE	Carboxyfluorescein succinimidyl ester
CRC	Colorectal cancer
CSF-1	Colony Stimulating Factor 1
CT	Computed Tomography
CXCL	Chemokine (C-X-C motif) ligand
CXCR	Chemokline (C-X-C motif) receptor
DAMPs	Damage Associated Molecular Patterns
DAPI	4',6-diamidino-2-phenylindole
DSB	Double Stranded Break
ECM	Extracellular matric
EDTA	Ethylenediaminetetraacetic acid
ELISA	Enzyme Linked immunosorbent assay
ELISPOT	Enzyme Linked Immunospot Assay
EMT	Epithelial-mesenchymal transition
FSC	Forward scatter
gMDSCs	granulocytic myeloid derived suppressor cells
Gy	Gray
HDI	Human Development Index
HMGPB1	High Mobility Group Protein Box 1
HRR	Homologous recombination repair
HSPs	Heath Shock Proteins
IFN	Interferon
IL	Interleukin
LPS	Lipopolysaccharide
MDSCs	Myeloid Derived Suppressor Cells
mMDSCs	monocytic myeloid-derived suppressor cells
MHC	Major Histocompatability Complex
MMP	Matrix metalloproteinase

mRNA	Messenger RNA
MSI	Microsatellite instability
NFkB	nuclear factor kappa B
NHEJ	Nonhomologous end joining
PBS	Phosphate Buffered Saline
PDAC	Pancreatic Ductal Adenocarcinoma
PET	Positron Emission Tomography
PGDF	platelet-derived growth factor
PRR	Pattern Recognition Receptor
PSCs	Pancreatic Stellate Cells
qPCR	quantitative Polymerase chain Reaction
PyMT	Polyoma virus middle T antigen
RIPA	Radioimmunoprecipitation assay
ROS	Reactive Oxygen Species
RPM	Revolutions Per Minute
RPMI	Roswell Park Memorial Institute medium
SEM	Standard Error of the Mean
SMAD-4	Mothers against decapentaplegic homohlog 4
RPMI	Roswell Park Memorial Institute medium
STAT	Signal transducers and activators of transduction
STING	Stimulator of Interferon Genes
SSB	Single Stranded Break
SSC	Side scatter
TAM	Tumour-associated macrophage
TGF-β	Transforming Growth Factor
TNFα	Tumour Necrosis Factor-alpha
TBK1	TANK binding kinase 1
TLRs	Toll-like receptors
VEGF	Vascular Endothelial Growth Factor

CONTENTS

Page N°

ABSTRACT II

ACKNOWLEDGEMENTS III

SPECIFIC ACKNOWLEDGEMENTS IV

ABBREVIATIONS V

CONTENTS VIII

LIST OF FIGURES XII

LIST OF TABLES XVI

1. CHAPTER 1 INTRODUCTION 1

1.1 Background to the work presented in this thesis. *1*

1.2 A brief history of radiation and immunity *2*

1.2.1 Innate immunity 3

1.2.2 Adaptive immunity 6

1.3 Tumour Associated Macrophages (TAMs) *9*

1.3.1 Macrophage phylogeny and role in normal tissue development and homeostasis 10

1.3.2 Macrophages in primary tumourigenesis 12

1.3.3 Macrophage phenotypes 13

1.3.4 Tumour-associated macrophages 15

1.4 Rationale for the experimental models used. *20*

2. CHAPTER 2 METHODS 23

2.1 Tumour cell lines *23*

2.1.1 Colony forming assays 23

2.2 Animal work and associated experiments *24*

2.2.1 Animals and husbandry 24

2.2.2 Tumour challenge and treatment experiments 24

2.2.3 In vivo antibody treatments 24

2.2.4 Murine serum collection 25

2.3 Tumour sectioning *25*

2.4 Haematoxylin and Eosin staining *25*

2.5 Immunofluorescent staining *26*

2.6 ELISA and cytokine arrays *26*
2.7 Flow Cytometry *26*
2.8 Fluorescence Activated Cell Sorting *28*
2.8.1 RNA extraction from sorted cell populations. 28
2.9 Magnetic bead separation of macrophages *31*
2.10 Real-Time quantitative PCR *31*
2.11 Bone Marrow Derived Macrophage (BMDM) culture *33*
2.11.1 BMDM co-culture experiments 33
2.11.2 BMDM conditioned media experiments 33
2.11.3 T cell suppression assay 34
2.12 IFN-γ Elispot assay *34*
2.13 Protein extraction *34*
2.14 Immunoblotting *35*
2.15 Statistical analysis *35*
3. CHAPTER 3: Radiation induces Colony-Stimulating Factor-1 (CSF-1) upregulation and increases macrophage numbers in murine tumours. 37
3.1 Introduction *37*
3.2 Aims *39*
3.3 Results *40*
3.3.1 Radiation induces CSF-1 upregulation and increases macrophage recruitment to tumours 40
3.3.2 Radiation increases macrophage numbers in murine subcutaneous xenografts. 43
3.3.3 Tumour associated macrophages are polarised towards an immunosuppressive 'M2' phenotype 46
3.3.4 Gene expression in isolated TAMs demonstrates a variable response to radiation, skewed towards an immunosuppressive phenotype. 50
3.3.5 TAMs from irradiated tumours suppress CD8 T cell proliferation. 52
3.3.6 Tumour cell conditioning can polarise macrophages towards an immunosuppressive phenotype. 54
3.3.7 Tumour conditioned macrophages suppress T cell proliferation 59
3.3.8 Adoptive transfer of tumour-conditioned macrophages promotes tumour growth 61
3.3.9 Changes in other immune cell populations 63
3.4 Discussion *66*
3.4.1 Upregulation of CSF-1 following irradiation 66

3.4.2 Increased alternatively activated macrophages in the tumour microenvironment following irradiation 67

4. CHAPTER 4: Macrophage depletion delays tumour growth following radiation. 72

4.1 Introduction 72

4.1.1 Macrophage depletion strategies 72

4.1.2 CSF-1(R) blockade 73

4.2 Aims 74

4.3 Results 75

4.3.1 aCSF treatment reduces TAMs 75

4.3.2 aCSF treatment selectively depletes M2 macrophages 77

4.3.3 aCSF treatment is associated with macrophage repolarisation 79

4.3.4 aCSF treatment combined with radiation delays tumour growth 81

4.3.5 sCSF does not affect tumour cell radiosensitivity 83

4.3.6 Macrophage depletion is associated with increased CD8+ T cells and penetrance into tumours 85

4.3.7 aCSF is associated with variable changes in other immune populations 89

4.3.8 Tumour growth delay is CD8 T cell dependent 92

4.3.9 Radiation stimulates specific adaptive immune priming 95

4.3.10 Radiation stimulates the expression of major Histocompatibility Complex I (MHC I) on tumour cells 99

4.3.11 Radiation induced antigen priming is sufficient to control distant tumours in aCSF treated mice 101

4.4 Discussion 103

4.4.1 aCSF is associated with a reduced TAM numbers and changes in their phenotype 103

4.4.2 Tumour growth delay is CD8 dependent 105

4.4.3 Combination therapy is required to achieve out-of-field responses 106

5. CHAPTER 5: Immune checkpoint blockade is required for tumour rejection 110

5.1 Introduction 110

5.2 Aims 111

5.3 Results 112

5.3.1 Radiation induces upregulation of PD-L1 on tumour cells 112

5.3.2 Immune checkpoint blockade combined with radiation shows a variable

response in vivo 114
5.3.3 Triple combination therapy with radiation, aCSF and aPD-L1 lead to tumour regression in a subset of KPC tumours 116
5.4 Discussion *119*
6. CHAPTER 6: Concluding remarks **121**
6.1 Synopsis *121*
6.2 Limitations *121*
6.3 Future directions *123*
7. References **125**

LIST OF FIGURES

Figure 2.1 – Initial flow cytometric gating strategy..... 28
Figure 3.2 – Macrophages are increased in tumours following irradiation. 45
Figure 3.3 – Flow cytometric gating strategy to measure iNOS and CD206 expression on tumour associated macrophages. 47
Figure 3.4 Macrophages in MC38 and KPC subcutaneous tumours are polarised towards an immunosuppressive phenotype. 49
Figure 3.5 - Gene expression in isolated TAMs demonstrate a variable response to radiation, skewed towards an immunosuppressive phenotype. 51
Figure 3.6 -TAMs from irradiated tumours are capable of supressing CD8 T cell proliferation. 53
Figure 3.7 – Tumour cells polarise bone marrow-derived macrophages (BMDMs). 56
Figure 3.8 – Co-culture with tumour cells significantly alters gene expression in bone marrow-derived macrophages (BMDMs)..... 57
Figure 3.9 – BMDMs co-cultured with tumour cells supress CD8 T cell proliferation..... 60
Figure 3.10 – Adoptive transfer of tumour-conditioned macrophages promotes tumour growth. 62
Figure 3.11 – Irradiation significantly alters the immune landscape in MC38 tumours 64
Figure 3.12 – Irradiation significantly alters the immune landscape in KPC tumours..... 65
Figure 4.1 – aCSF effectively reduces TAM number in MC38 and KPC tumours with a and without irradiation. 76
Figure 4.2 – M1 and M2 TAM populations are differentially affected by aCSF 78
Figure 4.3 – aCSF treatment is associated with TAM repolarisation..... 80
Figure 4.4 – Irradiation combined with aCSF treatment increases tumour growth delay. 82
Figure 4.5 – aCSF does not affect tumour cell radiosensitivity 84
Figure 4.6 – aCSF treatment is associated with increased numbers of CD8+ T cells 87
Figure 4.7 – CD8 T cells are homogenously distributed in MC38 tumours, but penetrate the tumour core in KPC tumour treated with irradiation and aCSF. 88

Figure 4.8 - aCSF is associated with changes in other immune populations in MC38 tumours 90
Figure 4.9 - aCSF is associated with changes in other immune populations in KPC tumours 91
Figure 4.10 – Tumour growth delay following aCSF treatment is CD8 T cell dependent..... 93
Figure 4.11 – Irradiation stimulates specific anti-tumour immunity..... 97
Figure 4.12 - Radiation stimulates the expression of MHC I on tumour cells..... 100
Figure 4.13 – Radiation induced antigen priming is not associated with control of distant tumours unless aCSF is concomitantly administered..... 102
Figure 5.1- Radiation stimulates PD-L1 expression on tumour cells..... 113
Figure 5.2 Radiation combined with immune checkpoint blockade shows a variable response in vivo..... 115
Figure 5.3 Triple combination therapy with radiation, aCSF and aPD-L1 lead to tumour regression in a subset of KPC tumours..... 118

LIST OF TABLES

Table 1 – List of fluorescently conjugated antibodies used in flow cytometry experiments.....27
Table 2 – List of primers used in real-time quantitative PCR experiments. 32

1. CHAPTER 1 INTRODUCTION

1.1 Background to the work presented in this thesis.

Here, I present a thesis investigating the immune response to irradiation in murine models of colon and pancreatic cancer. I focus particularly on tumour-associated macrophages (TAMs), and their role in the irradiated tumour microenvironment. Our interest turned to TAMs as a result of recent experimental evidence generated in our laboratory. We found that the formation of murine hepatic metastasis was dependent upon the presence of neutrophils[1]. Analysis of mRNA expression revealed upregulation of fibroblast growth factor 2 (FGF-2, bFGF) in neutrophils colonising the liver. Further experiments identified neutrophils as being the main source of FGF-2, and treatment with an antibody targeting FGF-2 reduced the metastatic burden. Subsequent immunohistochemical analysis of tumours revealed a pattern of vascular normalisation in mice treated with anti-FGF2. Together, these data suggested that neutrophils promote the growth of metastasis via FGF-2 mediated angiogenesis and vascular normalisation. In addition to metastasis, our lab also has an interest in studying the effects of irradiation on tumour vasculature. We therefore questioned whether neutrophils play a role in the irradiated tumour microenvironment, possibly as a source of vascular growth factors. We first sought to determine whether tumoural FGF-2 levels are altered after irradiation. Significantly increased levels of FGF-2 were found in the tumours after irradiation (unpublished data from our lab). However, whereas we previously found that FGF-2 was co-localised with neutrophils, this was not evident in the irradiated tumours. After staining for other myeloid cells, we found that the FGF-2 was co-localised with F480+ TAMs. In addition, there were significantly more TAMs in the irradiated tumours. Following on from these initial observations, I sought to investigate the effect of irradiation on the number and phenotype of TAMs, the kinetics of their recruitment, and their effect on tumour growth. In the following introductory chapters, I discuss how our understanding of the relationship between the immune system and irradiation has evolved over recent years. I will also present a brief summary of the role of macrophages under normal physiological conditions, followed by what is known about their role in tumours. Finally, I will discuss the rationale behind the experimental models used to generate the experimental data presented in this thesis.

1.2 A brief history of radiation and immunity

The clinical application of radiotherapy has traditionally been based upon the principle that it exerts its effects primarily via DNA damage. Whilst this is still the case today, the capacity for radiation to illicit an immune response was observed not long after its discovery and introduction just over a century ago. In 1917, James Ewing reported the presence of a polymorphonuclear exudate at the site of radium treatment in a patient with cervical cancer[2]. It wasn't until much later in the century that substantial progress was made towards understanding the effects of irradiation on immunity. In the 1950s and 1960s, a series of experiments demonstrated that vaccination with ex-vivo irradiated tumour samples improved the efficacy of radiation in murine xenografts[3–5]. Then in 1970, Suit et al demonstrated that the curative success of radiation was dependent upon the immune status of the mice [6]. Nine years later, Slone et al showed that the radiation dose required to control 50% of tumours (TCD50) in immunocompromised mice (thymectomy and whole body irradiation) was double that required in immune competent hosts [7]. Common amongst these experiments was the use of mice with chemically or virally induced tumours that tended to be highly immunogenic, that may have exaggerated the immune dependent effects. Hewitt et al reinforced this theory when they reported the results of experiments with spontaneous tumour isotransplantation in 20,000 mice. Apart from a small subset, no tumours were rejected, and in fact it was reported that pre-inoculation with lethally irradiated cells actually increased graft rate [8]. These striking and seemingly unequivocal results marked the beginning of a period of research senescence in the field of radiation immunity.

Interest in the immunological effects of radiation was rekindled following reports of 'abscopal' effects. Abcopus is a term derived from the Latin words *ab* meaning away and *scopus* meaning target. A term first coined by Mole in 1953, it refers to tumour shrinkage outside the field of radiation [9]. One of the possible explanations was a systemic immune response. There were sporadic reports of clinical cases where shrinkage or disappearance of metastases was noted following radiation of the primary tumour [10]. However subsequent clinical trials reported highly variable results with no clear evidence of abscopal effects [11]. Since then a number of preclinical reports have demonstrated variable immune dependency amongst tumours, probably as a result of each individual tumour or cell line to generate immunity [11]. This would explain the highly variable results reported across the pre-clinical and clinical field. A Lancet paper in 2010 which reported

improved survival in metastatic melanoma patients treated with ipilimumab heralded a new era of intense interest in tumour immunology [12]. This time, further clinical case reports of abscopal effects were supported by experimental evidence demonstrating synergy between radiation and immune checkpoint blockade [13–16]. Testament to this resurgence is the fact that 2016 alone saw 34 ongoing clinical trials combining radiotherapy with immune therapy across multiple tumours types [17].

1.2.1 Innate immunity

One of the prime functions of the innate immune system is to launch an initial response to the presence of foreign antigens, as well as tissue injury. Innate immunity is non-specific and provides the first line of defence. Adaptive immunity takes days or weeks to develop, and hence the innate immune system is critical for preventing infections from overcoming the host. Innate immunity is also important in the response to sterile tissue damage where immune cells contribute to repair and remodelling. A key step in the recognition of pathogens is the sensing of Pathogen-Associated Molecular Patterns (PAMPs) by cells of the innate immune system. First described by Janeway in 1989, PAMPs are evolutionary conserved across whole groups of pathogens and allow the detection of non-self[18]. One of the most widely recognised PAMPs is lipopolysaccharide (LPS) [19]. Others include other lipids such as lipoproteins, lipoteichoic acids, lipoglycans, glycoproteins, peptidoglycans and nucleic acids [20]. In addition to pathogenic stimuli, cells can also release Damage-Associated Molecular Pattern molecules (DAMPs) in response to sterile trauma [21]. This can include insults such as physical trauma, burns, myocardial infarction, neurological injury, and foreign bodies [22]. Importantly, both PAMPs and DAMPs are recognised by a conserved set of pattern recognition receptors (PRRs). These germline encoded receptors include transmembrane proteins such as C-type lectin receptors, Toll-like receptors (TLRs), and cytoplasmic proteins such as the NOD-like receptor (NLR) [23]. Originally, PRR ligands were linked to pathogenic organisms such as bacteria and viruses. However it is now understood that almost all PRRs recognise DAMPs [24]. Upon sensing DAMPs there is upregulated transcription of genes involved in inflammation. These include inflammatory cytokines (TNFα, il1, il6), type 1 interferons and chemokines. This response can then be propagated to other nearby immune cells.

The release of DAMPs from tumour cells may happen after spontaneous cell death, but is more well documented after cell death resulting from anti-tumour therapies, including radiation [25,26]. These molecules, including high mobility group protein box 1 (HMGPB1), adenosine

triphosphate (ATP), heat shock proteins (HSPs), can be recognised by pattern recognition receptors (PRRs) present on innate immune cells [27]. As 'first responders', these cells accumulate at the site of tissue injury and include phagocytic cells such as macrophages, neutrophils and dendritic cells (DCs), basophils, eosinophils and natural killer cells.

In addition, phagocytosis of DAMPs by DCs can prime naïve cytotoxic T cells via Major Histocompatibility Complex II (MHCII) presentation [28]. This process is one of the first in a series of events which contribute to the generation of a specific adaptive immune response. The presence of DNA within the cytoplasm can also act as a potent DAMP. DNA or nucleic acid fragments within the cytoplasm are indicative of cellular damage or infection (commonly viral). As part of the normal host response, the cGAS (cyclic guanosine monophosphate adenosine synthase)-STING (STimulator of INterferon Genes) pathway is activated. cGAS binds to DNA and becomes catalytically active, generating cyclic guanine monophosphate (cGAMP). cGAMP then binds to STING which in turn activates type I interferon (interferon α/β) production via TANK binding kinase 1 (TBK1) [29]. It is thought that tumour cell stress may increase the pool of cytosolic DNA, including in response to conventional treatments such as chemoradiation. This process may occur within tumour cells or following phagocytosis of tumour cell fragments by APCs. The subsequent effects of type 1 interferons on mediating the anti-tumour response are less well understood. There is evidence that dendritic cell activation may improve CD8 T cell priming and anti-tumour cytotoxic activity [30,31].

Radiation may also stimulate the recruitment of myeloid cells as a result of increased production of cytokines and chemokines. Unlike DAMPs, cytokines produced by tumour cells can act to both recruit and condition myeloid cells. Alterations in the secretome of tumours cells following radiation tends to be over a relatively short period (<48 hours) and highly variable across cell lines [32–34]. Increased production may result from the direct effects of IR on tumour cells or bystander effects, however mechanistic evidence is lagging behind. It is likely that response mechanisms vary across tumours, however there is convincing evidence that the NF-kappaB (NFKB) and signal transducer and activation of transcription 1 and 3 (STAT1/3) are activated [35,36]. Some of the cytokines upregulated following irradiation in vitro and in vivo include TNFα, il1α, il1β, il6, interferon α/β, GM-CSF, il4, M-CSF, il5, il10, il12, il18 and TGFβ [37–43]. The response of individual tumours and cell lines is variable and time-dependent. In addition, patterns may change

when comparing the same cell line following in vivo exposure compared with in vitro exposure to stimuli [44]. In addition to tumour cell production, stromal cells can also secrete cytokines in response to radiation [45,46]. This can be in an autocrine fashion but also affect tumour cells and other cells in the stroma. The net effect of the cytokine repertoire will either serve to promote a stimulatory or suppressive microenvironment. Ultimately, the antitumour effects elicited by radiation have to overcome immune suppression in order to eradicate the tumour.

Cells involved in the innate response include macrophages, dendritic cells, myeloid derived suppressor cells, neutrophils and Natural Killer (NK) cells. Mirroring the diversity in cytokine responses, the extent to which these cells infiltrate tumours is highly variable. The literature is largely restricted to pre-clinical models examining the response of macrophages and MDSCs. There is a paucity of data from clinical samples and this probably reflects the difficulty in obtaining tumour tissue within a short time-frame following the application of radiotherapy. The trend amongst these reports is of significant, transient elevations in myeloid cells and variable effects on polarisation or phenotype [47]. One of the explanations behind the heterogeneity amongst these observations is the variety of radiation doses and regimens, as well as the analytical time points. In a review by Vatner and Formenti, the majority of animal studies examining the response to radiation focused on CD11b+F480+ macrophages (13/18), some looked at MDSCs (6/18) and very few looked at neutrophils (2/18). Macrophages will be discussed in more detail in chapter 1.5.

MDSCs (Gr1+) have been found to increase in tumours following irradiation. Deng et al used anti-CCR2 to deplete MDSCs recruited after 20Gy irradiation to MC38 and LLC xenografts. This resulted in a decrease in immunosuppression and delayed tumour growth [48]. Xu et al reported a substantial increase (9.8 vs 3.4) in MDSCs in the blood, spleen, lung, lymph nodes and tumours [49]. It has also been noted that MDSCs tend to accumulate within or around areas of necrosis and hypoxia, contributing to post radiation vasculogenesis, [50], a phenomenon also noted in additional reports [51]. In one study combining irradiation with anti-PD-L1, MDSCs were found to be decreased following radiation, though the tumours were harvested at day 10 [52]. Notably, one of the widely reported functions of MDSCs is immunosuppression, as their name denotes. Despite this, there is a paucity of reports that look specifically at the role of MDSCs in supressing adaptive immunity following radiation.

Neutrophils are also shown to be increased within tumours following radiation, though there are fewer reports [53,54]. A recent paper by Takeshima showed improved tumour responses following radiation by augmenting N1 neutrophils via GM-CSF [55]. The authors provide data suggesting that the effect is dependent upon increase reactive oxygen species (ROS) production by neutrophils. Analogous to the macrophages polarisation, tumour associated neutrophils (TANs) have been classified as antitumour 'N1' and pro-tumour 'N2' cells [56]. Interestingly, the marker used to determine neutrophils by flow cytometry was Gr-1, which is also used in the identification of granulocytic MDSCs (gMDSCs).

The application of local radiation not only exposes tumour cells to its ionising effects, but also components of the stroma, including immune cells. This is especially true when considering dose fractionation. If immune cells are recruited to the tumour following initial doses of radiation, they themselves may be exposed to subsequent fractions. As discussed previously, there is already an understanding of the radiosensitivity of various immune populations, particularly in the context of whole body irradiation for bone marrow transplantation. However the effects of fractionated radiation on immune cells residing within the tumour microenvironment is less well understood. Strikingly, it appears that terminally differentiated macrophages are far more radioresistant than originally thought [57].

1.2.2 Adaptive immunity

Unlike the innate immune system, adaptive immunity is highly specific. Responses are broadly categorised into antibody or cell mediated. In antibody mediated immunity, B lymphocytes endocytose foreign antigens within secondary lymphoid organs, and subsequently produce specific antibodies in an acquired response [58]. Cell mediated immunity involves T lymphocytes, of which there are several subtypes, including T helper 1 (Th1), T helper 2 (Th2), regulatory T cells (Tregs) and cytotoxic T cells. The main effector cells are CD8 cytotoxic T cells, which can selectively destroy target cells. This is brought about by antigen specific priming. Foreign antigens are endocytosed by phagocytic cells (dendritic cells), packaged by the proteasome and presented on the surface via major histocompatibility complex I (MHC I). Subsequent engagement with T cell receptors, along with co-stimulatory molecules, results in T cell activation. These activated clones then expand, and upon interaction with the specific MHC I antigen complex and activation of co-stimulatory receptors, they exert their cytotoxic effects [59]. Whilst the process of antigen specific

immunity is a long established concept in the immunology field, particularly in the context of viral infection, it is only really in the last couple of decades that robust experimental data has resulted in the widespread consensus that adaptive immunity may play a role in tumour immune surveillance and rejection [60].

One of the landmark contemporary papers contributing to our current understanding of the role immunity plays in cancer surveillance was published in 2001 by Shankaran et al of the Schreiber group [61]. They demonstrated that carcinogen induced tumours were kept in check by immunocompetent hosts compared with those lacking functional T cells. In addition, over a fifteen-month period, immune deficient hosts (T cells and IFNγ-/-) had a higher rate of spontaneous epithelial carcinoma. Schreiber went on to describe the relationship of the host immune system with developing tumours as the 'Three E's of Immunoediting', referring to elimination, equilibrium and escape [62]. His notion was that the adaptive immune system did not always protect the host against tumour progression, as suggested by the term 'immunosurveillance'. Elimination refers to immunogenic elimination of antigenic tumour cells by components of the innate and adaptive immune system. This continuous process can eliminate the progression of tumours, but those that escape may enter the equilibrium phase. By a process of Darwinian natural selection, less immunogenic clones escape the elimination phase. During equilibrium, there is ongoing pressure from lymphocytes resulting in control but not elimination of malignant cells. It has been suggested that this process may continue for many years. This is supported by the fact that tumours developing after carcinogen exposure often take years to develop [63]. In addition, interesting observations from the field of transplantation also support this theory. It was noticed that two kidney transplant recipients developed metastatic melanoma within 2 years of receiving their transplants [64]. Looking back, it was noted that the donor was in remission, having been successfully treated for melanoma 16 years prior. It was suggested that immune suppression initiated in the recipients may have contributed to the successful escape of the melanoma. Importantly, the donor did not progress to malignancy. Another case report of post-transplant melanoma showed that following removal of the graft and augmentation of host immunity with interferon alpha, complete remission was observed [65]. Eventually, acquired resistance to host immunity can results in tumour escape and subsequent progression. Many factors may contribute to the eventual ability of tumours cells to fully escape immune rejection. Concurrent with the

equilibrium phase, tumour cells undergo constant genetic and epigenetic alterations. Some of these intrinsic cell changes may confer immunogenic survival advantage. These include loss of antigenicity, loss of MHC I expression, production of suppressive mediators, and loss of immune cell ligands [62,66,67].

Whilst evidence supporting the theory of cancer immunoediting was emerging, the concept of the equilibrium phase relied largely on observational data from clinical reports. More robust pre-clinical data was reported in 2007 in another seminal paper from the Schreiber group. Mice were treated with low dose carcinogen and those failing to develop tumours were subsequently monitored for 300 days. In the experimental arm, tumour free mice were depleted of T cells at 200 days, with all of them rapidly developing lethal tumours [68]. Since this observation, further studies have shown through immune manipulation that immunity participates in tumour dormancy and escape [69,70]. In addition, the escape phase of immunoediting has resulted in a huge amount of activity and subsequent publications over recent years, coinciding with its inclusion as one of the hallmarks of cancer [71,72]. This may in part be due to the fact that many of the newly discovered immune escape mechanisms lend themselves to therapeutic targeting. Chief amongst these are immune checkpoint molecules. Cytotoxic T lymphocyte antigen 4 (CTLA-4), first reported by Brunet in 1987, is one of dozens of immune checkpoints which have since been identified [73,74]. Antibody targeting of these checkpoints has shown striking efficacy in subsets of patients with melanoma, colorectal cancer and lung cancer [75–77].

As discussed previously, there have been cases of tumour regressions beyond the radiation field (abscopal effect) reported sporadically over recent years. In addition, pre-clinical data has demonstrated improved tumour sensitivity to immune checkpoint blockade when combined with radiation [78–80]. These observations were swiftly translated into the clinical arena with many phase I and phase II trials recruiting patients for combined radiation with checkpoint blockade [81]. Despite the rapidity of these events, the underlying mechanisms behind how radiation elicits adaptive immunity remain incompletely understood.

One of the possible mechanisms gaining traction is the possibility that radiation improves tumour antigen availability. This may result from direct tissue damage, increased intracellular peptide pooling, neopeptides availability as a result of mutagenesis, and increased MHC I

expression. An elegant study by Reits et al in 2006 demonstrated that radiation caused an increase in the number of proteins available for MHC presentation as well as novel radiation specific proteins. When tested in vivo, this significantly augmented MC38 tumour response to gp70 specific T cell adoptive transfer [82]. However the exact nature of presented 'neopeptides' is yet to be elucidated. Emergent techniques for qualitatively and quantitatively measuring the immunopeptidome using mass spectrometry may help to determine whether this is indeed a true phenomenon. There are some indirect hints in the literature that radiation is capable of generating neoantigen priming. More readily accessible T cell receptor clonal analytical techniques have emerged over recent years. These techniques can measure both the number of expanded clones as well as the nature of individual clones. Deep sequencing of T cell receptor clones recently demonstrated that following radiation the receptor repertoire was both broadened and expanded [83,84]. These data are interesting but do not definitively discern the link between MHC presented peptides and correspondent T cell receptor specific priming.

Bridging the gap between innate and adaptive immunity, radiation can also increase the recruitment and activation of cross-presenting dendritic cells [85–87]. Also, radiation can stimulate the secretion of T cell chemokines including CXCL9, CXCL10 and CXCL16 [88,89]. Radiation is a double-edged sword, as adequate responses however are often thwarted by the coincident generation of a highly immunosuppressive microenvironment.

In summary, emerging evidence generally supports the possibility that radiation is capable of generating immunity in certain situations. It is clear that there are mechanisms within tumours which resist immunogenic death, and these are yet to be fully understood. The field is exciting and evolving rapidly, with avid interest due to the possibilities of augmenting existing immunotherapies.

1.3 Tumour Associated Macrophages (TAMs)

Before examining what is known about TAMs in the context of tumour irradiation, it is helpful to appreciate the role of macrophages in normal physiology. In addition to this role, there is abundant pre-clinical and clinical data that help in the understanding of how macrophages may contribute to promoting or inhibiting tumour growth.

1.3.1 Macrophage phylogeny and role in normal tissue development and homeostasis

The term phagocyte derives from the Greek terms 'phagos' (to eat) and 'cyte' (cell). The term was described by Elie Metchnikoff in 1882, who was recognised for his contributions to the discovery of the innate immune system, winning the Nobel prize in 1908 [90]. Metchnikoff also noticed how these phagocytic cells were attracted to bacteria, though the nature of the soluble substances responsible for this were not characterised until the latter half of the next century [91]. Macrophages, along with dendritic cells, make up the main cells of the mononuclear phagocyte system. Whilst our understanding of the role macrophages play in immunity is now greatly expanded, it would be inappropriate to consider these cells as a discrete immune sub-population. Macrophages are highly pleotropic, have different embryological origins, are present in almost all mammalian tissues, and are involved in multiple physiological processes [92].

For a long time it was thought that all macrophages, including tissue macrophages, were derived from circulating monocytes originating in the bone marrow [93]. However during embryogenesis, macrophage progenitors can be found in the primitive ectoderm within the yolk sac, which subsequently seeds progenitor populations in the fetal liver. The liver remains the primary source of monocyte precursors during embryonic development until bone formation begins after birth. At this stage the bone marrow emerges as the prime and definitive site of haematopoiesis [94]. These relatively new observations can be in part attributed to a series of fate-mapping experiments. A seminal paper by Ginhoux et al in 2010 demonstrated that adult brain microglia derive from primitive yolk sac progenitors before day 8 of gestation [95]. It has since been reported that many other tissue resident macrophage populations are derived from either yolk sac progenitors, liver progenitors or a combination of both. These include Kupffer cells (liver), Langerhans cells (skin), alveolar, peritoneal and splenic macrophages [96,97]. The dependence upon these resident macrophages for normal tissue development and homeostasis is highlighted by studies involving *Csf1*$^{op/op}$ mice. Colony-stimulating factor 1 receptors (CSF-1R) are found on almost all macrophages and CSF-1-CSF-1R signalling is the major lineage growth regulator in macrophages [98]. Csf1r (also known as macrophage-colony stimulating factor, M-CSF) is a homodimeric type II tyrosine kinase receptor encoded by the c-*fms* proto-oncogene [99]. CSF-1 promotes survival, differentiation, proliferation and chemoattraction of macrophages. CSF-1 deficient mice show severe depletion of almost all macrophage populations, although Csf1r

knockout mice show an even more severe phenotpye with loss of Langherhans cell and microglia [100]. One of the candidate second ligands for Csf1r is interleukin 34 [101]. Importantly, CSF-1 deficient mice harbour severe developmental abnormalities, including breast, bone and dental development, infertility and neuronal maturation [102].

The functional role of tissue resident macrophages depends upon their interaction with the client cells residing within the organ. Some of these functions have been elucidated by examining the characteristics of abnormally developed tissues in macrophage-depleted mice. Failure of osteoclast development in *Csf1*$^{op/op}$ mice results in severe osteoporosis. In addition, bone marrow macrophages maintain erythrocyte and neutrophil homeostasis by clearing defective or excess populations through phagocytosis [103]. The ability of macrophages to ingest 'self' cells has emerged as an important component of tumour surveillance and elimination [104,105]. Another functional role macrophages play in development is breast ductal branching and terminal bud formation during puberty [106]. Macrophages recruited via CSF-1 from epithelial cells produce growth factors and proteases facilitating outgrowth and maturation of ductal structures [107]. Macrophages also play a role in angiogenesis during organogenesis, including in the kidney, brain and retina [108–110]. Mechanisms of angiogenic regulation include the production of WNT7b, Vascular Endothelial Growth Factor (VEGF) production and engulfment of apoptotic endothelial cells [111–113]. Interestingly, gene expression profiles of fetal lung, kidney and brain macrophages showed a conserved pattern of genes involved in growth and proliferation [108]. Some of these genes, such as Mrc1 and CD163 are included in those considered to be markers of a 'M2', trophic phenotype.

Beyond embryonic and tissue development, macrophages continue to have important roles in tissue homeostasis. This includes tissue resident macrophages and also circulating monocytes originating in the bone marrow. Just some of the roles this heterogeneous population are involved in includes erythropoiesis, bone remodelling, modulation of gut inflammation, micronutrient metabolism, stem cell maintenance, tissue repair and remodelling, initiation of adaptive immunity and particulate clearance in the lungs. The number and diversity of these roles precludes further discussion in the scope of this thesis. Importantly, despite their genetic diversity, tissue resident macrophages can be supported by a reactive population of patrolling monocytes [114,115]. A field of ongoing investigation is the ontogeny of disease or tumour-associated macrophages. Experiments utilising bone marrow chimera models and microsphere labelled

macrophages confirmed that circulating monocytes were a major source of TAMs [116–118]. However, since it has become clear that macrophages can derive from different embryological origins, there is the possibility that proliferation of resident macrophages contribute to the TAM pool. Indeed, there have been a number of recent studies confirming that TAMs can be derived from both resident and circulating populations. Importantly, resident macrophages can exhibit pro-tumourigenic properties in the same way as recruited monocytes. In the Polyoma middle T (PymT) oncogenic murine breast cancer model it was shown that recruited monocytes as well as in situ proliferation swelled the TAM population, and that TAM but not resident macrophage depletion affected tumour growth [119]. In contrast, parabiosis models show that resident pancreatic macrophages are critical for the development of the fibrotic stromal compartment in genetically engineered models [120].

1.3.2 Macrophages in primary tumourigenesis

As distinct from macrophages present in established tumours, they have also been implicated in the initiation of cancer. One of the cornerstones of basic cancer biology is the acquisition of mutations in oncogenes or tumour-suppressor genes that lead to malignancy. Numerous environmental stimuli have been shown to accelerate this process and a well-recognised precipitant is chronic inflammation. This can include sterile chronic inflammatory states including autoimmune diseases and obesity [121]. In addition, there are very well established associations between pathogenic infections and cancer, such as viral hepatitis and hepatocellular carcinoma, and human papilloma virus and cervical cancer [122,123]. Macrophages are able to make significant contributions to this ongoing inflammation through their production of potent inflammatory molecules such as TNF-α and IFN-γ [124]. Experimentally, this was demonstrated in an inflammatory bowel disease associated colorectal cancer mouse model. Deng et al conditionally knocked out STAT3 in macrophages which led to reduced expression of anti-inflammatory genes with an associated increase in pro-inflammatory molecules (TNF-α, il6, il1α/β). Other studies using Csf1 gene knockout mice show how macrophages are critical for tumour initiation in models of spontaneous carcinogenesis [125,126]. One of proposed mechanisms behind these observations is the formation of a microenvironment characterised by ‘smoldering inflammation’ [127]. In this setting, it is proposed that macrophages directly foster a mutagenic environment through their production of reactive nitrogen and oxygen species [128,129]. Macrophages may also contribute to tumourigenesis

by secreting growth factors that promote the proliferation of epithelial cells with acquired tumourigenic gene mutations [121]. Finally, Modi et al showed that Langherhans cells were required for polyaromitc hydrocarbon induced skin carcinogenesis [130]. The role of macrophages during the initiation of cancer is largely related to their pro-inflammatory role. However once tumours are established, cancer cells can harness the pleotropic nature of macrophages to aid and abet progression. Thus, herein the role of macrophages in established tumours will be discussed, so-called tumour-associated macrophages (TAMs).

1.3.3 Macrophage phenotypes

Phenotypic characterisation of macrophages is a complex field of ongoing investigation. One of the main areas lacking consensus amongst investigators is the classification and nomenclature of macrophages [131]. An early attempt at macrophage classification resulted from work by Stein et al in 1992, who reported differential gene expression patterns in cultured macrophages exposed to LPS and il4. Whilst LPS stimulated an inflammatory, 'classically' activated phenotype, IL-4 induced the expression of the mannose receptor (MMR) and was described as 'alternative' activation [132]. These classifications are analogous to the now widely used terms 'M1' (classical) and 'M2' (alternative) macrophages. These terms, proposed by Mills et al in 2000, drew parallels with the established T_h1/T_h2 paradigm [133]. Recognising that exogenous in vitro stimulation of macrophages produces extreme phenotypes, additional subtypes were proposed to reflect the range of phenotypes existing between these poles [131,134,135].

Lipopolysaccharides are a major constituent of gram-negative bacterial membranes [136]. As a PAMP, LPS is recognised by toll-like receptors (TLR4-CD14 co-receptor) on macrophages which is followed by STAT3 dependent upregulation of TNF-α, il1β and nitric oxide synthase [137]. Conversely, STAT6 dependent M2 activation by il4 is associated with upregulation of genes associated with the resolution of inflammation. These include those associated with immune suppression, such as il10, arginase and TGF-β, as well as genes associated with wound healing and matrix remodelling, such as VEGF, MMPs and TIMPs [138–140]. Further transcriptional profiling of both human and murine activated macrophages has revealed hundreds of differentially expressed genes [141–143]. These findings highlight the functional diversity of macrophages, where the phenotypic patterns expressed in response to in vitro stimulation are unlikely to be mirrored in vivo. This has important implications when considering the role of TAMs. An important observation

regarding macrophage activation is their capacity to switch phenotype in response to external stimuli [144]. This plasticity can be manipulated by tumour cells, skewing the phenotype of macrophages towards a pro-tumourigenic profile. Factors produced by tumour cells which can induce M2 polarisation include IL-10, CSF-1, insulin like growth factor 1 (IGF-1), CCL2, and lactate [145–148]. Exposure of naïve monocytes to conditioned medium from multiple tumour cell lines induces macrophage polarisation [145,149–151]. In addition, other cells within the microenvironment can also produce polarisation factors, including il10 produced by regulatory T cells (Tregs) and tumour cells, il4 and IL-13 produced by Th2 T cells, CSF-1 and TGF-β produced by tumour cells, fibroblasts and macrophages [152]. The tumour environment is therefore a potentially rich source of multiple factors that can influence macrophage phenotype.

One of the possible reasons for a lack of consistency in the reporting of macrophage classification is the use of various markers used to identify the same M1 and M2 populations, with a lack of consistency across the literature. Macrophages are routinely characterised by their expression of CD11b and F480 in mice, and CD68 in humans [153,154]. These markers can largely distinguish macrophages from other myeloid cells. These are readily identified by routine laboratory techniques such as immunohistochemical staining and flow cytometry. Further sub classification is often based upon the expression of additional markers that are associated with particular phenotypes. Chief amongst these are markers indicative of M1 and M2 polarisation. In mice there are many established markers that reproducibly discriminate between macrophage sub-populations [141]. A lack of human homologs for many of these markers means comparisons between murine and human data is often precluded. In addition, in vitro murine studies usually source monocytes from the bone marrow or peritoneum, however circulating blood monocytes are usually harvested for use in human experiments. Nonetheless, a range of markers stereotypical of M1 and M2 polarisation has emerged. For M1 macrophages, these include inducible nitric oxide synthetase (iNOS), $MHCII^{hi}$, and CD80/CD86. For M2 macrophages, CD206 (mannose receptor), arginase in mice, and CD163 in humans.

Importantly, these markers are indicative of macrophage polarisation towards extremes of a spectrum of different phenotypes. Therefore in order to reveal more subtle differences between the functional characteristics additional analyses are required. These include gene expression profiles, functional studies of immunosuppressive capacity (T cell suppression assays),

cytokine secretion and effects on tumour cells and other stromal cells. In summary, the investigation and reporting of macrophage phenotype is fraught with challenges. The use of the archetypal M1 and M2 markers described above is useful for determining the basic landscape in tissues of interest, as well as monitoring changes in response to treatments or other stimuli. However in order to capture more subtle changes in this potentially highly heterogeneous population, additional experimental methods should be considered.

1.3.4 Tumour-associated macrophages

Independent of their role in primary tumourigenesis, substantial evidence also implicated them in promoting ongoing tumour progression. Macrophages are often the most abundant leukocyte population present in solid tumours [155]. Dozens of clinical reports have shown a correlation between high TAM numbers and poor survival in many solid organ tumours [156,157]. However these observations are not consistent, with some studies indicating improved outcomes with high TAM numbers [158–160]. There are a number of methodological considerations that limit the extent to which these clinical reports can be extrapolated. Firstly, almost all of the reports are retrospective in nature, almost ubiquitously using immunohistochemical staining for TAM quantification. Also, a majority use a single marker for macrophage identification and dichotomise TAM infiltrates within studies. For example, most studies differentiate patients into high TAM infiltrate (top 50%), and low TAM infiltrate (bottom 50%). The single marker used to identify TAMs is frequently CD68, however this marker can also be expressed on other cells within the stroma and even tumour cells [161]. Also, very few reports attempt to differentiate between different TAM phenotypes, therefore failing to account for the possible contribution of anti-inflammatory M1 macrophages [156]. Also, analysis of macrophages in isolation fails to capture the multifaceted nature of the immune microenvironment. The contribution of macrophages can both influence and be checked by the presence of other immune cells within the TME. This was highlighted in a seminal paper published in 2006 by Jerome Galon [162]. In colorectal tumour samples, they demonstrated that the type, density and location of myeloid cells and lymphocytes provided more informative prognostic information. Subsequently, a number of studies have demonstrated improved sensitivity of composite immune scoring methods [163,164]. More recently, the new paradigm of bioinformatics analyses of public gene array data has provided compelling evidence reinforcing the importance of the basal immune landscape on both prognosis and likely response to treatment [165]. This has been

made possible by the generation of cell-specific signatures able to discriminate between different immune cells and their contribution to the landscape of bulk tumour samples [166]. Despite some inconsistencies, it is generally agreed that TAMs are pro-tumoural. The source of TAMs, recruitment mechanisms and pro-tumoural mechanisms will now be discussed in further detail.

As discussed previously (Section 1.5.2 12), macrophages can be traced to either embryonic progenitors or recruited from circulating monocytes. Whilst it was originally thought that most, if not all, TAMs were recruited from the circulation, recent studies have demonstrated that embryologically distinct tissue resident macrophages can also contribute [120,167]. An important question is whether tissue resident macrophages behave differently in response to queues from tumour cells compared with less mature monocytes. An elegant study by van de Laar et al recently demonstrated that yolk sac, hepatic and bone marrow derived monocytes became transcriptionally and functionally identical upon lung colonisation [168]. In contrast, Pyonteck et al showed different responses to CSF1R blockade between brain microglia and recruited macrophages [169]. This was likely due to the ability of the recruited TAMs to resist CSF blockade by responding to GM-CSF, which did not support microglial resistance. Despite these observations, there is still a plethora of evidence demonstrating that circulating monocytes are recruited to tumours to become TAMs [116,148,154,170–173].

Macrophages are recruited via a range of chemokines and cytokines, a number of which are secreted by tumour cells. CSF-1 is not only the key lineage regulator of macrophages, it can also act as a potent chemoattractant. Overexpression of CSF-1 is associated with significantly higher TAM numbers, and multiple agents targeting the CSF-1/CSF-1R axis result in significantly lower TAM numbers [107,125,174,175]. However because CSF-1 is also critical for survival, these studies do not definitively prove that CSF-1 recruits TAMs. More convincing evidence is provided by a study using organ specific epithelial cell overexpression of CSF-1, which resulted in higher TAM infiltrates [176]. Given that TAMs are generally associated with a poor prognosis, and CSF-1 is potentially acting as a chemoattractant, it is unsurprising that CSF-1 overexpression itself is a predictor of worse survival [126,177,178]. Another chemokine mediating monocyte recruitment is CCL2 (macrophage chemoattractant protein-1, MCP-1), acting on the CCR2 receptor found on monocytes [148,179–181]. Circulating inflammatory (Ly6Chi) monocytes express high levels of CCR2 and normal tissues can respond to injury or infection by secreting CCL2 [182]. Elevated levels of

CCL2 in both the serum of patients and within tumours is an independent poor prognostic marker [183,184]. CXCL12 (stromal derived factor-1, SDF-1) can also recruit monocytes, acting on the receptor CXCR4. Interestingly, fibroblasts constitutively express CXCL12 and can be a major source in the tumour microenvironment [185]. Also, tumour cells can also express its ligand CXCR4, resulting in increased proliferation upon activation [186]. CXCL12 is also implicated in tumour cell adhesion, the metastatic cascade and angiogenesis [187]. As such, it is not an attractive target for examining the role of TAMs in tumour progression. In addition, macrophages have been shown to accumulate in hypoxic or necrotic areas within tumours [188,189]. These macrophages co-localise with blood vessels and express VEGF, suggesting a role in neoangiogenesis [190]. Interestingly, VEGF has also been identified to independently recruit macrophages. In the PyMT model VEGF gain-of-function resulted in recruitment of pro-angiogenic TAMs which drove tumour progression [191]. Loss of VEGF led to inhibition of tumour growth associated with a reduction in angiogenesis and invasion [192]. These data suggest that VEGF can attract macrophages, which also secrete VEGF in an autocrine loop as part of their pro-tumoural, M2 phenotype. Interestingly, studies in rat models of mycocardial infarction and the murine matrigel plug assay show VEGF mediated macrophage localisation and also exhibited an M2 phenotype [193]. Polarisation in this setting may be as a result of hypoxia inducible factor 1 alpha (HIF1α) activation and lactate production [146].

Once macrophages are recruited to the tumor microenvironment, their functional differentiation can affect tumour progression via a range of mechanisms. Firstly, TAMs can influence the intrinsic properties of tumour cells. By producing growth factors, such as EGR, macrophages can increase the proliferation rate of tumour cells [194,195]. Also, there is an abundance of evidence supporting the pro-angiogenic role of macrophages. A key functional characteristic of the M2 phenotype, the effects of macrophages on angiogenesis likely reflects their role in tissue remodelling during the resolution phase of inflammation in response to injury or infection. In human tumours, there is a correlation between TAM numbers and vascular density, which combined predict poor outcomes [189,196,197]. Experimental studies have provided insights into the mechanisms by which TAMs are able to augment angiogenesis. Lin et al used the PyMT spontaneous breast cancer model, crossed with CSF-1 knockout mice, demonstrating that tumours macrophages appeared to be instrumental in regulating the angiogenic switch. Importantly, restoration of VEGF expression rescued tumour growth, suggesting that TAMs are a key source of VEGF within

tumours [191]. This is supported by other reports that demonstrate TAMs drive angiogenesis through their production of VEGF, which is particularly important during the initial stages of tumour growth [198–200] Possible stimuli include hypoxia via the HIF1ALPHA pathway, and CSF-1 mediated NF-kB upregulation [201,202]. In addition to VEGF, TAMs have also been shown to produce MMP9, which can also promote angiogenesis, both directly and by further release of VEGF contained within the extracellular matrix. In some cases MMP9 is critical for VEGF expression. In a murine cervical cancer model, MMP9 blockade inhibited the release of VEGF from TAMs [203]. Interestingly, in a CCR2 deficient mouse model, the lack of TAM derived MMP was compensated for by elevated tumour associated neutrophil production [180]. Finally, a specific subset of highly pro-angiogenic TAMs has been identified. These TAMs are characterised by their expression of the angiopoietin 2 (ANG2) receptor Tie2. Increased expression of ANG2 by endothelial cells in tumours localises Tie2 TAMs to the lumen of blood vessels [204]. Blocking either ANG2 or Tie2 inhibits tumour angiogenesis in models of breast and pancreas cancer [205]. Transcriptional profiling of these TAMs show significantly higher expression of pro-angiogenic genes compared with their Tie2 negative counterparts [199]. Here, CSF-1 is yet again critical by increasing Tie2 expression on the surface of macrophages [206].

Another way in which TAMs exert their pro-tumoural effects is by contributing to immune suppression. Immune suppression is another typical characteristic associated with M2 polarisation. Macrophages constitutively express programmed death ligand 1 (PD-L1), and along with other antigen presenting cells they are the only source of PD-L2. PD-L1 expression can be further increased upon LPS or IFN-γ stimulation, whereas PD-L2 is only induced following IL-4 mediated alternative activation [207]. TAMs in a range of human tumours, including hepatocellular carcinoma, glioblastoma and pancreatic cancer, have been shown to express PD-L1 [208–210]. Furthermore, conditioned media from tumour cells upregulates macrophage PD-L1 expression in culture [209]. Macrophages also express the ligands to cytotoxic T lymphocyte antigen 4 (CTLA-4), CD80 and CD86. Engagement of these ligands with programmed death-1 (PD-1) and CTLA-4 on CD8+ T cells inhibits T cell receptor signalling, regulates their cell cycle and reduces activation. This results in what is referred to as a ‘exhausted’ phenotype. Determining the relative contribution of these inhibitory molecules on the surface of TAMs is experimentally challenging as many other cells within the microenvironment also express them. Two elegant studies, using a combination of MC38

tumour cell PD-L1 deletion and knockout mice, reported different conclusions [211,212]. The paper by Lau et al demonstrated that host PD-L1, particularly macrophages-derived, contributed to escape from immune checkpoint blockade [212]. In contrast, Juneja et al show that deletion of PD-L1 on MC38 tumour cells alone is enough to allow effective immune checkpoint blockade mediated tumour regression [211]. Quantifying the relative checkpoint expression amongst the different cell populations within the tumour microenvironment, and how these contribute to immune suppression and sensitivity to treatment is complex and clearly warrants further investigation.

Immunity is also suppressed by the release of a variety of cytokines, chemokines and enzymes by TAMs. Arginase is an enzyme which catalyses the breakdown of L-arginine to L-ornithine and urea. L-arginine is required for effector T cell activation, and its loss inhibits the re-expression of the CD3 in antigen stimulated T cells, and also inhibits their proliferation [213]. Arginase expression is most commonly associated with alternative M2 activation, although it can also be expressed at lower levels in other activation states [214]. As well as inhibiting T cell function, the products of L-arginine breakdown, polyamines and L-proline, both known to involved with cell proliferation and collagen deposition [215]. Whilst it is clear that T cell suppression and the promotion of cell growth and ECM deposition promote tumour growth, these functions have been extensively characterised in the non-tumour setting. Interestingly, L-arginine is also a substrate for nitric oxide synthetase, a prototypical M1 marker. However the product in this case is nitric oxide, a potent pro-inflammatory agent [216]. Another feature of alternatively activated TAMs is their low expression of IL-12 and high expression of IL-10. IL-12 promotes the activation of Natural Killer cells and differentiation of CD4 T cells into Th1 effector cells [217]. IL-10 prevents dendritic cell activation, promotes regulatory T cell recruitment and function, and inhibits effector T cells [218–220]. In addition, IL-10 prevents the release of IL-12 from TAMs in an autocrine fashion, and also acts to promote alternative activation. Another potent anti-inflammatory cytokine produced by TAMs is TGF-BETA, which also suppresses effector T cell function [221,222]. TAMs also secrete a number of cytokines involved in the recruitment of regulatory T cells, including CCL3,CCL4, CCL5, CCL20 and CCL22 [223–226]. In summary, TAMs have the capacity to create an immunologically hostile tumour microenvironment, largely by inhibiting adaptive T cell antitumour activity through the expression of a variety of immune modulating molecules.

Macrophages can promote metastasis by augmenting the extravasation of tumour cells and subsequent invasion, angiogenesis and growth [227]. Even before tumour cells arrive at metastatic sites macrophages have been shown to be present, contributing to the so-called 'pre-metastatic niche' [228]. In lung cancer metastasis, platelet-mediated tumour cell clots recruit Ly6C+ monocytes via CCL2 which promote extravasation via VEGF secretion [229]. Both genetic and drug based depletion of these myeloid cells inhibits the seeding and growth of metastases [230]. Myeloid cells can also promote tumour cell mesenchymal to epithelial transition by secreting versican in the ECM, which attenuated the phosphor-Smad 2 pathway [231].

Finally, a growing body of evidence suggest that TAMs are implicated in the maintenance of cancer stem cells. Cancer stem cells are highly plastic and can drive treatment resistance and tumour recurrence [232]. In a breast cancer xenograft model, IL-6 mediated STAT3 induction [233]. A similar mechanism was identified in a pancreatic cancer model, where TAMs enhanced the survival of stem cells and their depletion conferred an improved chemotherapy response [234]. Furthermore, TAM-derived IL-6 promoted the proliferation of CD44+ stem-like cells in a hepatocellular cancer (HCC) cell line, and analysis of human HCC tumours revealed a correlation between TAM numbers and CD44+ cells [235].

Overall, a vast body of evidence shows that TAMs are generally pro-tumoural in nature. They contribute to tumour initiation, progression and metastasis. These effects are mediated via a number of mechanisms, which illustrates the functional plasticity of macrophages. In contrast, there is far less known about the role of TAMs in irradiated tumours.

1.4 Rationale for the experimental models used.

All experiments were carried out using the murine colon cancer cell line, MC38, and the pancreatic adenocarcinoma cell line, KPC. Our lab has extensive experience using these cell lines for both in vitro and in vivo work. This prior knowledge was particularly useful in the design of animal experiments, where important details such as cell inoculation numbers and tumour growth kinetics were already known. This facilitated the optimisation experiments I carried out early on during the project. We started our investigation using the murine colon cancer cell line, MC38. To complement the data generated from this cell line, we chose to repeat the experiments using a second cell line. Whilst there were other syngeneic murine cancer cell lines available for which our group has similar prior experience, KPC was selected for specific reasons discussed below. Firstly,

both cell lines are derived from C57 black 6 (C57/BL6) mice. C57/BL6 are genetically unaltered, therefore they have a fully functional immune system complete with all components of the innate and adaptive system. Although we focused on macrophages, any interplay with the adaptive immune system would be precluded if immune compromised models were used. This does however limit our models to one mouse strain. Also, the use of immune competent mice limited our work to murine cell lines. Another strain of mouse used frequently in syngeneic studies is BALB/c. The main difference between these strains is that the immune system in C57/BL6 is Th1 dominant, whereas it is Th2 dominant in BALB/c [236].

MC38 is a murine colon cancer cell line that is generally considered to be generate immunogenic tumours in vivo. One of its biological characteristics that may contribute to this observation is its hypermutated state. MC38 is microsatellite unstable due to impaired DNA mismatch repair. It is thought that this increases the pool of tumour antigens, possibly augmenting adaptive immunity through improved T cell priming. Although there is no direct evidence supporting this theory, experimental evidence involving mouse models suggests that MC38 xenografts are relatively sensitive to immune based therapies. In particular, a number of papers report MC38 xenograft regression in response to anti-PD-L1 monotherapy. These responses are in line with murine tumours known to be sensitive to checkpoint blockade, including B16-F10 and CT-26 [237]. The potential effect this has on generating immunity has recently been revealed following clinical trials in human patients. In patients with colorectal cancer, the immune checkpoint inhibitor Pembrolizumab was only effective in those with microsatellite instability [238]. In addition, data from our lab, as well as previous reports, show that MC38 is infiltrated by CD8+ T cells [237]. The presence of CD8+ T cells are required for effective immunotherapeutic targeting of tumours [239]. As well as its ability to generate immunity, MC38 tumours are also reported to contain modest numbers of macrophages. Given that we aimed to investigate the effect of irradiation on TAMs, a tumour with at least some macrophage infiltration is important if the number and phenotype of TAMs in the unirradiated tumour is to be established. Finally, data from previous clonogenic experiments conducted in our lab, as well as in the literature, demonstrate that MC38 is a relatively radiosensitive cell line. Modest doses of radiation (10Gy single dose, 18Gy in 9 fractions of 2Gy) are able to significantly delay the growth of MC38 tumours in vivo. This is also important given that we also aimed to investigate the effect TAMs may have on tumour growth after radiation. Of

course, the dose applied can be changed in order to achieve optimal baseline growth kinetics. However, higher doses carry increased risk of normal tissue damage that may not be tolerated in the mice. Together, the growth kinetics, the nature of the tumour microenvironment and the immune phenotype make MC38 a suitable cell line for the investigation of the immune response to irradiation.

The KPC cell line is derived from spontaneous pancreatic ductal adenocarcinoma tumours arising in the pancreas of transgenic mice. In homozygous mice, the combination of a p53 and Kras mutation leads to the development of pancreatic intraepithelial neoplasia (PanIN) lesions followed by invasive carcinoma. The tumour microenvironment in KPC tumours is highly reflective of that observed in human tumours, and it is therefore an excellent pre-clinical model of the disease. The microenvironmental characteristics it shares with human tumours includes desmoplasia with a dense stromal compartment, high macrophage and myeloid-derived suppressor cell (MDSC) numbers, and pattern of metastasis. These features also render it highly resistant to conventional chemotherapy agents as well as radiation, which are also seen in patients with PDAC. Using the KPC cell line therefore complements our use of MC38 insofar that most of its characteristics contrast directly with MC38.

2. CHAPTER 2 METHODS

2.1 Tumour cell lines

The murine MC38 cell line was purchased from American Type Culture Collection. KPC cells were derived from primary pancreatic tumours spontaneously arising in KrasLSL^{G12D}/+;p53^{R172H}/+;Pdx1-Cretg/+ (KPC) mice. The mice were a gift from Owen Samsom (Cambridge, UK). Tumours were harvested and dissociated to form single cell suspensions. Cells were cultured in RPMI supplemented with 10% FBS and penicillin (100µg/ml) and streptomycin (100µg/ml). All cells were cultured in a sterile incubator with 5% CO_2 at 37°C and kept for no more than 10 passages. For in vivo injection models cells were used when they reached 80% confluency. Cells were tested regularly for mycoplasma negativity. Cell culture experiments were performed under sterile conditions in a laminar flow hood. For irradiation experiments, cells were transported under sterile conditions to a Caesium^{137} irradiator and radiation applied.

2.1.1 Colony forming assays

Cells were cultured as described previously and used for clonogenic assays when they reached 80% confluency. Cells were trypsinised using trypsin-EDTA and filtered through a 50µm filter to remove cell clumps. Cells were re-suspended (1x10^6/ml) and immediately irradiated using a Caesium^{127} laboratory irradiator for the required amount of time to generate doses of 0,2,4,6,8 and 10Gy. Cells were then counted using a hemocytometer and re-suspended at a stock concentration before serial dilution to the required concentrations for seeding. Cells were seeded into 100mm cell culture dishes in triplicate. Cells were then cultured for 5-8 days and monitored for colony formation. Clones were determined to be present if there were >50 cells in a colony. For colony counting, plates were washed and fixed with 75% laboratory grade ethanol with 1% crystal violet. Colony counting was performed on an Oxford Optronix™ GelCount system using the corresponding software. The surviving fraction at each sequential radiation dose was normalised to the unirradiated control. Plating efficiency (PE) was calculated by dividing the number of colonies counted by the number of cells seeded and multiplying by 100. The surviving fraction was calculated by dividing the PE of the treated sample by the PE of the control sample and multiplying by 100. Survival curves were fitted using indirect curve fitting in GraphPad Prism 5.0. Three independent experiments were conducted.

2.2 Animal work and associated experiments

2.2.1 Animals and husbandry

Animal procedures were carried out in accordance with UK Animal law (Scientific Procedures Act 1986), including local ethics approval. Female C57BL/6 and CD1-Nu mice were purchased from Charles River Laboratories (Kent, UK). Experiments were conducted within the limits of the Home Office issued project licence (Project licence number 30/2922). Animals were housed in specific pathogen-free facilities with temperature controlled conditions (24±1°C) and humidity was controlled at 55%±10%. Light was set at 12 hour light/dark cycles continuously and mice had unlimited access to food and water. Mice were weighed three times weekly and health monitored daily. Mice were only entered into an experiment if their weight was in excess of 17.0g. If there was >10% weight loss once entered into an experiment mice were culled. Tumours were monitored for ulceration and mice culled if wet ulceration was detected.

2.2.2 Tumour challenge and treatment experiments

For the MC38 model, $0.5x10^6$ MC38 cells diluted in Phosphate Buffered Saline (PBS) were injected into the flank(s) of anaesthetised mice. For the KPC model, $0.25x10^6$ KPC cells diluted in PBS were injected into the flank(s) of anaesthetised mice. Tumours were measured daily in three dimensions using digital callipers and tumour volume calculated using the formula *0.5 x Length x Width x Height*. When tumours reached $80mm^3$ mice were randomly assigned to treatment groups.

2.2.3 In vivo antibody treatments

For in vivo treatments mice were randomly assigned treatment groups when tumour volume reached a pre-determined volume. For macrophage depletion studies anti-CSF was started when tumours reached a volume of $80mm^3$. Tumour volume was monitored twice daily and if the volume exceeded $90mm^3$ mice were excluded from the experiment. As each mouse entered the experiment they were sequentially entered into each treatment arm until all arms were complete. Anti-CSF (Bioxcell, clone 5A1) was administered intraperitoneally at a dose of 10mg/kg diluted in 100uL phosphate buffered saline three times weekly. For anti-PD-L1 treatments the first dose was given when tumours reached $80mm^3$, twenty-four hours prior to the first dose of radiation. The second dose was administered twenty-four hours following radiation, the third on day 5 and the final dose on day 9. Anti-PD-L1 (Bioxcell,clone 10F.9G2) was administered at a dose of 10mg/kg diluted in 100uL phosphate buffered saline injected intraperitoneally. Anti-CD8a (Bioxcell, clone 2.43) was

administered intraperitoneally at a dose of 250ug diluted in 100uL phosphate buffered saline on days -1,3,6 and 9. Radiation was initiated when tumours reached 100mm^3 (±10mm^3), delivered via a Gulmay 320 irradiator under inhalational isofluorane anaesthesia. If tumours exceeded 100mm^3 they were excluded from the experiment. The tumours were exposed and the remainder of the body and tail shielded using lead shields. Experimental end-point was pre-defined as tumour volume at or exceeding 500mm^3 and mice were culled early in the case of tumour (wet) ulceration. In vivo tumour growth studies were analysed by comparing mean end-point data (days) or tumour volume at specific time points by unpaired *t* test or one-way ANOVA for multiple comparisons.

2.2.4 Murine serum collection

Mice were sacrificed using an intraperitoneal injection of pentobarbital (200mg/kg). Shortly following injection, once mice were unconscious, the thoracic cage was opened and the vena cava divided immediately superior to the diaphragm. Blood was aspirated using a 1ml syringe and transferred to an eppendorph 1.5ml tube. The blood was placed on ice for 30minutes and then centrifuged at 12,000 RPM for 20 minutes at 4^{O}C. The supernatant was then transferred to a new tube and samples were stored at -80 until analysis.

2.3 Tumour sectioning

Subcutaneous tumours were excised immediately following sacrifice and subcutaneous fat dissected away from the tumour tissue. Tumours were then embedded in optimal cutting temperature (OCT) compound (25608-930 TissueTek) and immediately frozen and stored at -80^{o}C. Sections were prepared using an OTF 5000 cryostat (Bright). 10-15µm sections were mounted on to SuperFrost plus miscroscope slides (ThermoFisher).

2.4 Haematoxylin and Eosin staining

Tissue sections were brought to room temperature and fixed in ice-cold acetone for 10 minutes. Sections were then rehydrated in PBS (3x5 minutes), then immersed in filtered Harris Haematoxylin solution (Sigma) for 3 minutes. After this sections were immediately washed with running tap water for 5 minutes. Sections were then immersed in differentiation solution (2mls concentrated hydrochloric acid in 98mls 70% ethanol) for 25 seconds. Sections were then rinsed in tap water for five minutes. Sections were then immersed in 95% ethanol for 1 minute followed by immersion in 1% aqueous Eosin (Sigma) for 2 minutes. Sectiones were then gradually dehydrated

using 50%, 70%, 90% and 95% ethanol by immersing for 10-20 seconds each. They were then cleared using Xylene twice (fresh solution each time) for 5 minutes. Coverslips were mounted suing Permount mounting medium (ThermoFisher) and dried overnight.

2.5 Immunofluorescent staining

For immunofluorescence staining, sections were brought to room temperature, fixed in ice-cold acetone, rehydrated, blocked with 20% goat serum, and incubated for 2 hours at room temperature or overnight at 4 degrees. A full list of antibodies used for immunofluorescent staining can be seen in table XX. The following day, the slides were washed in PBS before being incubated with Alexa Fluor 546 secondary antibodies against rabbit (Life Technologies) for 1 hour at RT. The sections were washed and mounted using the ProLong® Diamond Antifade Mountant with DAPI (P36962; Fisher). Immunofluorescence was visualised utilising an inverted epifluorescence microscope (DM IRBE, Leica Microsystems) with a digital camera. The images were processed using either ImageJ (National Institutes of Health, Bethesda, MD) or Adobe Photoshop CS4 (Adobe Systems).

2.6 ELISA and cytokine arrays

CSF-1 mouse ELISA kit (MBS701429, MyBioSource) was used according to manufacturer`s instructions for determination of CSF-1 levels. ELISA was performed using 10 µL protein lysates diluted 1:10. Proteome profiler array panel A (R+D systems) was used to analyse tumour cell conditioned media.

2.7 Flow Cytometry

Tumours were manually dissociated immediately following excision using a scalpel to create fragments <1mm. Tumour fragments were incubated in Hanks Balanced Salt Solution (with calcium/magnesium ThermoFisher Scientific 14170112) with 200uL Collagenase II (Worthington, UK) and incubated on an automatic shaker at 37° Celsius for 40 minutes before being passed through a 70µm filter (Falcon, BD). The cell pellet was re-suspended in 3 mls of red cell lysis buffer and incubated for 3 minutes, spun and re-suspended in 5% fetal bovine serum at a concentration of $10x10^6$/ml for staining. For T-cell stimulation $1x10^6$/ml of cells were incubated in RPMI supplemented with 10% fetal bovine serum with 2µL/ml of Cell Stimulation Cocktail with Brefeldin A (Biolegend 423304) for 4 hours. Prior to staining for surface and intracellular antigens cells with incubated with Fc

block (anti-CD16/CD32) for 5 minutes. For surface staining antibodies were incubated at room temperature for 45 minutes before being washed three times and re-suspended in 300μL PBS with added 5% fetal bovine serum. For intracellular staining the eBiosciences FOXP3 intracellular staining kit was used according to the manufacturer's instructions (00-5523-00). A list of antibodies used can be seen in the Table 1. Data were acquired on a BD FACS Canto™ II or BD FACSCalibur™. For acquisition of tumour samples, the total number of events collected was constant across samples and determined on the live gate of single cells. The initial gating strategy can be seen in Figure 2.1. Data were analysed using FlowJo version 10.0.

Table 1 – List of fluorescently conjugated antibodies used in flow cytometry experiments.

Antibody	Supplier	Catalogue number
Cell viability dye	ThermoFisher	65-0867-18
CD11b PeCy7	ThermoFisher	25-0112-81
CD8a PeCy7	ThermoFisher	25-0081-82
CD4 APC	ThermoFisher	17-0041-82
FOXP3 BV 421	Biolegend	126410
CD3 APC-Cy7	ThermoFisher	47-0031-82
CD25 PerCP Cy5.5	Biolegend	101911
F480 BV 421	Biolegend	123132
MHC II APC	Biolegend	17-5321-82
CD11c PE	ThermoFisher	12-0114-81
NK 1.1 APC Cy-7	Biolegend	108724
Granzyme B	ThermoFisher	515405
Interferon-y APC	ThermoFisher	17-7311-81
Ki67 PE	ThermoFisher	12-5698-80
PD1 BV 421	Biolegend	135221
LAG-3 PE	ThermoFisher	369306
PDL-1 BV 421	Biolegend	124315
Ly6C APC Cy-7	Biolegend	128026
Ly6G-Gr1 BV 510	Biolegend	108438
Ly6G-Gr1 APC	ThermoFisher	17-9668-80
FasLigand PerCP Cy5.5	Biolegend	46-5911-80
CD206 PerCP Cy 5.5	Biolegend	141715
iNOS PE	Santa Cruz	Sc-7271

CD45 BV 510	Biolegend	103138
CTLA-4 PerCp Cy 5.5	Biolegend	106315
CD31 APC	ThermoFisher	17-0311-82

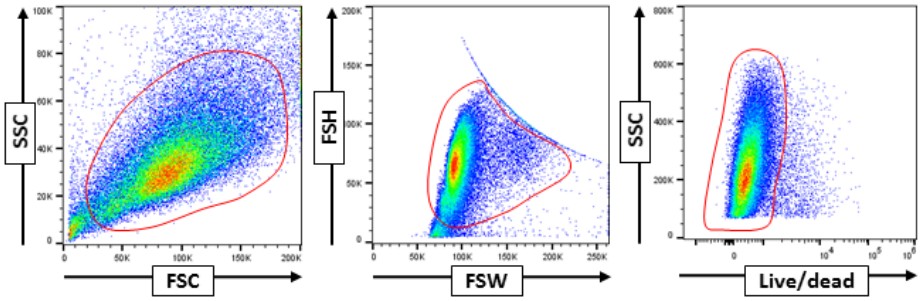


Figure 2.1 – Initial flow cytometric gating strategy. Cells were first identified based upon their forward and side scatter profiles (left). Doublets were then excluded by analysing width and height profiles (middle. Finally, dead cells were excluded using a fixable cell viability dye (right).

2.8 Fluorescence Activated Cell Sorting

Tumours were manually dissociated immediately following excision using a scalpel to create fragments <1mm. Tumour fragments were incubated in Hanks Balanced Salt Solution (with calcium/magnesium ThermoFisher Scientific 14170112) with 200uL Collagenase II (Worthington, UK) and incubated on an automatic shaker at 37° Celsius for 40 minutes before being passed through a 70µm filter (Falcon, BD). The cell pellet was re-suspended in 3mls of red cell lysis buffer and incubated for 3 minutes, spun and re-suspended in 5% fetal bovine serum at a concentration of $10x10^6$/ml for staining. The cell suspension was first incubated with anti-CD16/32 (eBiosciences) for 5 minutes in order to block Fc receptors. Cells were stained with surface antibodies for 45 minutes at room temperature. Cells were washed with 3mls 5% fetal bovine serum and re-suspended at $10x10^6$/ml in 5% fetal bovine serum. Samples were sorted on a Beckman Coulter Legacy MoFlo high speed cell sorter. The cell sorting was kindly performed by Dr Andrew Worth of the Jenner Institute, University of Oxford. All cells were stained with cell viability dye (APC Cy-7) and only live cells collected. Macrophages were gated on expression of CD11b+ and F480+. Tumours cells were GFP+. The gating strategy for isolation of cell populations can be seen in **Error! Reference source not found.**.

2.8.1 RNA extraction from sorted cell populations.

Prior to RNA extraction an RNAse free workspace was designated within the laboratory. Surfaces were cleaned with 100% ethanol and gloves worn at all times and changed frequently. All plastic ware was autoclaved before use and sprayed with 100% ethanol before introduction to the workspace. Immediately after cells were isolated by FACS tumour cells were lysed in 1ml of TRIzol reagent by pipetting for 1 minute. Following lysis, the cell suspension was incubated for 5 minutes at room temperature before 200µl of chlorophorm was added. Samples were then shaken vigorously for 30 seconds before being incubated at room temp for 3 minutes. Samples were then centrifuged at 12,000RPM for 15 minutes at 4^{O}C. The aqueous phase was then transferred to a new sterile eppendorph tube containing 2µl glycogen, then 500µl of isopropanol was added. Samples were incubated on ice for 20 minutes before being spun at 12,000RPM for 10 minutes at 4^{O}C. The supernatant was then decanted and 1ml of 75% ethanol (constituted with nuclease free water) added. Samples were spun again at 7500g for 5 minutes at 4^{O}C. The supernatant was decanted and a further wash with 75% ethanol performed. Samples were spun at 7500g for 5 minutes at 4^{O}C and the supernatant decanted then aspirated to remove all excess alcohol. Samples were then air dried until all traces of the ethanol were evaporated. RNA pellets were re-suspended in 20-50µl nuclease free water. RNA was fully dissolved by incubating the tubes for 30 minutes at 37^{O}C. RNA yield and purity was determined by analysing 1µl RNA suspension on a spectrophotometer (NanoDrop™ One, ThermoFisher). For immune cell populations, due to the low cell counts RNA was extracted using the Arcturus™ PicoPure™ RNA isolation kit according to the manufacturer's instructions.

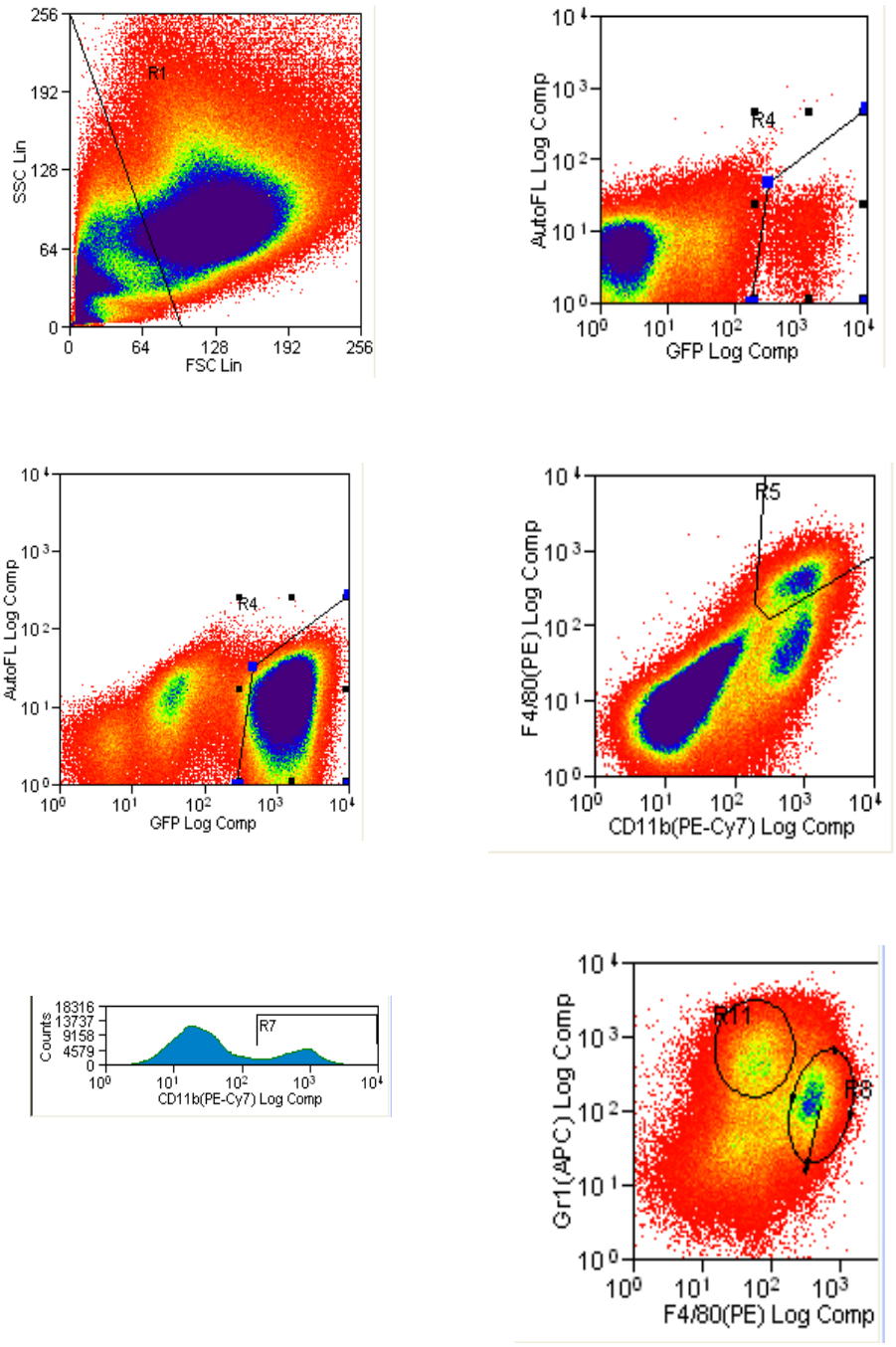


Figure 2.2

Fluorescence activated sorting of tumour cell and myeloid populations. Cellular populations were first gating according to their forward and side scatter profiles (top left), then dead cells were excluded as defined by their expression of cell viability dye (top right). Tumour cells were identified according to their GFP expression (middle left). For myeloid sorting, macrophages were gated according to their expression of $CD11b^{hi}$ and $F480^{hi}$ (middle right). To distinguish MDSCs from macrophages, cells were first pre-gated on CD11b expression (bottom left), then separated based upon Gr1 and F480 expression (bottom right). $Gr1^{hi}$ cells were determined to be MDSCs.

2.9 Magnetic bead separation of macrophages

Whole mice were immediately immersed in 70% ethanol following cervical dislocation and tumours harvested using sterile instruments. Immediately after dissection, tumours were placed in sterile PBS. Tumours were kept on ice until manual dissociation using a scalpel was performed using sterile instruments under a laminar flow hood. Tumour fragments were incubated in sterile Hanks Balanced Salt Solution (with calcium/magnesium ThermoFisher Scientific 14170112) with 200uL Collagenase II (Worthington, UK) and incubated on an automatic shaker at 37° Celsius for 40 minutes before being passed through a sterile 50µm filter (Falcon, BD). Cells were washed in cold, sterile PBS and filtered again through a sterile 50µm filter (Falcon, BD). Cells were then counted and re-suspended at a concentration of 10^7 cells per 90ul MACS buffer (sterile PBS pH 7.2, 0.5% bovine serum albumin, 2mM EDTA). Fc receptors were blocked by incubating the cell suspensions at room temperature for 5 minutes with anti-CD16/32. 10ul/10^7 total cells of magnetic ultrapure F480 beads were then added and the cells incubated at 4^OC for 15 minutes. Cells were then washed with 2mls MACS buffer, spun at 300g for 10 minutes at 4^OC. The supernatant was aspirated and cells re-suspended at 10^8 in 500ul MACS buffer and kept on ice. MS columns were prepared by adding 1ml MACS buffer before applying the cell solution. After three washes with 500ul MACS buffer the cells were re-applied to an additional MS column. The column was washed three times with 500ul MACS buffer before cells eluted and used in downstream applications.

2.10 Real-Time quantitative PCR

RNA was extracted from cultured cells using TRIzol (Sigma Aldrich). Cells were washed with PBS and TRIzol (stored at 4^oC) added. Cells were incubated with TRIzol for 5 minutes until they were detached. For highly adherent cells such as macrophages, cells scrapers were used. The cell lysates were passed several times up and down a 1ml pipette. After a further 5 minutes room temperature incubation, 200uL chlorophorm was added and samples shaken vigorously for 30 seconds. Samples were then centrifuged at 12,000rpm for 20 minutes. 3-500uL of the aqueous phase was transferred into new eppendorph tubes containing 2uL of glycogen. 500uL of isopropyl alcohol was then added to each sample and incubated for 20 minutes at -20^oC. Samples were then centrifuged at 12,000rpm for ten minutes. The supernatant was aspirated and 1ml of 75% ethanol added. Cells were then spun for 5 minutes at 7500g. The supernatant was aspirated and a further 1 ml of 75% ethanol added. Cells were spun at 7500g for 5 minutes. The supernatant was carefully

aspirated leaving a small RNA pellet. Tubes were then left in the hood until all of the 75% ethanol had evaporated. Samples were then re-suspended in 30-50uL of nuclease free water and re-suspended by incubating at 37^{o}C for 30 minutes. RNA quality and quantity was measured using a NanoDrop^{TM} One UV-Vis spectrophotometer with readings at 260nm and 280nm. The 260nm/280nm absorbance ratio was measured to determine sample quality. Pure RNA was determined to be present if the ratio was 1.8-2.0. Samples outside of this range were discarded. For tissue samples, small (1-2mm^3) tissue samples were homogenised using a Tissue Tearor homogeniser (Biospec) for 30 seconds in 1ml of TRIzol. Following 5 minutes incubation at room temperature the same protocol as outlined above (for cultured cells) was used to extract RNA. Following RNA extraction, genomic DNA was eliminated using the TURBO DNA-free kit (ThermoFisher Scientific) according to the manufacturer's instructions. RNA quantity was then re-measured to gain accurate measurements. cDNA was synthesised using the High Capacity RNA-to-cDNA Kit^{TM} (ThermoFisher Scientific) according to the manufacturer's instructions. For quantitative polymerase chain reaction (qPCR) reactions, 25ng of cDNA was loaded with SYBR green (Thermofisher) and amplified in the following conditions: 40 cycles at 95 degrees (15 seconds), 60 degrees for 30 seconds and 72 degrees for 30 seconds. mRNA expression and fold change was analysed using the delta ct method, normalising for the housekeeping gene (ß-actin).

Table 2 – List of primers used in real-time quantitative PCR experiments.

Gene	**Forward primer**	**Reverse primer**
β-actin	GATGTATGAAGGCTTTGGTC	TGTGCACTTTTATTGGTCTC
Csf1	TAGAAAGGATTCTATGCTGGG	CTCTTTGGTTGAGAGTCTAAG
NOS2	CATCAACCAGTATTATGGCTC	TTTCCTTTGTTACAGCTTCC
Il12	GAAGACATCGATCATGAAGAC	CTCTTGTTGTGGAAGAAGTC
Tnfα	GTAGCCCACGTCGTAGCAAA	ACAAGGTACAACCCATCGGC
Il1α	AACCCATGATCTGGAAGAGACC	TGGTGCTGAGATAGTGTTTGTCC
Il1ß	CAGGCAGTATCACTCATTGTGG	GTGCAGTTGTCTAATGGGAACG
Arg	CTGACCTATGTGTCATTTGG	CATCTGGGAACTTTCCTTTC
Il6	ACAAAGCCAGAGTCCTTCAGAGA	CTGTTAGGAGAGCATTGGAAATTG
ym1	TCTGGTGAAGGAAATGCGTAAA	GCAGCCTTGGAATGTCTTTCTC
ccl2	CAAGATGATCCCAATGAGTAG	TTGGTGACAAAAACTACAGC
Il10	CAGGACTTTAAGGGTTACTTG	ATTTTCACAGGGGAGAAATC

2.11 Bone Marrow Derived Macrophage (BMDM) culture

Bone marrow was harvested from the tibia and femur of C57BL/6 mice under sterile conditions. Mice were culled by cervical dislocation and immediately immersed in 70% ethanol. Bones were then harvested using sterile instruments without breaching the abdomen. Harvested bones were briefly immersed in 70% ethanol, washed in sterile PBS then stored in ice cold PBS. Any bones where the cortical integrity was breached were discarded. Further work was carried out under sterile conditions in a laminar flow hood. Each end of the bones was transected and the bone marrow pulp washed out using sterile PBS and a syringe and 23G needle. Following filtration and washing, $3x10^6$ cells were re-suspended in RPMI supplemented with penicillin (100µg/ml) and streptomycin (100µg/ml), 10% fetal bovine serum and 20% L929 conditioned medium and incubated for 5 days. L929 conditioned medium was prepared by culturing confluent L929 cells in the presence of serum free media for 48 hours. Media was filtered through 20µm filter and stored at -20. Purity was assessed by flow cytometry, with macrophages defined as $CD11b^{hi}$ $F480^{hi}$.

2.11.1 BMDM co-culture experiments

For co-culture experiments, differentiated macrophages were seeded into 6 well plates ($1x10^6$/well). Tumour cells were seeded into Millicell® 0.4µm cell culture inserts ($0.5\text{-}1.0x10^6$/well) 24 hours prior to transfer to the 6 well plates. Irradiation was performed on tumour cells immediately prior to transfer. Transwell inserts were transferred into the wells containing macrophages using sterile forceps under a laminar flow hood. Plates/transwells were then cultured for the time indicated in individual experiments. The minimum co-culture period was 24 hours and the maximum was 120 hours. Transwell inserts were removed; BMDMs were washed with PBS and then harvested for downstream analysis. For flow cytometric analysis cells were harvested using trypsin-EDTA. For RNA extraction cells were harvested using a cell scraper.

2.11.2 BMDM conditioned media experiments

BMDMs were obtained as described in 2.11. Following 5 days of culture with RPMI supplemented with penicillin (100µg/ml) and streptomycin (100µg/ml), 10% fetal bovine serum and 20% L929 conditioned medium. Conditioned media was collected from MC38 and KPC cells. Cells were grown to 70% confluency, the media changed and then collected after 48 hours of culture. For irradiation experiments cells were irradiated at 0 hours and media collected after 48 hours of culture. The conditioned media was filtered through a 20um filter and spun at 1500rpm for 5 minutes to

eliminate any contamination by tumour cells. Conditioned media (CM) was then stored at -80 until use. After 5 days of culture, media was aspirated and fresh media applied supplemented with 20% tumour conditioned medium. After a period of further culture (as indicated in each experiment), media was aspirated and cells harvested for downstream analysis.

2.11.3 T cell suppression assay

Spleens from naïve C57BL6 wilt-type mice were manually dissociated using a scalpel and incubated for 45 minutes at 37 degrees in HBSS supplemented with type II collagenase (Worthington, UK). Cell suspensions were then strained through a 50µm cell strainer before being incubated with 3mls of red cell lysis buffer for 3-5 minutes. Cells were washed in PBS supplemented with 5% fetal bovine serum and counted. $1x10^7$ cells were incubated with anti-CD8 microbeads (Miltenyi Biotech) and separated using LD columns according to the manufacturer's instructions and labelled with 1mM Carboxyfluorescein succinimidyl ester (CFSE, Invitrogen) in PBS at 37 degrees for 20 minutes. T cells were re-suspended in RPMI supplemented with 10% FCS, 1% pen/strep, 0.5% (1mM) L-Glutamine, 0.1% (55uM) 2-mercaptoethanol and recombinant il2 (30units/mL). Tumour macrophages were added at the indicated ratios and incubated for 55 hours in wells pre-coated with anti-CD3 (10ug/mL) and anti-CD28 (2ug/mL). T cells were analysed for CFSE expression by flow cytometry (Attune NxT flow cytometer, ThermoFisher).

2.12 IFN-γ Elispot assay

The Ebiosciences mouse interferon-gamma ELISPOT kit was used according to the manufacturer's instructions. Spleens were harvested from naïve and tumour bearing mice from control, anti-CSF, 10Gy and 10Gy+anti-CSF treated groups. CD8 t cells were isolated as described above and seeded in a sterile 96 well high protein binding immunobiolon-P membrane culture plate (Millipore) with control or irradiated (10Gy) MC38 tumour cells ($1x10^5$ cells at a ratio of 1:1). Recombinant mouse interferon gamma (Biolegend, UK) was used as a positive control. IFN-γ spots were quantified using the EliSpot plate reader (Oxford Biosystems).

2.13 Protein extraction

For cell culture samples, cells were washed with PBS then detached using Trypsin-EDTA solution. Cell suspensions were then spun at 4^oC for 5 minutes and the supernatant aspirated. Samples were then re-suspended in radioimmunoprecipitation assay buffer (RIPA) supplemented with

1% protease/phosphatase inhibitor (Cell Signalling Technologies). For tissue samples, small fragments (2-3mm^3) of tissue were transferred from -80 to flat bottomed eppendorph tubes and then homogenised using a Tissue Tearor homogeniser for 30 seconds (Biospec). Samples were then incubated at 4^{o}C with constant agitation for 3 hours. Samples were spun at 10,000rpm for 10 minutes and the supernatant containing the protein transferred to a new tube and stored at -80^{o}C until use.

2.14 Immunoblotting

Sample protein concentrations were measured using the Bradford Protein Assay (Biorad). Equal amounts of protein (8-20ug) were added to LDS sample buffer at a ratio of 4:1 and loaded into lanes in 4-12% Bis-Tris precast gels (NP0321 Life Technologies). Nupage MES SDS running buffer (NP0002-02 ThermoFisher) was added to the module. Proteins were separated at 100V for 120 minutes. Proteins were transferred on polyvinylidene fluoride membranes (IPVH00010 Millipore) at 30V on ice for 60 minutes. Membranes were blocked with either 5% bovine serum albumin (A2153 Sigma) or 5% powdered milk in tris-based sline (TBS) supplemented with 0.05% Tween (TBST) for 60 minutes. Membranes were then incubated with primary antibody overnight at 4^{o}C at concentrations of 1:600-5000. Membranes were then washed for 10 minutes three times on a rolling device in TBST. Horseradish peroxidase conjugated secondary antibodies were added at a dilution of 1:1000 and incubated at room temperature for 60 minutes. Protein bands were visualised by adding Amersham ECL detection reagent (RPN2106 GE healthcare) and acquiring images using the Odyssey® image system.

2.15 Statistical analysis

Statistical analyses were performed using Graphpad Prism® 5. The number of mice used in animal experiments is indicated in the corresponding figure legends. In addition, where indicated, animal experiments were repeated more than once. For the analysis of tumour growth delay end-point data (days) were compared between groups by unpaired *t* test or one-way ANOVA for multiple comparisons (with post-hoc analysis). For time-point analyses, tumour volumes were compared between groups by unpaired *t* test or one-way ANOVA for multiple comparisons (with post-hoc analysis). Volumetric data points are presented as mean±SEM. Throughout the figures asterisk symbols are used to denote statistical (p) significance values: *p=<0.05 **p=<0.01 ***p=<0.001.

For the analysis of flow cytometry data, FlowJo version 10 was used. Unless otherwise stated, red cells, debris, doublets and dead cells were first excluded via pre-gating. Pre-determined acquisition gates were then set in order to collect the same number of events from each sample. Percentages of immune cells were calculated using the total cells analysed as the denominator. Relative expression of specific markers on sub-sets (e.g iNOS, CD206) was calculated using mean fluorescence intensity (MFI). Flow cytometry data are presented as mean±SEM and analysed by unpaired *t* test or one-way ANOVA for multiple comparisons (with post-hoc analysis).

3. CHAPTER 3: Radiation induces Colony Stimulating Factor-1 (CSF-1) upregulation and increases macrophage numbers in murine tumours.

3.1 Introduction

One of the main mechanisms by which TAMs are recruited to tumours is in response to chemoattractants and cytokines (page 15). These cytokines are expressed variably in a range of solid tumours, and data from human patients show that overexpression is often associated with increased TAM numbers as well as poor prognosis [240–243]. The source of incumbent macrophages to the tumour microenvironment is likely to be circulating Ly6C+ monocytes derived from the bone marrow, although contributions from tissue resident macrophages have been demonstrated in some models [244]. These are the same monocytes which are mobilised and recruited in response to pathogenic infections [182]. Despite there being a plethora of evidence demonstrating that tumours are a rich source of cytokines involved in monocyte chemotaxis, literature pertaining to alterations in these factors following radiotherapy is more limited. In the context of human data, this may be due to the limited availability of tumour tissue obtained contemporaneously with the administration of radiation. Due to the dynamic nature of immune responses, analysis of tumour samples taken after a significant period of time has passed since the radiation was administered may be of limited benefit. This is best illustrated in patients receiving neoadjuvant radiotherapy for rectal cancer, where a greater than 50% complete pathological response is frequently observed, leaving no tumour tissue for analysis [245,246]. Interestingly, investigation into radiation toxicity as well as radiation associated fatigue has resulted in a number studies reporting changes in cytokine profiles in the blood of patients receiving radiotherapy, including many inflammatory cytokines [247–252]. Furthermore, irradiation of human tumour cell lines *in vitro* demonstrates significant alterations in cytokine expression [34,253]. These studies are primarily interested in exploring the bystander effect (the effect of dying tumour cells on other cells adjacent to those receiving radiation). Two studies measuring cytokine expression *in vitro* showed significant increases in some cytokines involved in monocyte recruitment, including VEGF and GM-CSF [34,253]. In addition to these human data, some studies have reported alterations in cytokine levels following irradiation in animal models. In a murine transgenic pancreatic cancer model, a high dose (20Gy) of irradiation resulted in significantly elevated levels of CCL2, which resulted in the recruitment

of CCR2+ monocytes to tumours [254]. In another model of pancreatic cancer, CSF-1 mRNA levels were significantly higher in whole tumour samples 3 days after 12Gy irradiation [151]. The advantage of these pre-clinical models is that via the use of blocking antibodies (anti-CCL2/CSF-1), the authors were able to demonstrate a significant reduction in monocyte/macrophage numbers, confirming the role of these cytokines in chemotaxis.

The precise mechanism behind the cytokine response observed in tumour cells following radiation is yet to be fully elucidated. At the most basic level, one first has to look at how gene expression may change in response to radiation. Very early gene responses, under the control of promoters laden with CpG islands, involve constitutively active chromatin and do not require the nucleasomal remodelling [255]. Many genes associated with inflammation, including TNFα, G-CSF, VEGF and interferons are included in this group associated with very early (2 hour) upregulation[40]. Increased activation of intracellular signalling pathways involve in inflammation can also be elicited following radiation. These include the nuclear factor kappa B (NFkB) and STAT pathways [36,256]. In vitro, the response of mammalian cells to the potent NFkB inducer TNFα is comparable with the response observed following radiation[257]. NFkB, a ubiquitous transcription factor, regulating the expression of hundreds of genes, has been shown to induce the expression of inflammatory genes in a variety of tumours [258]. The activation of NFkB has been shown to result through ataxia telangiectasia mutated (ATM) and DNA-dependent protein kinase pathways [259].

Within the tumour microenvironment itself, other stromal cells may also produce cytokines. Assays detecting cytokine levels in whole tumour lysates do not provide any information on which cell is responsible for its production. Cellular injury or death, particularly apoptosis, may result in the release of DAMPs. Following interaction with pattern recognition receptors (PRRs), activated immune cells may in turn produce cytokines into the tumour microenvironment [260]. Furthermore, PRRs can be present on non-immune cells, including epithelial cells [261,262]. The release of DAMPs may cause the release of pro-inflammatory cytokines in neighbouring viable tumour cells via activation of TLRs in a self-propelled cycle of inflammation [263]. In particular, macrophages have been shown to produce cytokines responsible for their own survival and recruitment (CSF/CCL2).

Cytokine production within tumours following radiation is a transient process that typically occurs early after the dose is delivered. Cytokine levels in the brain following whole body irradiation in

mice peaked within hours and most returned to baseline within a few days [264]. However the response of tumours is complex and dependent upon factors including dose, fractionation and the response of additional sources of cytokines such as stromal cells. In summary, the available evidence confirms that radiation can alter the expression of cytokines, and some of these may be involved in the recruitment of immune cells to the tumour microenvironment.

3.2 Aims

1. To characterise the cytokines associated with macrophage recruitment secreted by tumour cells in response to ionising radiation.
2. To determine whether macrophages are increased in tumours following radiation.
3. To characterise the functional phenotype of tumour associated macrophages following irradiation.

3.3 Results

3.3.1 Radiation induces CSF-1 upregulation and increases macrophage recruitment to tumours

In order to examine the milieu of cytokines secreted by tumour cells after radiation, we analysed conditioned medium from MC38 tumour cells with and without exposure to radiation. Tumour conditioned media was collected 48 hours after irradiation, filtered and concentrated using a protein concentrating column. Protein concentrations were quantified using a Bicinchoninic assay (BCA) and equal amounts from each sample were added. Relative cytokine levels were measured using a cytokine array. This array allows for the quantification of 26 different cytokines. Importantly, analysis of the conditioned media confirms that the cytokines are present in their secreted forms. An alternative approach would be to analyse changes in mRNA expression. Whilst this more easily allows for the analysis of a large number of genes, downstream protein expression would need to be confirmed using an additional assay (ELISA). The cytokines included in the array were pre-selected to cover those involved with an inflammatory response. Therefore, whilst many are not known to be involved with macrophage recruitment, all of the key candidate cytokines were included.

Tumour cell irradiation resulted in variable changes in multiple cytokines. The highest relative increases were observed for il10, il13 and il12 (**Error! Reference source not found.**). Included within the array were cytokines known to be responsible for macrophage chemo-attraction, including GM-CSF, SDF-1, CCL2 and CSF-1. Amongst these cytokines, CSF-1 was the most highly upregulated (Figure 3.1). To confirm these findings we measured changes in gene expression at various time points following 10Gy irradiation of tumour cells in vitro. To account for early gene induction, we measured changes in gene expression at 2,4,6 and 8 hours (Figure 3.1 B). There was a trend towards increased gene expression at 8 hours in MC38 and 6 hours in KPC cells, however no statistically significant changes were detected. We therefore examined gene expression at later time points. In MC38 cells, CSF-1 was significantly upregulated at 24 hours following radiation and declined thereafter. Induction of CSF-1 in KPC cells appeared later, at 48 hours, and remained elevated at 72 hours (Figure 3.1 C). We next sought to confirm if the changes in gene expression resulted in increased protein expression. To do this we collected conditioned media from tumour cells and measured CSF-1 protein levels by ELISA. For MC38 cells, media was collected after 48 hours of culture as the peak gene expression appeared at 24 hours. In order to detect changes in KPC cells media was collected after 72 hours of culture as the peak upregulation occurred later, at 48 hours.

CSF-1 protein was detected at significantly higher levels in both cells lines after irradiation, though absolute levels were lower in KPC (Figure 3.1 D). These data confirm that tumour cells responded to ionising radiation by upregulation of CSF-1 gene expression and subsequent secretion. These changes took place at 24 hours or beyond, with variable responses between tumour cell lines. In order for CSF-1 to mobilise and recruit monocytes from the bone marrow, it has to be present in the serum. To determine whether there were systemic increases in CSF-1 following tumour irradiation, we measured CSF-1 levels in the sera of tumour bearing mice by ELISA. Interestingly, mice bearing unirradiated KPC tumours contained higher levels of CSF-1 in the serum compared with mice bearing MC38 tumours (Figure 3.1 E). However after 10Gy tumour irradiation there was a significant increase in CSF-1 in the sera of MC38 tumour bearing mice on day 3, which normalised by day 10. In KPC tumour bearing mice CSF was elevated on day 3 but maximally elevated on day 7 (Figure 3.1, E).

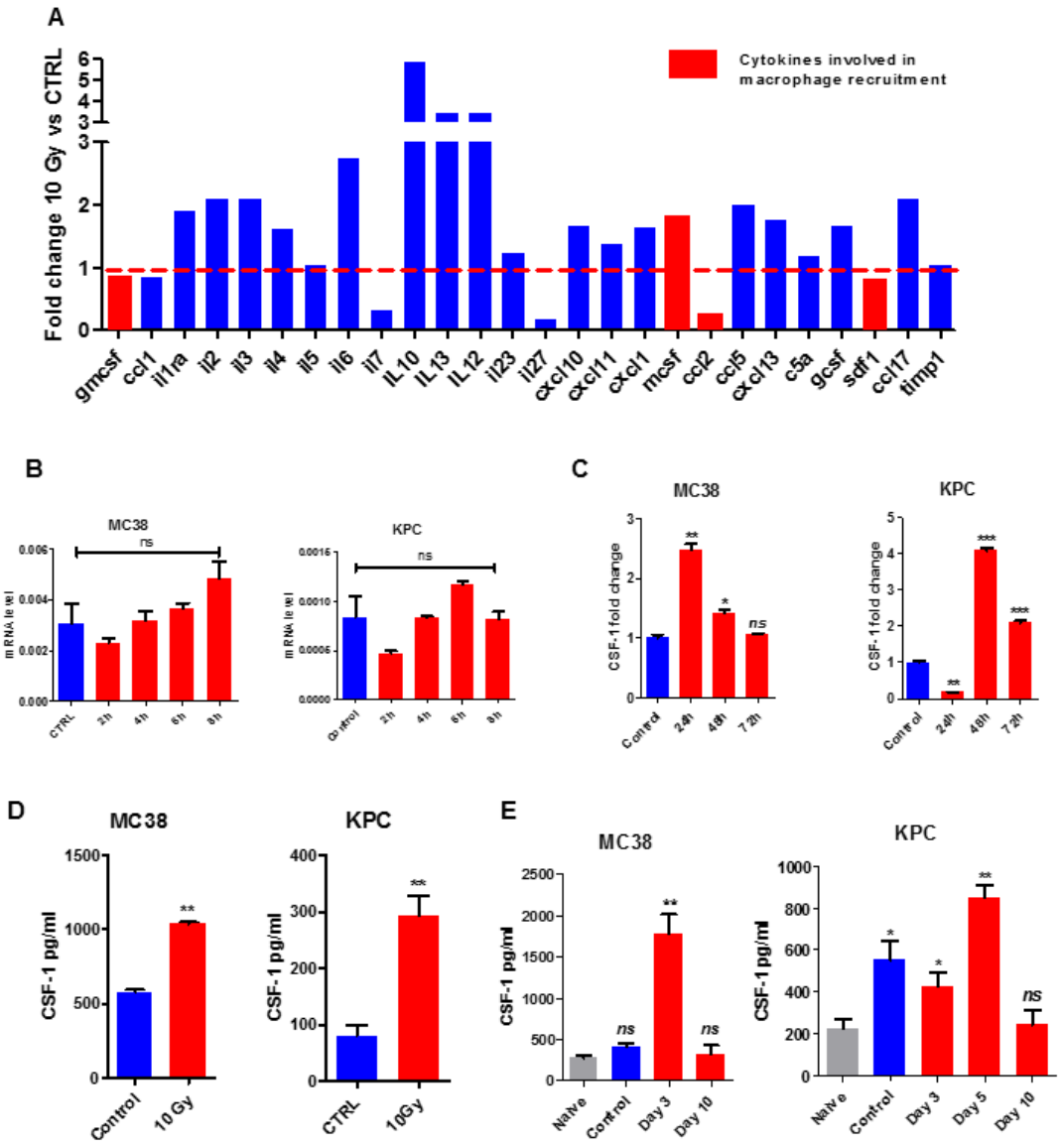


Figure 3.1 Colony stimulating factor (CSF-1) is increased in response to irradiation.

A To determine how irradiation alters cytokines produced by tumours cells, conditioned medium was analysed by protein array. Briefly, MC38 cells in tissue culture were treated with mock (0Gy) and 10Gy irradiation. Conditioned medium (CM) was collected after 48 hours and assayed for the indicated cytokines. Fold-changes in the amounts of the cytokines are shown. Cytokines involved in macrophage recruitment are indicated in red.

B CSF-1 mRNA expression was measured in MC38 and KPC cells exposed to 10Gy IR compared with mock irradiated cells. Cells were harvested at 24, 48 and 72 hours after irradiation and RNA expression was analysed by RT-qPCR. Data are presented as mean ± SEM and analysed by Kruskal-Wallis test with Dunn's multiple comparison (n=3).

C CSF-1 mRNA expression in tumour cells at various time points after 10Gy irradiation analysed by RT-qPCR**.** Data are presented as mean ± SEM and analysed by Kruskal-Wallis test with Dunn's multiple comparison (n=3).

D CSF-1 protein (pg/mg total protein) in CM collected from MC38 and KPC cells 48 hours after exposure to 10Gy IR compared to mock-irradiated cells. Data are presented as mean ± SEM and analysed by Mann-Witney (n=3)

E CSF-1 protein (pg/mg total protein) measured by ELISA in the sera of naïve mice, mice bearing mock-irradiated tumours, and mice bearing irradiated tumours analysed at time points as indicated (n=4/group). Data are presented as mean ±

3.3.2 Radiation increases macrophage numbers in murine subcutaneous xenografts.

We next examined whether the changes in CSF-1 expression were associated with altered macrophage numbers in tumours after radiation. To do this we analysed immune cell populations in subcutaneous MC38 and KPC tumours by flow cytometry. Following pre-gating to identify live cell populations, macrophages were identified by their co-expression of CD11b and F480 (CD11b+ F480+). In order to appreciate the temporal changes in macrophage numbers we performed a time course experiment. MC38 tumours were relatively radiosensitive compared with KPC tumours, and tumour growth delay extended to between 20 to 30 days after radiation. Therefore we analysed tumours on days 1,3,5,10,14 and 21. KPC tumours were more radio resistant and end-point was delayed by 5-7 days following 10Gy radiation. Large numbers of mice were required to generate tumours of comparable sizes, harvested and analysed on the same day in order to limit variation between flow cytometric analyses. In addition, data from the MC38 time course experiment gave us an impression of the kinetics of the immune response, therefore in order to avoid using excessively high numbers animal, we limited our time points to days 5,7,10 and 14. All mice were injected on the same day, irradiation applied when tumours reached a volume of 100mm^3 (+/-10mm^3). Flow cytometric analyses was subsequently performed at the indicated time points. In MC38 tumours, there was a period of tumour volume stasis after radiation, lasting approximately ten days. After 10-14 days, tumour growth recurred and reached end-point (500mm3) by day 21. There was a significant increase in macrophages 24 hours following irradiation, which continued until a peak at day 5 (Figure 3.2 A). Interestingly, macrophage numbers began to decline beyond day 5, coinciding with tumour regrowth. However relative numbers still remained significantly higher than control tumours. On day 5, the point of maximal increase, there was a nearly two-fold increase in the number of macrophages present within tumours (9.14 vs 5.23 p=<0.05) (Figure 3.2 B). In KPC tumours, whilst there was a delay in tumour growth, there was no discernible period of growth stasis. Nonetheless, as was observed in MC38 tumours, macrophages were significantly increased on day five following radiation (22.50 vs 12.32 p=<0.05). The increase in macrophage numbers was transient, returning to baselines levels by 1 week following irradiation (Figure 3.2 D,E). To confirm our findings of increased macrophage numbers we performed immunofluorescent staining of subcutaneous tumour sections

harvested 5 days following irradiation (Figure 3.2 C,F). Significantly greater numbers of macrophages were observed in irradiated tumours compared with control tumours.

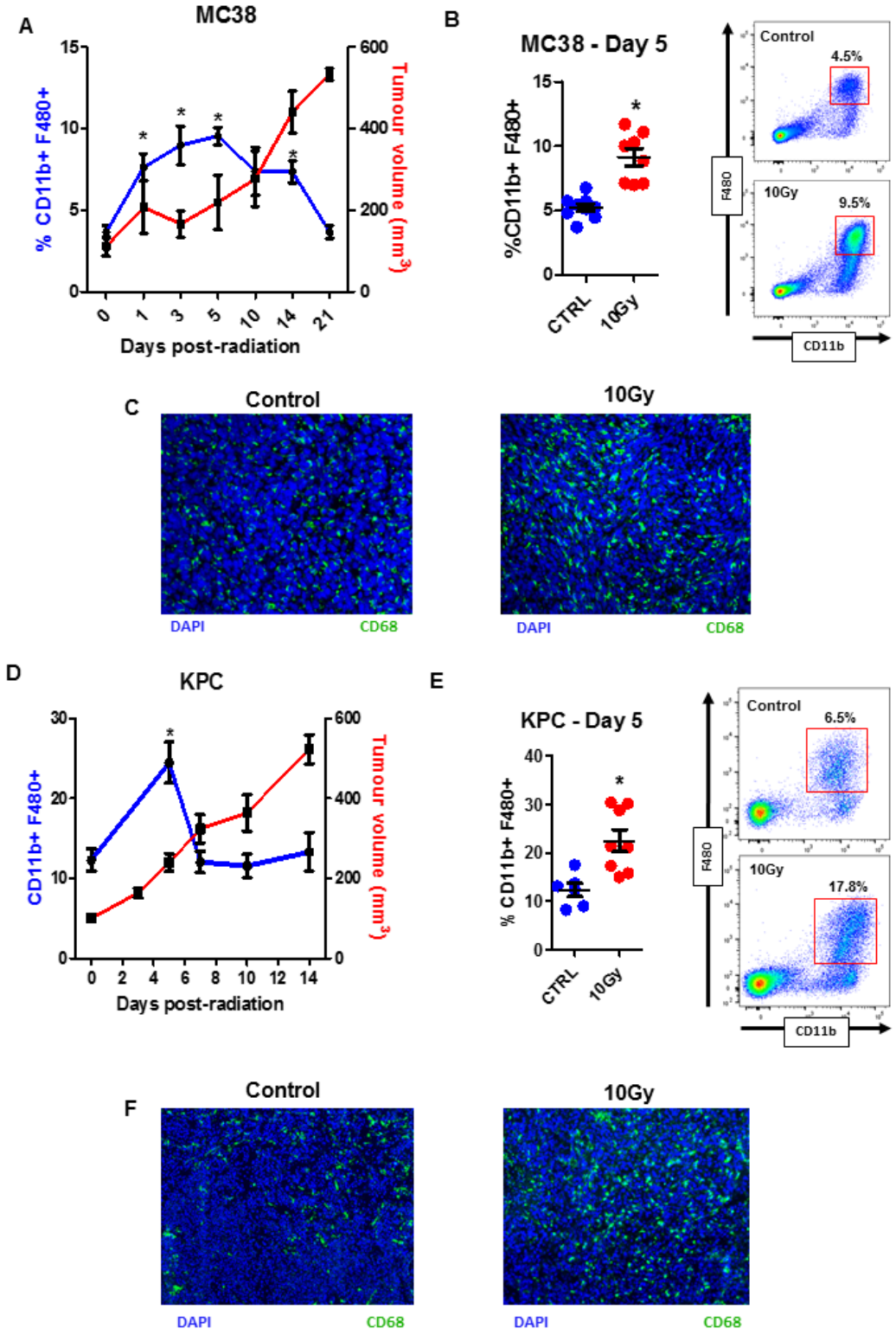


Figure 3.2 – Macrophages are increased in tumours following irradiation.

A, D – MC38 (A) and KPC (D) tumours were irradiated with 10Gy. Average tumour volume (red line) is shown with mean TAM infiltrate (blue line) for each time point. For TAM quantification, tumours were disaggregated and CD11b+/F480+ TAMs identified by flow cytometry. Data are presented as mean ± SEM for TAMs and SEM for tumour volume (n=6 mice/group).
B,E – Quantification of macrophage numbers on day 5 following irradiation with representative flow cytometry plots. Data are presented as mean ± SEM and analysed by flow cytometry. For TAM quantification, tumours were disaggregated and CD11b+/F480+ TAMs identified by flow cytometry
C,F – Immunofluorescence images of subcutaneous tumour sections from MC38 (C) and KPC (F) tumours harvested 5 days following irradiation (Blue=nuclear DAPI staining, Green=CD68+ macrophages).

3.3.3 Tumour associated macrophages are polarised towards an immunosuppressive 'M2' phenotype

We next examined the phenotype of the tumour-associated macrophages present within MC38 and KPC tumours. We firstly analysed macrophages by flow cytometry. For M1 characterisation, we used the marker iNOS (inducible nitric oxide synthetase) [265]. For M2 characterisation we measured expression of the mannose receptor CD206. The gating and analysis strategy can be seen in Figure 3.3. We adopted two different approaches for the measurement of M1 and M2 markers by flow cytometry. We firstly measured the expression of iNOS and CD206 on pre-gated CD11b+F480+ macrophages. This allowed not only quantification of positive cells but also measurement of the mean fluorescence intensity (MFI). This quantifies the mean signal emitted on a cell-by-cell basis. This allowed us to measure changes in overall expression of markers. In addition, we calculated the total number of iNOS+ and CD206+ macrophages as a percentage of all of the cells analysed. These data allowed us to quantify absolute numbers of individual M1 and M2 populations as well as changes in expression between treatment groups.

Relatively few TAMs in MC38 tumours expressed iNOS and this decreased following tumour irradiation (20.25% vs 6.3% p=<0.05) (Figure 3.4, A). This corresponded with a reduction in the absolute number of iNOS+ macrophages present in tumours after radiation (1.28% vs 0.36% p=<0.05) (Figure 3.4, B). The majority of TAMs expressed the M2 marker CD206 and this was also significantly reduced following exposure to radiation (58.6% vs 36.5% p=<0.05) (Figure 3.4, C). However compared with iNOS expression, significantly more TAMs expressed CD206 in the irradiated tumours (36.5% vs 6.3%). Notably, whilst the relative expression of CD206 decreased, the substantial overall increase in TAMs in MC38 tumours meant that the absolute number of M2 TAMs actually increased (Figure 3.4, D). The overall decrease in the number of M1 TAMs, and the overall increase in the number of M2 TAMs resulted in a significantly decreased M1:M2 ratio (Figure 3.4, E).

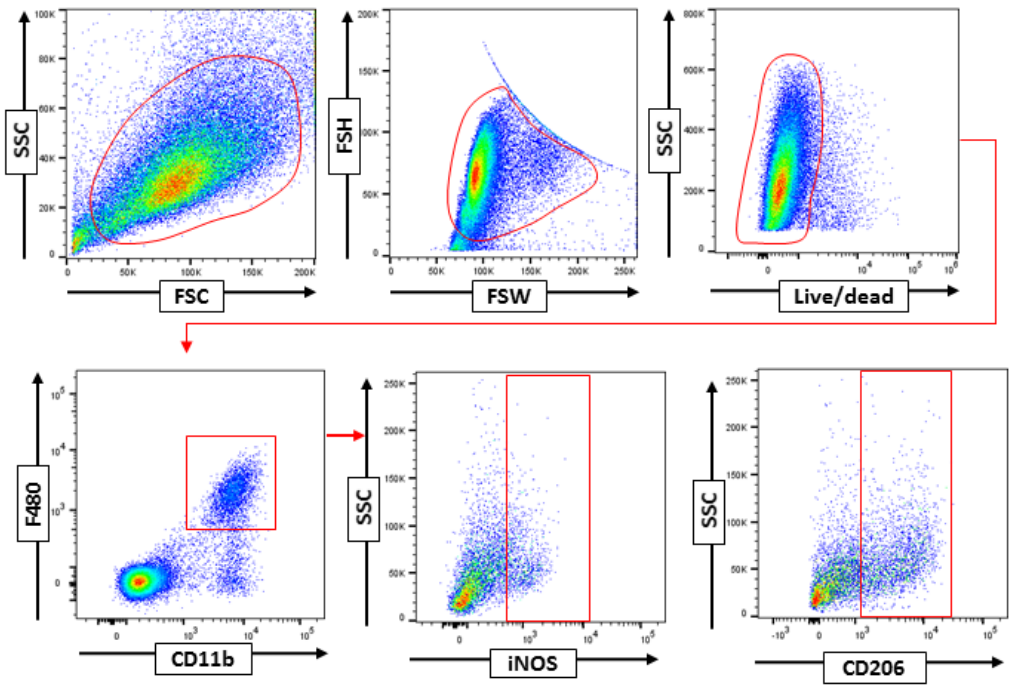
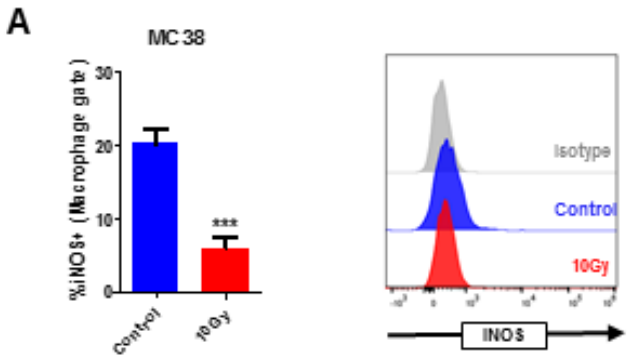
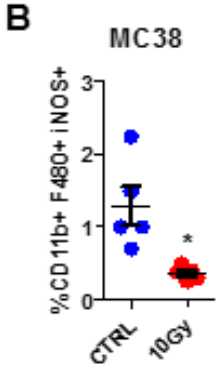


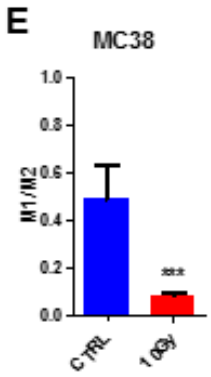
Figure 3.3 – Flow cytometric gating strategy to measure iNOS and CD206 expression on tumour associated macrophages. Debris, doublets and dead cells were first excluded, then macrophages identified by their co-expression of CD11b and F480. iNOS and CD206 expression was then measured on cells within the macrophage gate. In order to determine absolute numbers, positive cells (iNOS/CD206) were compared with the total live cells analysed.

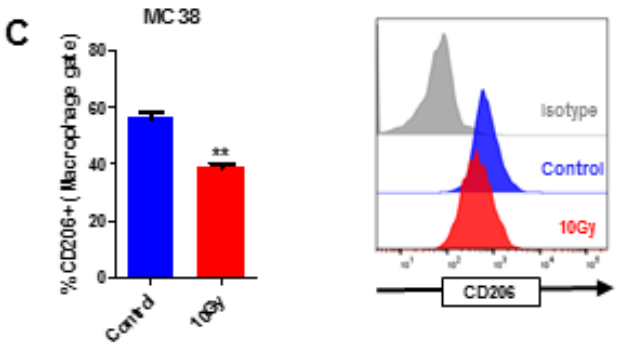
In KPC tumours there was higher baseline expression of iNOS amongst TAMs compared with MC38 tumours. In addition, in response to radiation there was an increase in iNOS expression (11.2% vs 25.5% p=<0.05) (Figure 3.4, A). Combined with the overall increase in TAM numbers, this led to a significant increase of iNOS+ TAMs in KPC tumours after radiation (2.10% vs 6.05% p=<0.05) (Figure 3.4, B). Similar to MC38 tumours, TAMs in KPC tumours expressed high levels of CD206. Interestingly, this remained unchanged after radiation (Figure 3.4, C) however due to the overall increase in TAMs there were again far more CD206+ present in tumours after radiation

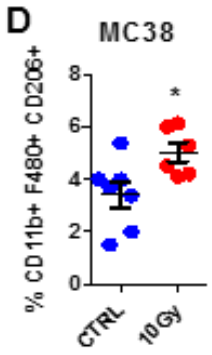
MC38


A
MC38
%iNOS+ (Macrophage gate)
***
Control
10Gy
Isotype
Control
10Gy
INOS

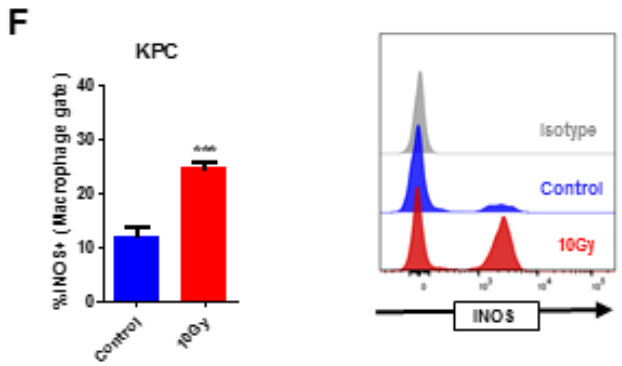

B
MC38
%CD11b+ F480+ iNOS+
*
CTRL
10Gy

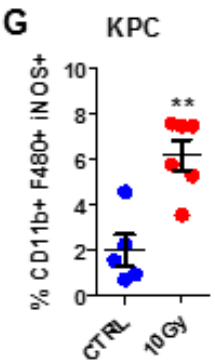

E
MC38
M1/M2
***
CTRL
10Gy

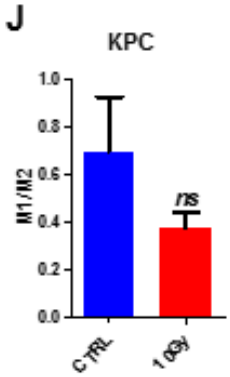

C
MC38
%CD206+ (Macrophage gate)
**
Control
10Gy
Isotype
Control
10Gy
CD206

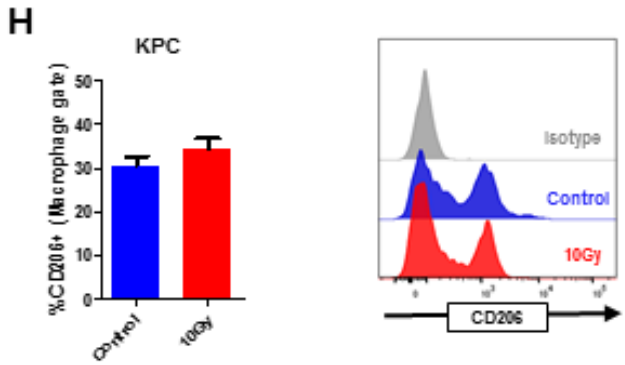

D
MC38
% CD11b+ F480+ CD206+
*
CTRL
10Gy

KPC


F
KPC
%iNOS+ (Macrophage gate)
***
Control
10Gy
Isotype
Control
10Gy
INOS


G
KPC
% CD11b+ F480+ iNOS+
**
CTRL
10Gy


J
KPC
M1/M2
ns
CTRL
10Gy


H
KPC
%CD206+ (Macrophage gate)
Control
10Gy
Isotype
Control
10Gy
CD206

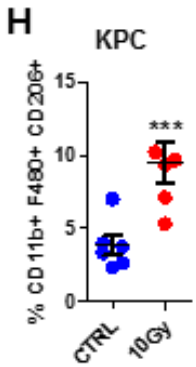

H
KPC
% CD11b+ F480+ CD206+
***
CTRL
10Gy

Figure 3.4 Macrophages in MC38 and KPC subcutaneous tumours are polarised towards an immunosuppressive phenotype.

A – M1 polarisation was determined by iNOS expression. iNOS expression on TAMs contained in MC38 tumours (CD11b+ F480+) was analysed by flow cytometry. Representative histogram plots also shown (right panel)*.
B – Percentage of CD11b+F480+iNOS^{hi} macrophages contained in MC38 tumours measured by flow cytometry*.
C – M2 polarisation was determined by CD206 expression. CD206 expression on TAMs contained in MC38 tumours (CD11b+ F480+) was analysed by flow cytometry. Representative histogram plots also shown (right panel)*.
D – Percentage of CD11b+F480+CD206^{hi} macrophages contained in MC38 tumours measured by flow cytometry*.
E – Ratio of M1 (iNOS+) to M2 (CD206+) macrophages in MC38 tumour with and without radiation*.
F – M1 polarisation was determined by iNOS expression. iNOS expression on TAMs contained in KPC tumours (CD11b+ F480+) was analysed by flow cytometry. Representative histogram plots also shown (right panel)*.
G – Percentage of CD11b+F480+iNOS^{hi} macrophages contained in KPC tumours measured by flow cytometry*.
H – M2 polarisation was determined by CD206 expression. CD206 expression on TAMs contained in KPC tumours (CD11b+ F480+) was analysed by flow cytometry. Representative histogram plots also shown (right panel)*.
I – Percentage of CD11b+F480+CD206^{hi} macrophages contained in KPC tumours measured by flow cytometry*.
E – Ratio of M1 (iNOS+) to M2 (CD206+) macrophages in KPC tumour with and without radiation*.

*Data are presented as mean ± SEM and statistical significance determined by unpaired t-test.

3.3.4 Gene expression in isolated TAMs demonstrates a variable response to radiation, skewed towards an immunosuppressive phenotype.

In order to further characterise TAM phenotype, we isolated macrophages (F480+CD11b+) by FACS from tumours 5 days following radiation. RNA was extracted and gene expression analysed by qPCR. TAMs from MC38 tumours showed significantly increased expression of iNOS, whilst other inflammatory genes remained unchanged (Figure 3.5, A). Compared with most of the inflammatory genes analysed, there were higher baseline levels of some genes associated with immune suppression (Arg1, ccl2, Figure 3.5, A). TAMs from irradiated tumours showed significantly higher expression of Arginase and Ym1, both markers of immune suppression.

TAMs isolated from KPC tumours showed a different gene expression pattern. Of the inflammatory genes analysed, il1b and il1a were both significantly increased in the irradiated group (Figure 3.5, B). The expression of immunosuppressive genes was also variable. There was significant upregulation of Arginase and il10, and a reduction in ccl2 (Figure 3.5, B).

Together, these data indicate that TAMs present in irradiated tumours have altered expression of genes involved in immune regulation. In both MC38 and KPC tumours there was a variable pattern, though a general trend towards immune an immune suppressive phenotype was observed. These data indicate that macrophage phenotype is highly variable, even within populations that appear to be highly polarised based upon flow cytometry analysis.

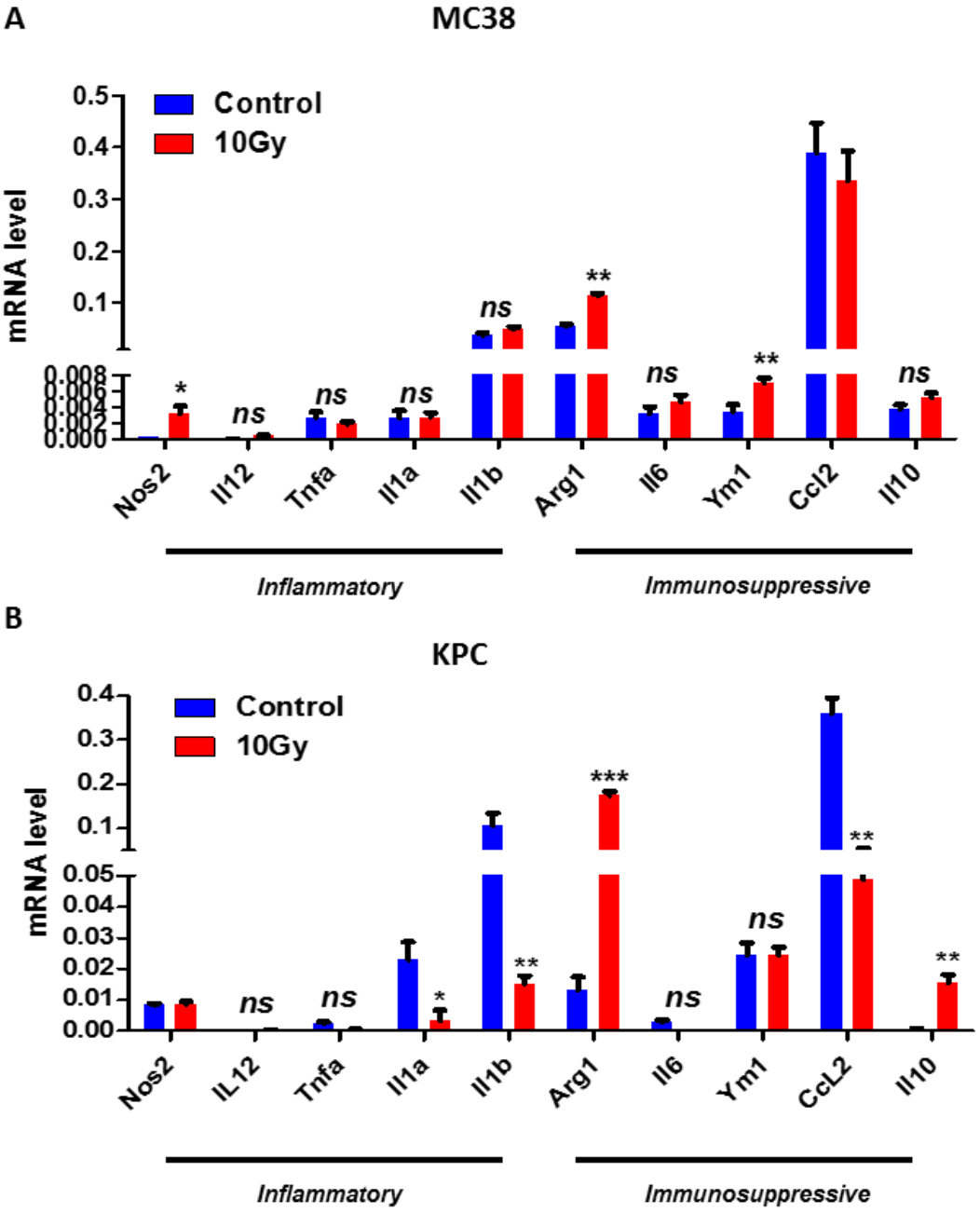


Figure 3.5 - Gene expression in isolated TAMs demonstrate a variable response to radiation, skewed towards an immunosuppressive phenotype.

A,B - Tumours were collected 5 days following 10Gy irradiation from MC38 (A) and KPC (B) tumours and pooled (5 mice/group). Macrophages were isolated by FACS (CD11b+ F480+) and RNA extracted from cell pellets. A selection of typical immune stimulatory and suppressive genes were analysed by qPCR. Data are shown as mean ± SEM and statistical significance determined by unpaired t-test.

3.3.5 TAMs from irradiated tumours suppress CD8 T cell proliferation.

Thus far the characterisation of TAMs suggests they are skewed towards an immunosuppressive phenotype. A hallmark feature of immunosuppressive myeloid cells, particularly M2 TAMs, is their capacity to inhibit T cell proliferation[266]. We used a CFSE based T cell suppression assay to study the effects of TAMs on T cell proliferation. This assay is based upon the principle that the signal emitted from an intravital dye (CFSE), halves with every cell division. Therefore, undivided cells emit fluorescent signal at the highest intensity. With each cell division, this intensity halves, allowing for an estimation of the number of divisions over time. TAMs isolated from MC38 and KPC tumours with and without radiation were cultured with naïve C57/BL6 CD8+ splenic T cells. The medium used in this assay is supplemented with recombinant IL-2 to drive T cell proliferation. TAMs isolated from MC38 tumours significantly suppressed T cell proliferation irrespective of whether the tumour was irradiated (Figure 3.6, A). Interestingly, TAMs isolated from irradiated tumours were less suppressive than those from unirradiated tumours. TAMs isolated from unirradiated KPC tumours did not significantly suppress T cell proliferation whilst those from irradiated tumours were suppressive (Figure 3.6, B). These results suggest that macrophages are more T cell suppressive following tumour irradiation. Importantly, whilst providing further evidence that irradiation promotes an immunosuppressive TAM phenotype, T cell suppression is not a proxy marker for activation. However, it has been proposed that the likely mechanisms contributing to the suppression of proliferation are likely to overlap with activation. These include stimulation of the co-inhibitory pathways due to the expression of molecules such as PD-L1 on the surface of TAMs. Also, the TAMs and T cells are cultured in a 1:1 ratio. This is the ratio typically used to identify differences between experimental groups, and we found that higher TAM numbers led to excessive suppression in all groups. Importantly, these ratios do not reflect the changes is cell numbers observed in the tumours. For example, after irradiation the significantly increased number of TAMs may compound the switch to a suppressive phenotype observed at the individual cell level.

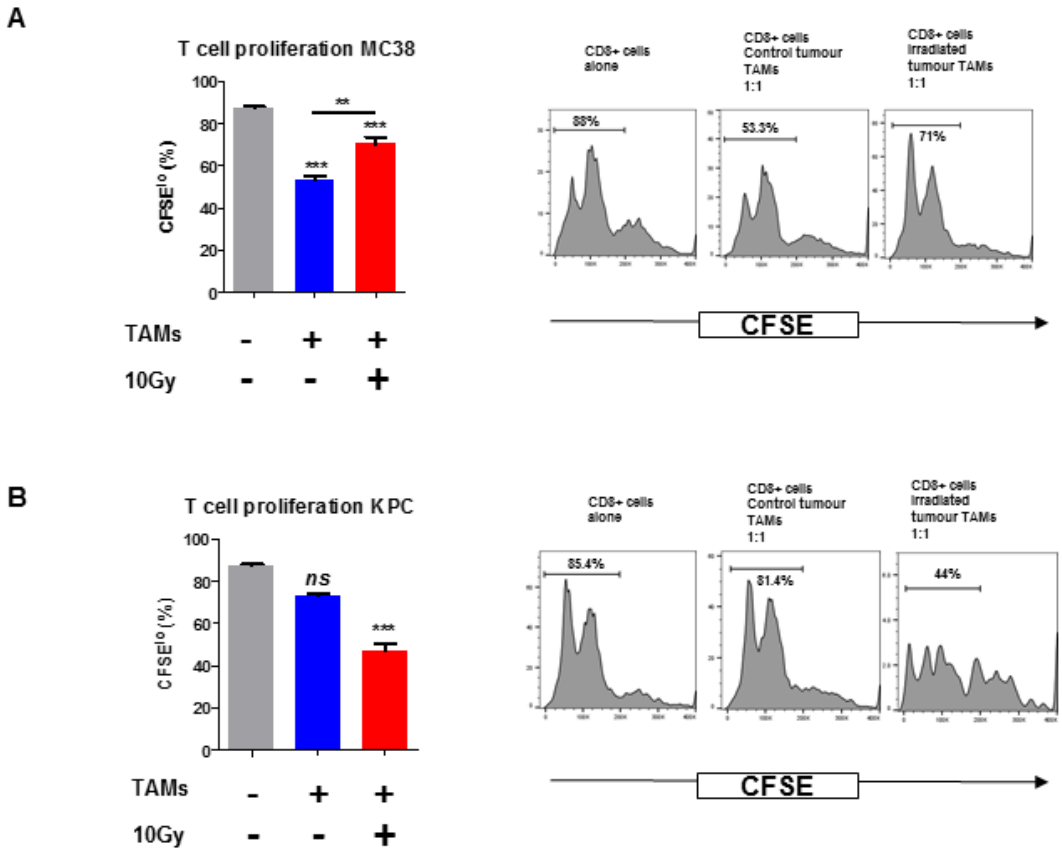


Figure 3.6 -TAMs from irradiated tumours are capable of supressing CD8 T cell proliferation.

A, B - Naïve CD8+ splenic T cells were isolated from C57/BL6 mice by magnetic bead separation and labelled with CFSE. Culture plates were pre-coated with anti-CD3/CD28 and medium supplemented with recombinant IL-2 in order to stimulate proliferation. TAMs were isolated from MC38 (A) and KPC (B) tumours by magnetic bead separation and added to the wells containing T cells in a 1:1 ratio. TAMs from 3 control tumours and 3 irradiated tumours were harvested. CD8 T cells and TAMs were cultured for 55 hours before being analysed by flow cytometry. CD8 T cells were gated (CD45+CD3+CD8+) and their CFSE fluorescence measured. Data are presented as mean ±SEM and analysed by one-way ANOVA.

3.3.6 Tumour cell conditioning can polarise macrophages towards an immunosuppressive phenotype.

The data thus far confirm that TAMs show variable and significant alterations in their phenotype after radiation. We hypothesised that these changes may be caused by changes in cytokines secreted by tumour cells. Previous reports demonstrate that the tumour cell secretome plays an important role in shaping the phenotype of TAMs [267–270]. We utilised a transwell co-culture technique whereby tumour cells could be cultured in synthetic inserts adjacent to macrophages in cell culture plates. This allowed for passive diffusion of secreted proteins but no cell-to-cell contact. Naïve BMDMs had almost no iNOS expression and little (10%) CD206 expression (Figure 3.7, A). After 72 hours exposure to tumour cells both iNOS and CD206 expression were significantly increased (8.5% and 34.5% respectively). Co-culture with irradiated tumour cells was associated with almost complete diminution of iNOS expression (0.1%) and slightly reduced CD206 expression (26.1%) (Figure 3.7, A). Interestingly, whilst these results cannot be directly compared with TAM analysis, the expression pattern resembles macrophages in MC38 tumours with and without radiation (Figure 3.4, A,C). Following co-culture with KPC cells, there was no increase in iNOS expression but a significant increase in CD206 expression, which remained unchanged following exposure to irradiated cells (Figure 3.7, B). Gene expression analysis of the same genes involved in inflammation and immune suppression were also analysed. After 72 hours of co-culture with either naïve or irradiated (10Gy) tumour cells via a transwell assay, RNA was isolated and qPCR performed. Co-culture of naïve BMDMs with naïve and irradiated tumour cells significantly altered gene expression in both MC38 and KPC (Figure 3.8). In BMDMs co-cultured with MC38 cells, there was a reduction in the expression of some pro-inflammatory markers, including iNOS, il12 and il1b, and an increase in TNFα and il1a. Changes in expression of immunosuppressive markers was also variable, with a substantial increase in arginase expression, increased il10 expression and decreased Ym1, Ym2 and CCL2. Following co-culture with irradiated MC38 cells, iNOS was further decreased, along with TNFα and il1a, however there was an increase in il12 and il1b. There was a general trend of increased expression across most immunosuppressive markers. These results suggest that macrophages are activated following co-culture with tumour cells, and irradiated tumour cells stimulate a more immunosuppressive phenotype. Co-culture with naïve KPC cells resulted in variable changes in pro-inflammatory gene expression, with increased iNOS, decreased il12, unaltered TNFα and substantial increases in il1a and il1b. Co-culture with irradiated KPC cells was associated with a reduced in iNOS expression, a

reduction in il12 comparable to control cells, and substantial increases in il1a and il1b, again comparable to control cells. Changes in genes associated with immunosuppression largely mirrored those observed with control tumour cell co-culture, aside from a reduction in il10. The variability in gene expression seen in KPC co-cultures is similar to that observed in the CM38 co-cultures. However the difference in gene

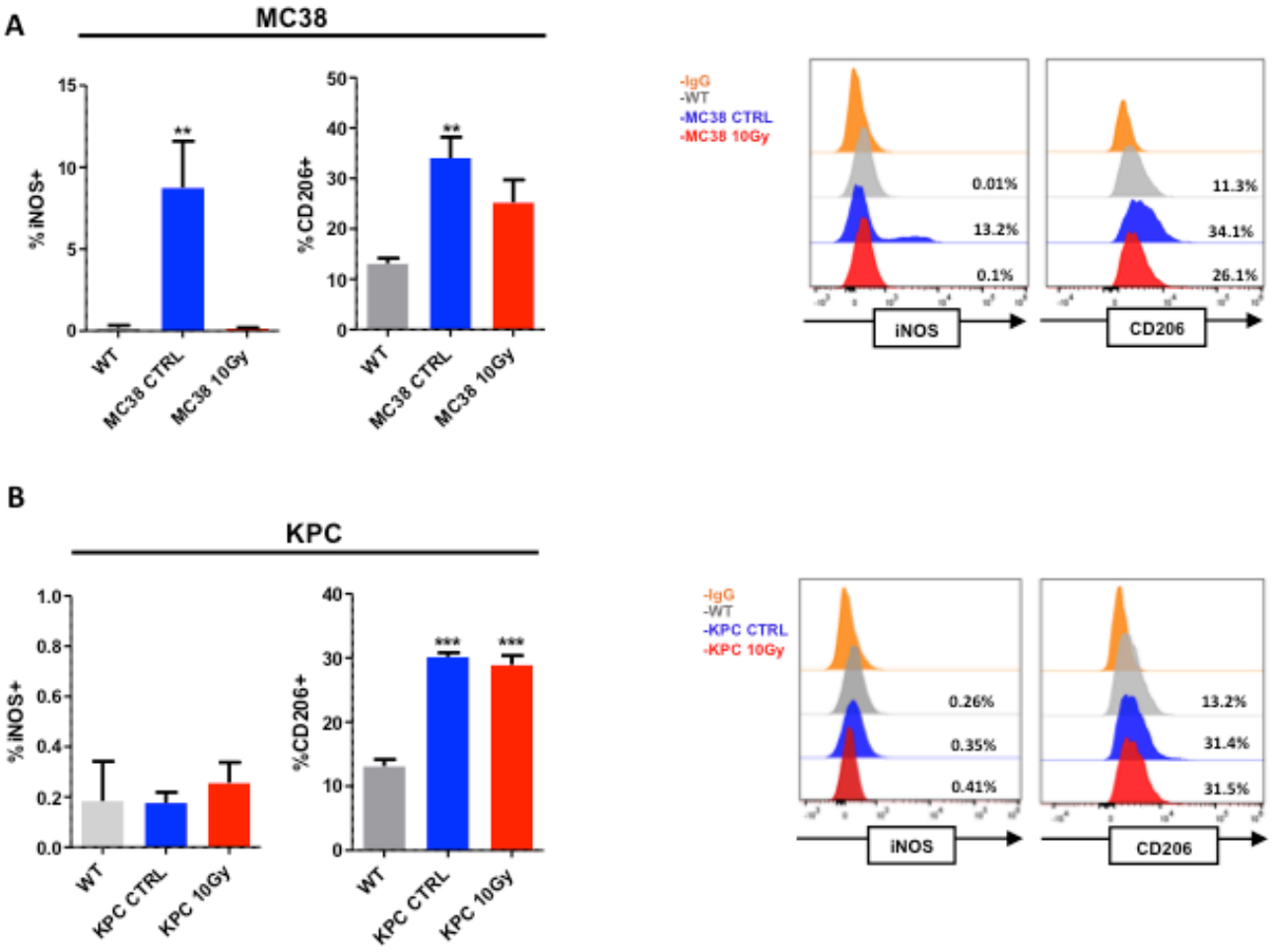


Figure 3.7 – Tumour cells polarise bone marrow-derived macrophages (BMDMs).

A,B - Bone marrow monocytes were differentiated into macrophages by culturing for 5 days in the presence of L929 (fibroblast) conditioned media. L929 is a murine fibroblast cell line that produces CSF-1 and is commonly used for BMDM culture. For co-culture experiments, MC38 (A) and KPC (B) tumour cells were added to Millicell® 0.4µm cell culture inserts (0.5-1.0x10^6/well) and added to wells containing BMDMs. For radiation groups, tumour cells were irradiated immediately prior to transfer. BMDMs and tumour cells were co-cultured for 72 hours prior to analysis. Only macrophages were analysed by removing the cell culture inserts containing tumour cells prior to BMDM harvest and staining. WT refers to BMDMs without tumour cell conditioning, MC38 CTRL refers to BMDMs exposed to naïve MC38 cells, and MC38 10Gy refers to BMDMs exposed to irradiated MC38 cells. This nomenclature also applies to the KPC experiments presented in B. Data are presented as mean ± SEM and analysed by one-way ANOVA. Representative histogram plots are also shown (right panels).

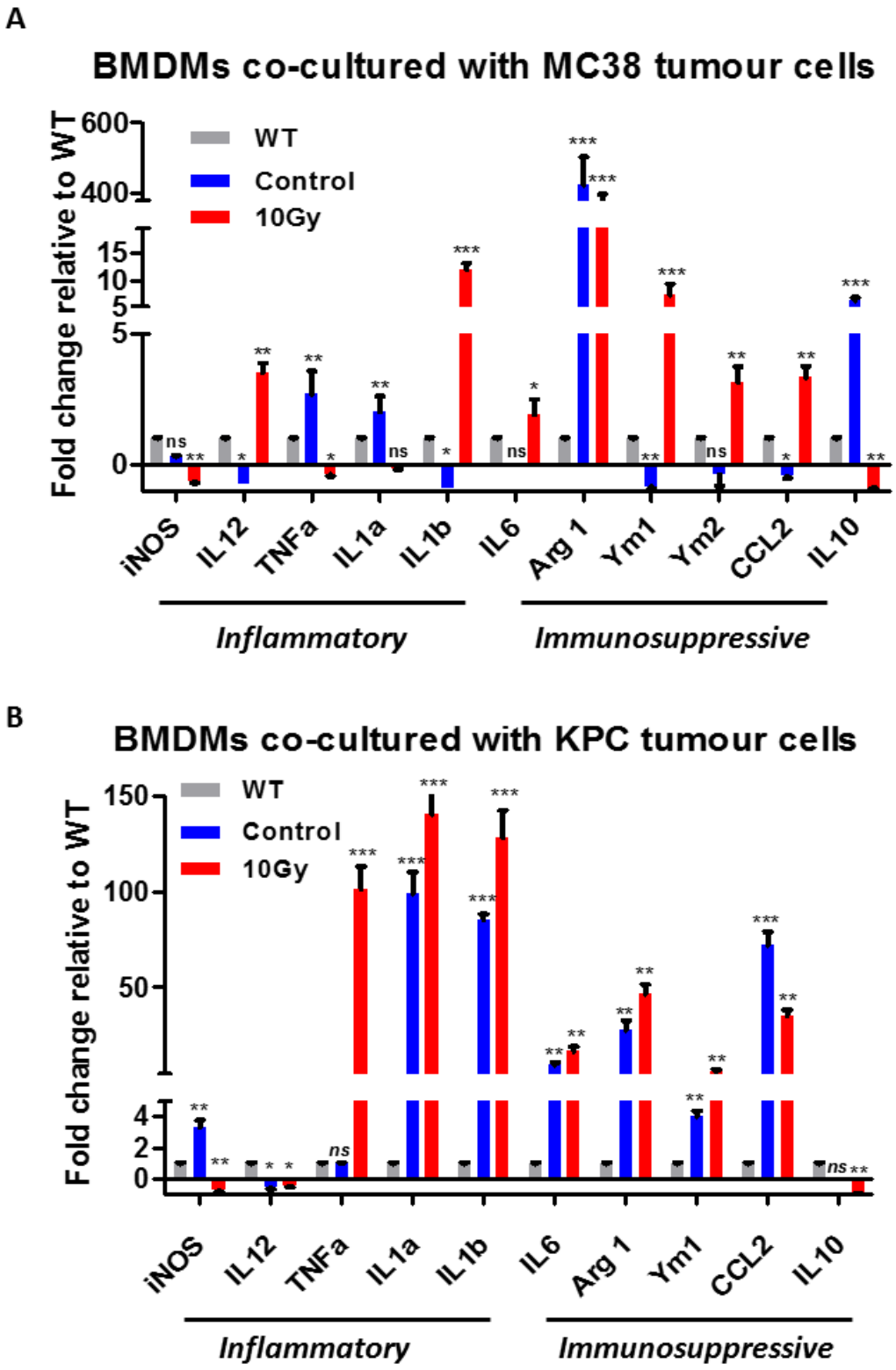


Figure 3.8 – Co-culture with tumour cells significantly alters gene expression in bone marrow-derived macrophages (BMDMs).

A, B - Gene expression analysis of RNA extracted from BMDMs co-cultured with MC38 (A) and KPC (B) tumour cells (+/-10Gy irradiation). BMDMs were generated from bone marrow harvested from wild-type C57/BL6 mice and cultured in media supplemented with L929 conditioned medium for 5 days. Tumour cells were cultured in Millicell® 0.4µm cell culture inserts (0.5-1.0x10^6/well). Irradiation was applied immediately before transfer of inserts. Cells were co-cultured for 72 hours then RNA extracted using TRIzol and RT-qPCR performed. Fold changes in gene expression in experimental samples are compared with naïve BMDMs. Data are presented as mean fold change. Data are shown

as mean ± SEM and statistical significance determined by unpaired t-test. Experiments were performed with biological and technical triplicates.

3.3.7 Tumour conditioned macrophages suppress T cell proliferation

Based upon the flow cytometric and gene expression analyses, co-culture of BMDMs with irradiated tumour cells appeared to induce an immune suppressive phenotype. Flow cytometric and mRNA analysis showed that macrophages were polarised to an immunosuppressive phenotype, similar to the pattern observed in TAMs. Therefore, we next tested the capacity of tumour cell conditioned macrophages to supress T cell proliferation. Naïve BMDMs and BMDMs co-cultured with either naïve or irradiated MC38 and KPC cells were co-cultured with CFSE labelled naïve splenic CD8 T cells. Naïve BMDMs did not alter T cell suppression (Figure 3.9, A). BMDMs co-cultured with naïve MC38 tumour cells did not significantly suppress T cell proliferation, however those cultured with irradiated tumour cells significantly suppressed proliferation. BMDMs co-cultured with both naïve and irradiated KPC tumour cells substantially suppressed CD8 T cell proliferation (Figure 3.9, B). In line with the phenotypic characterisation, these data confirm that irradiated tumour cells condition BMDMs towards an immunosuppressive phenotype capable of suppressing CD8 T cell proliferation. Interestingly, the gene expression profiles indicated that the difference between control and irradiated conditioned BMDMs was greater for the KPC group than the MC38 group (Figure 3.8, A,B). These findings are consistent with the T cell proliferation data, where suppression levels were similar in both the naïve and irradiated KPC conditioned BMDMs (Figure 3.9, B). In addition, these results suggest tumour cells are at least partly responsible for the immunosuppressive macrophage phenotype observed in these experiments.

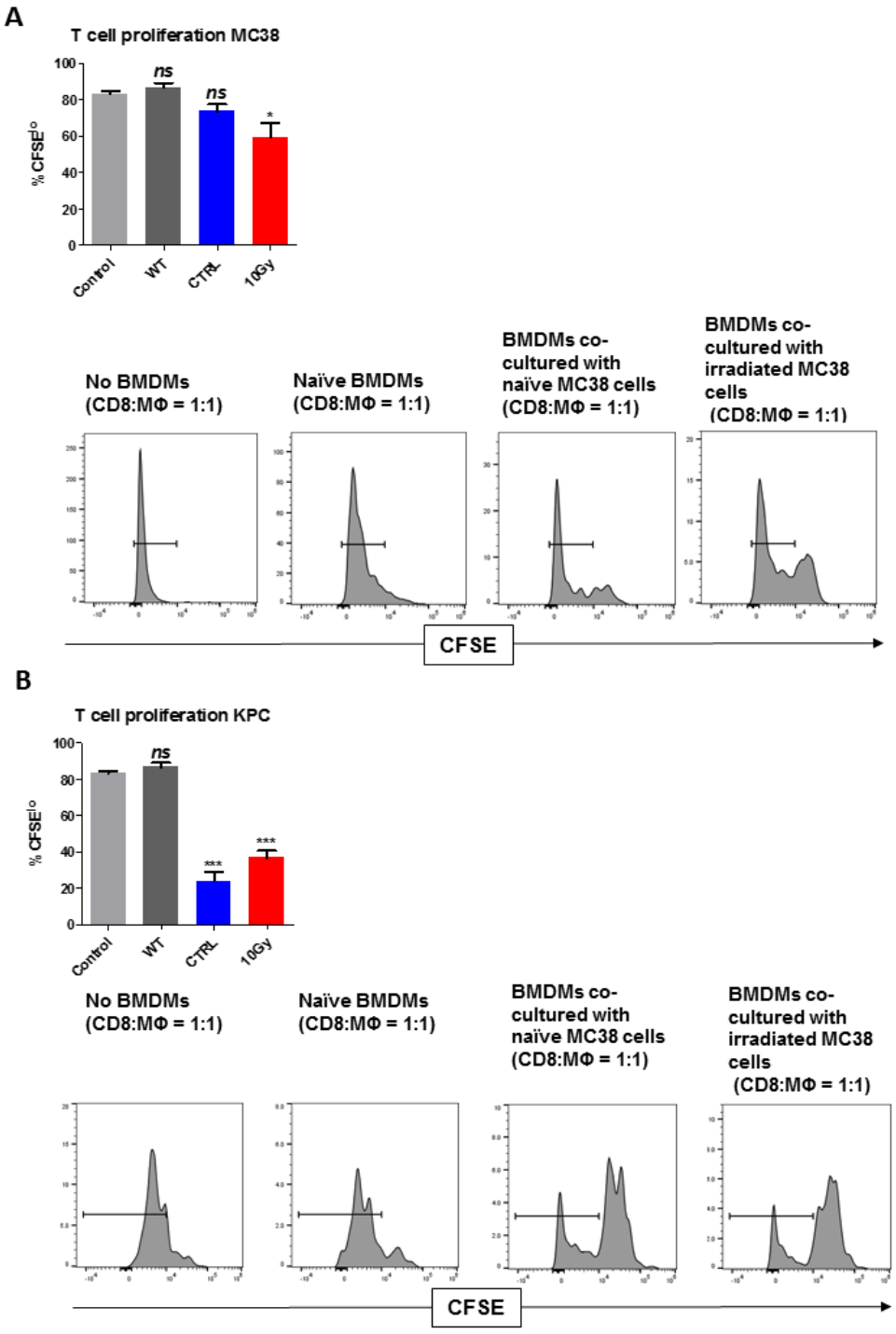


Figure 3.9 – BMDMs co-cultured with tumour cells supress CD8 T cell proliferation

A,B - BMDMs were generated from bone marrow harvested from wild-type C57/BL6 mice and cultured in media supplemented with L929 conditioned medium for 5 days. Tumour cells were cultured in Millicell® 0.4µm cell culture inserts (0.5-1.0x10^6/well). Irradiation was applied immediately before transfer of inserts. Cells were co-cultured for 72 hours and then harvested and seeded into wells (96-well plate) with CFSE labelled splenic naïve CD8+ T cells from wild-type C57/BL6 mice. After 55 hours cells were harvested and CFSE expression quantified on CD45+CD8+ cells by flow cytometry. Biological and technical triplicates were analysed. Experimental groups were compared to the control group (no BMDMs), data presented as mean ± SEM and statistical significance determined by one-way ANOVA with post-hoc adjustment.

3.3.8 Adoptive transfer of tumour-conditioned macrophages promotes tumour growth

Naïve macrophages co-cultured with tumour cells demonstrated polarisation towards an M2, pro-tumourigenic phenotype. Therefore we questioned whether these macrophages are capable of promoting tumour growth. To do this, pre-conditioned macrophages were co-injected with MC38 tumour cells to generate subcutaneous xenografts. Co-injection of tumour cells with naïve BMDMs did not alter the growth rate of tumours. However co-injection of tumour cells with BMDMs co-cultured with control and irradiated (10Gy) BMDMs significantly increased the growth rate (Figure 3.10, A). To determine if BMDMs from the initial inoculation with tumour cells were present in established tumours, they were tracked with CFSE labelling (Figure 3.10, B). When tumours were 100mm^3, 15% of the total macrophages were CFSE positive (Figure 3.10, B). These data indicate that adoptively transferred BMDMs are retained within tumours, and may promote tumour growth.

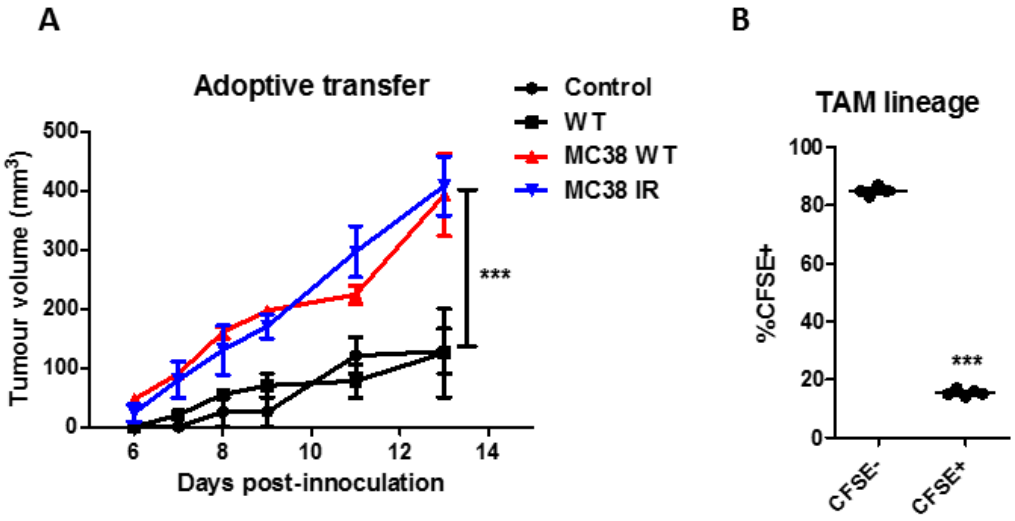


Figure 3.10 – *Adoptive transfer of tumour-conditioned macrophages promotes tumour growth.*

A - BMDMs from wild-type C57/BL6 mice were generated from bone marrow –derived monocytes cultured in media supplemented with L929 conditioned media for 5 days. MC38 tumour cells were cultured in Millicell® 0.4µm cell culture inserts (0.5-1.0x10^6/well). Irradiation was applied immediately before transfer of inserts. Macrophages and MC38 cells were subsequently co-cultured for 72 hours, then harvested and injected subcutaneously with MC38 tumour cells in a 1:1 ratio.

B – Prior to injection, wild-type BMDMs were labelled with CFSE. When tumours were harvested (100mm^3), the numbers of CFSE+ macrophages were quantified by flow cytometry. Statistical significance was determined by paired t test.

3.3.9 Changes in other immune cell populations

In addition to alterations in macrophage numbers, radiation has also been associated with changes in other leukocyte and lymphocyte populations [271]. Therefore we used flow cytometry to quantify changes in additional immune cell populations, including neutrophils, granulocytic myeloid derived suppressor cells (gMDSCs), monocytic myeloid derived suppressor cells (mMDSCs), CD4 and CD8 T cells. To appreciate the immune landscape at the point of maximal macrophage infiltration, we analysed tumours on day 5. In MC38 tumours, all myeloid populations were significantly elevated after 10Gy radiation, including neutrophils (Figure 3.11, A), and MDSCs (granulocytic and monocytic populations Figure 3.11, B,C). Interestingly, the granulocytic ($Ly6G^{hi}$) population of MDSCs comprised a small minority of the total MDSC infiltrate, compared with mMDSCs ($Ly6C^{hi}$ Figure 3.11,C) In addition, both CD4 and CD8 T cells were significantly elevated, although the total number is comparatively smaller than the myeloid cell populations.

In KPC tumours, there was also a significant increase in myeloid cells, including neutrophils and MDSCs (Figure 3.11, A-C). There was a reduction in mMDSCs however these comprised a minority of the MDSC subset (Figure 3.11, C). There were relatively few CD4 T lymphocytes and these increased following radiation (Figure 3.11, D). There were very few CD8 T lymphocytes and these remained unchanged following radiation (Figure 3.11, E). These data demonstrate that 5 days following tumour irradiation there are significant alterations in the number of immune cells. The immune infiltrate is predominantly comprised of myeloid cells. There are also significant differences between MC38 and KPC tumours, particularly in terms of the total myeloid cell infiltrate which is significantly higher in KPC tumours, as well as CD8 T cell numbers, which are very low in KPC tumours.

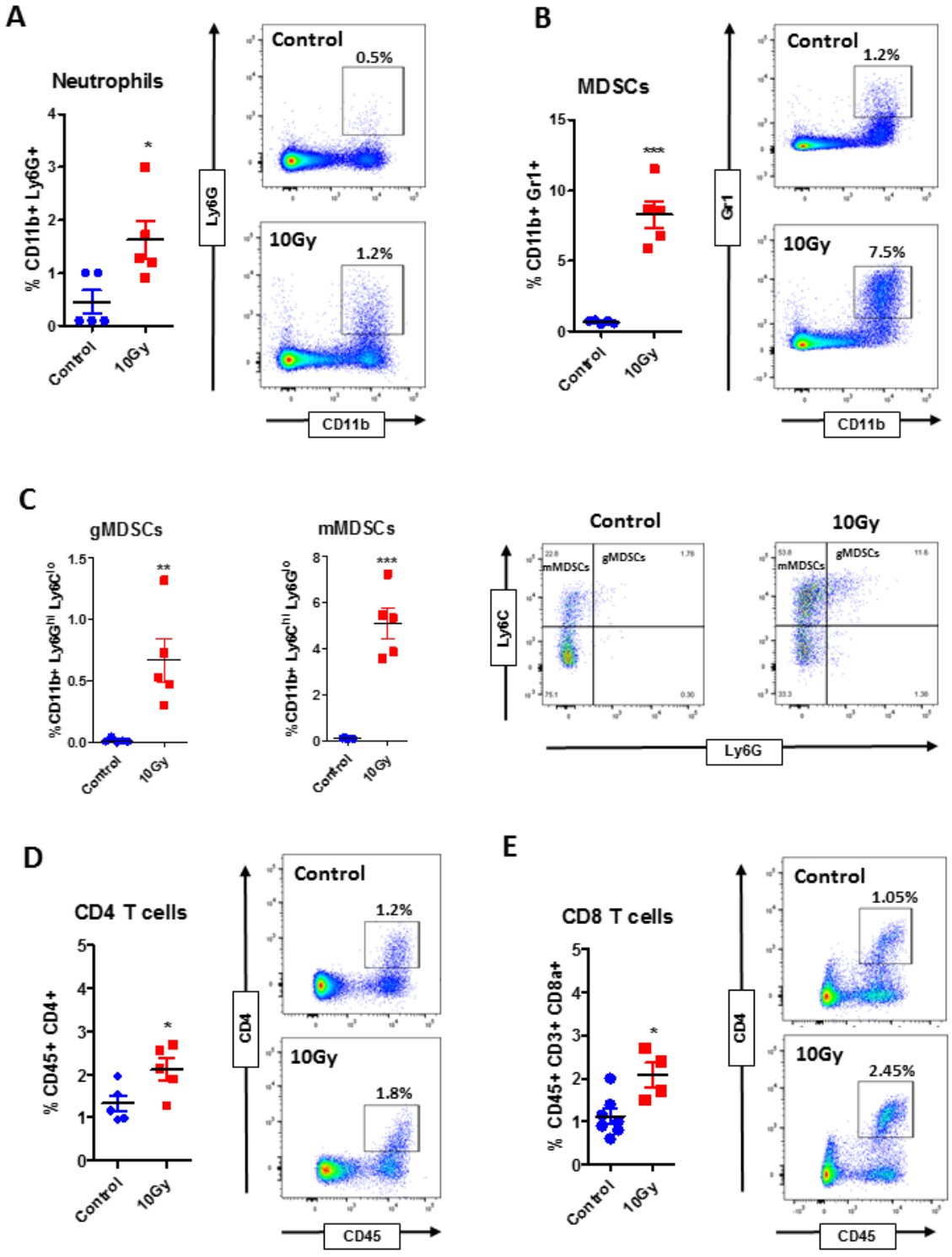


Figure 3.11 – Irradiation significantly alters the immune landscape in MC38 tumours

A-E – Flow cytometric analysis of immune cell populations in MC38 tumours 5 days following 10Gy irradiation, compared with control tumours. Immune populations were gated as indicated in the y axes. Total populations are expressed as a percentage of total cells analysed. Data are presented as mean ± SEM and statistical significance determined by unpaired t-test.

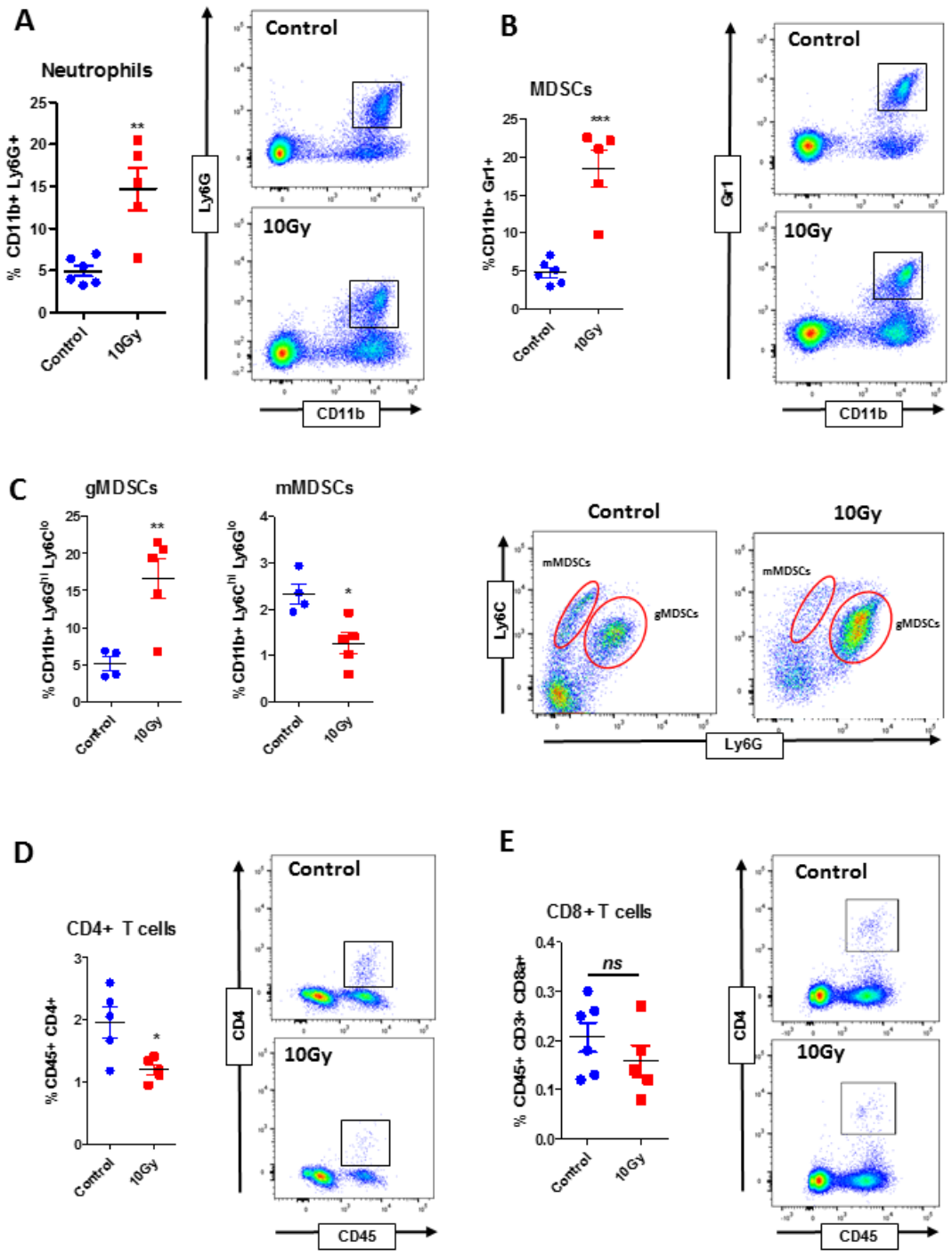


Figure 3.12 – Irradiation significantly alters the immune landscape in KPC tumours.

A-E, Flow cytometric analysis of immune cell populations in KPC tumours 5 days following 10Gy irradiation, compared with control tumours. Immune populations were gated as indicated in the y axes. Total populations are expressed as a percentage of total cells analysed. Data are presented as mean ± SEM and statistical significance determined by unpaired t-test.

3.4 Discussion

Here we demonstrate that CSF-1 is upregulated by tumour cells following exposure to ionising radiation. Upregulation in vitro corresponded with a transient increase in the serum of tumour bearing mice receiving radiation. This in turn corresponded with a significant increase in macrophage numbers present in MC38 and KPC tumours after irradiation in vivo. Macrophage phenotype showed a variable response, but they were functionally immunosuppressive. Finally, adoptive transfer of tumour pre-conditioned macrophages significantly increased tumour growth.

3.4.1 Upregulation of CSF-1 following irradiation

We screened for a number of cytokines and chemokines and identified CSF-1 as a candidate cytokine responsible for macrophage recruitment. As a result of alternative splicing there are 5 different CSF-1 mRNA isoforms which give rise to three different proteins; two secreted forms and one membrane bound glycoprotein [272,273]. Importantly, all three of these forms of CSF-1 are functionally active as they have been shown to reverse the phenotypes observed in the CSF-1 knockout mouse (*op/op*) [274–276]. A number of different drivers are thought to contribute to CSF-1 gene expression [277–280]. Interestingly, CSF-1 is secreted by dental follicle cells where it stimulates the recruitment of monocytes which in turn differentiate into osteoclasts involved in the dental eruption pathway [281]. In this setting, platelet-derived growth factor (PDGF) and basic fibroblast growth factor (bFGF) secreted by adjacent cells acted as mitogens, stimulating CSF-1 mRNA expression [277,281]. In addition to increased synthesis of CSF-1, levels may be elevated following shedding of the membrane bond protein isoform. In breast cancer cells, this has been shown to be mediated by tumour necrosis factor converting enzyme (TACE) [201]. In summary, there are a number of reported mechanisms by which CSF-1 is regulated, but these are limited to settings not involving radiation. In the context of tumor irradiation, Xu et al reported that the non-receptor tyrosine kinase ABL1 was translocated to the nucleus and subsequently bound to the CSF-1 promoter region resulting in significantly increased transcription of CSF-1 [282]. The proposed mechanism is supported by previous studies which report that ABL1 responds to DNA damage via the DNA-PK, ATM and p53 pathways [283–285]. They also showed a significant increase in CSF-1 mRNA expression in 8 out of 9 murine and human tumour cells analysed by qPCR at 24 hours. Importantly, they show that CSF-1 was elevated (not statistically significant) in the serum of patients with prostate cancer undergoing radiotherapy.

Two studies have previously demonstrated upregulation of CSF-1 gene and protein expression in response to radiation. The first involved a fractionated regime delivered to prostate cancer xenografts, and the second involved a single dose (12Gy) to murine pancreatic cancer xenografts [151,286]. Xu et al showed increased levels at 8 and 24 hours, which also resulted in increased CSF-1 in tumour conditioned medium. They also examined changes in SDF-1 and CCL2 which are known to attract macrophages [148,185]. Similar to our findings, these were comparably lower and did not increase following radiation. Seifert et al irradiated orthotopic KPC tumours and detected increased CSF-1 mRNA expression as well as protein levels in tumours on day 3. The orthotopic tumours grew at a significantly slower rate and the experimental end-point was at 8 weeks, at which point CSF-1 had returned to baseline levels [287].

In our hands, there was no significant increase in gene expression within the first 8 hours following irradiation. This may indicate that CSF-1 does not belong to the family of inflammatory genes which are upregulated in the acute phase after radiation (<2 hours) [40]. After peaking at 24 and 48 hours, the trend towards decreased expression by 72 hours may be due to the death of the lethally irradiated tumour cells. The transient induction of tumor cell CSF-1 gene expression was reflected in a similar pattern of protein secretion in vivo, with transient peaks in CSF-1 levels in both tumour models. Notably, circulating levels of CSF-1 in KPC tumour bearing mice were depressed 72 hours following radiation, but significantly increased on day 5. KPC tumours grew more rapidly than MC38 tumours, which had a period of growth stasis prior to regrowth. Therefore it is possible that repopulation of tumour cells in KPC produce CSF-1 independent of the effects of radiation. Without additional time points it is not possible to ascertain this from these data. However, the in vitro data does indicate that radiation induces CSF-1 expression in KPC cells. In summary, we show that irradiation of tumour cells both in vitro and in vivo results in increased CSF-1 expression, suggesting an intrinsic tumour cell response. These observations are comparable to results from two previous publications. Mechanistic data is limited to one study and requires further investigation.

3.4.2 Increased alternatively activated macrophages in the tumour microenvironment following irradiation

The induction of CSF-1 by radiation would be expected to both recruit and enhance survival of macrophages in tumors [153]. Indeed increased numbers of macrophages in tumors following radiation coincided in time with increased CSF-1. In the literature, the effect of radiation on both the

recruitment and functional status of macrophages appears to be dependent on the experimental model, radiation dose, and the time at which tumors are isolated and analysed. Whilst some reports find recruitment of macrophages [51,53,282,288], others do not identify any significant change [289,290]. Seifert et al report significant macrophage increases in orthotopic pancreatic tumors which disappeared by 8 weeks [291]. Crittenden et al identified an increase as early as 24 hours with a substantially higher peak at day 7 [288], whilst Shiao et al report maximum numbers at day 14 [292]. Importantly, the radiation dosing strategy varies significantly amongst these studies, ranging from three separate does of 20Gy, a single fraction of 12Gy and 5 fractions of 3Gy. We found considerable increases in macrophages early following radiation, coinciding with increased CSF-1, and peaking on day 5. The reduction in macrophages over time suggests that there is a diminution of the initial stimulus responsible for recruitment.

To assess the phenotype of TAMs we used a combination of flow cytometry, mRNA expression, CD8 T cell suppression assay. Analysis of TAM polarisation by flow cytometry is restricted to a small number of markers that are largely indicative of either M1 or M2 polarisation. These markers are typically selected because they indicate significant skewing towards either end of a polarisation continuum. It is important to note that these phenotypic extremes were first identified following the stimulation of monoctyes in vitro with either LPS or IL-4 for M1 and M2 polarisation respectively. Some of the most widely reported murine markers of M1 and M2 polarisation using flow cytometry are iNOS and CD206 respectively [293]. Inducible nitric oxide synthetase (iNOS) is a key enzyme involved in the inflammatory macrophage response. iNOS mediates the oxidation of L-arginine to L-citrilline, generating nitric oxide (NO). This has been reported to result in direct antimicrobial activity, production of reactive oxygen species, and direct T cell suppression, all associated with the innate immune response. CD206, known as the mannose receptor or c-type lectin, is a pattern recognition receptor (PRR). It interacts with glycoproteins present on the surface of pathogens, and plays a role in mediating macrophage functions typical of alternatively activated macrophages. The expression of these markers therefore indicates that macrophages are in a state representing two extremes of a normal physiological activation. The main limitation to this approach is the inability to characterise TAMs lying somewhere in the middle of these extremes. Whilst other flow cytometric markers were available, they also characterise macrophages as either M1 or M2. It is for this reason that we selected one reliable and reproducible marker for M1 and M2. During optimisation

experiments, additional markers were included in the flow cytometry panel, including Arginase and IL-10 for M2, and MHC II and CXCL10 for M1. Analysis of Arginase and MHC II yielded results comparable to those obtained from analysing iNOS and CD206. IL-10 and CXCL10 are cytokines that require ex vivo stimulation and protein transport blockade, increasing the risk of experimental variation as well as the burden associated with multiple flow cytometry analyses. Data for these optimisation experiments are not presented. The issues surrounding analysis by flow cytometry are important for interpreting the data presented in figure 3.4. Our results suggest that irradiation alters the number of M1 and M2 macrophages present in tumours. However, further exploration of the intermediate and functional phenotype, alternative approaches are required. One such approach includes, but is not limited to, mRNA expression analysis. This has the advantage of allowing for analysing a substantially higher number of markers, as well as more sensitive quantification of differences.

Previous reports show a variable response in TAMs following tumour irradiation. Shiao et al analysed tumour macrophages harvested 24 hours following 5Gy irradiation, finding upregulation of genes in both pro-inflammatory and immune suppressive pathways, suggestive of generalized activation [292]. Of note, in the same report the authors state that low dose (2Gy) irradiation did not result in any significant changes in TAM gene expression. Murine pancreatic tumours from genetically engineered models and allografts showed a significant shift towards M2 polarisation following radiation [288,291]. The disparate results between studies reflect the pleiotropy of macrophages, particularly in response to treatment. For gene expression analysis, we isolated TAMs by fluorescence activated cell sorting (FACS). The isolation of specific cell populations is restricted by the flow capacity of cell sorting cytometers. In situations where the desired cell populations make up a fraction of a large sample, the time taken to for isolation is significantly increased. This has to be balanced against the reduction in quality of samples associated with length acquisition times. This is especially true in the collection of RNA. We found that attempts at collecting RNA from TAMs isolated from single tumours yielded insufficient RNA for downstream analysis. Pooling of tumours from 5 or more mice generated enough good quality RNA to perform mRNA analysis of 10 genes in total (in triplicate). To avoid using excessively high numbers of mice, we limited our analysis to a carefully selected panel of genes representative of both immune suppression and stimulation. The selected genes were previously reported in studies examining tumour macrophage polarisation. Importantly, as

well as being markers reflective of polarisation, each gene plays a functional role in the immune phenotype of the macrophages.

Our results highlight the heterogeneous nature of response amongst tumor types, with a more inflammatory phenotype in KPC tumors compared to MC38, though the general trend was towards M2 polarisation. Consideration of the dynamics of macrophage recruitment may explain these differences, particularly in the context of radiation. In murine subcutaenous xenografts there are no tissue resident macrophages. Therefore it can be assumed that any TAMs have been recruited from the circulation. Newly arrived Ly6C+ monocytes are functionally naïve but can become terminally differentiated by exogenous signals within the tumour. Therefore it is perhaps unsurprising that established populations of TAMs from within non-irradiated tumours are often found to be highly M2 polarised [242]. However when radiation is applied, especially at relatively high single ablative doses, there may be a transient but significant influx of naive inflammatory monocytes. The extent to which these are subsequently conditioned by the tumour microenvironment may vary across tumours.

The extent to which factors secreted by tumour cells can affect macrophage phenotype was highlighted in the results from the co-culture experiments. Generally, conditioning by tumour cells resulted in significant alterations in gene expression, and these were different between cell lines. In addition, the results from flow cytometric analyses indicated that there were only slight changes in iNOS expression, a marker indicative of M1, inflammatory activation. However gene expression analyses revealed that many other inflammatory markers were highly upregulated, particularly in KPC conditioned macrophages. This suggests that conclusions drawn from analyses of TAM phenotype based on single makers analysed by flow cytometry should be interpreted with caution. These markers may be useful for measuring changes in polarisation over time or in response to treatment, however additional characterisation may be required for a deeper appreciation of their functional status. It was interesting to compare the alterations in macrophage phenotype between those isolated from tumours with those co-cultured with tumour cells. TAMs were generally immunosuppressive in nature, with further increases in immunosuppressive genes following irradiation. This was confirmed by their ability to significantly suppress CD8 T cell proliferation. However macrophages co-cultured with tumour cells had relatively higher levels of expression of inflammatory genes after radiation. Whilst the experimental approaches preclude direct comparison of the results, it is interesting to note the differential response seen *in vitro*. Firstly, co-cultured macrophages were analysed 3 days after

radiation. The release of DAMPs form dying tumour cells possibly means that macrophages are still responding to the effects of TLR activation. In addition it is likely that tumour-derived factors are only partly responsible for macrophage conditioning. Additional stimuli produced by non-tumour cells may contribute to the more suppressive phenotpye observed in the TAMs.

Finally, despite the variable gene expression profiles in BMDMs and TAMs, those exposed to irradiated tumour cells significantly inhibited T cell proliferation. Arginase was abundantly expressed in TAMs and conditioned BMDMs suggesting that the tumor cells are partly responsible for the immunosuppressive phenotype observed. Arginase in tumoral macrophages or co-cultured macrophages further increased following irradiation of the tumor or radiation of the tumor cells used in co-culture respectively. Arginase mediated L-arginine depletion can profoundly limit T cell function and metabolism [291,292,294], which may underlie our finding of enhanced macrophage mediated T cell suppression following radiation. TAMs are also known to constitutively express immune checkpoint molecules, and engagement of these with their cognate ligands on CD8 T cells can induce anergy [207]. CD163+ TAMs isolated from oral squamous cell carcinoma patients showed high levels of PD-L1 and induced apoptosis when cultured with T cells [295]. There are other reports of T cell suppression induced by TAMs, but we were unable to find any which looked specifically at macrophages isolated from irradiated tumours [296].

In summary, macrophages we found significantly increased numbers of macrophages in tumours following irradiation. Phenotypically, these TAMs were characterised by altered expression in a range of inflammatory and immune suppressive genes. In general, TAMs were skewed more towards a suppressive phenotype, which was confirmed by their ability to suppress T cell proliferation in vitro.

4. CHAPTER 4: Macrophage depletion delays tumour growth following radiation.

4.1 Introduction

4.1.1 Macrophage depletion strategies

We have thus far identified that there is a significant increase in TAMs following tumour radiation. These macrophages are functionally immunosuppressive. However, to determine whether they impact on tumour growth following radiation, we next sought to deplete them. A number of therapeutic strategies have been developed which either aim to deplete macrophages, or alter their activation status. A common way in which macrophages are targeted in pre-clinical models is via the blocking of chemokine-mediated recruitment. The challenge with this approach is the multiple different chemokines and cytokines involved macrophage migration, as well as the effects some of them have on other immune cells. A frequently reported approach is targeting of the CCL2-CCR2 axis, which has been shown to reduce macrophage numbers in a range of tumour models [181,234,297,298]. Experimentally, targeting CCL2 to specifically target macrophages is less favourable due to its expression on a number of other cells, including fibroblasts, tumour cells, as well as other immune cells [299]. Also, despite a majority of studies demonstrating an inhibition of tumour growth with anti-CCL2 therapy, a report from Bonapace et al showed that in four different models showed that blocking CCL2 was associated with an increased rate of metastasis [300]. Nonetheless, a number of anti-CCL2 monoclonal antibodies have entered clinical trials. Whilst phase I trials have shown that these agents are safe, a phase II trial in metastatic prostate cancer showed no objective response [301–303]. Promising results were shown in a phase Ib trial of a small molecule CCR2 inhibitor combined with FOLFIRINOX chemotherapy (oxaliplatin and irinotecan, plus leucovorin and fluorouacil). As well as showing tolerability, 49% of patients had an objective response and 97% stable disease.

Another common target is the CSF-1/CSF-1R axis. As discussed previously (section 1.3), CSF-1 is involved in the migration, survival and differentiation of macrophages. In addition, it is almost exclusively expressed on monocytic cells, predominantly macrophages [155]. Agents targeting the axis include monoclonal antibodies directed against either CSF-1 or CSF-1R, and a number of small molecule inhibitors targeting the CSF-1R tyrosine kinase [304]. Antibody blocking of CSF-1 and CSF-1R has been extensively reported in the pre-clinical setting, showing effects on both macrophage

numbers and their activation status [169,286,305–308]. Anti-CSF-1(R) antibody-mediated macrophage depletion alone is not always associated with delayed tumour growth, however is reported to work synergistically in combination with other immune stimulatory agents [305,309]. There are a large number of clinical trials currently evaluating the use of CSF1(R) inhibitors as monotherapy or in combination with other agents, all currently in phase I or phase II [304].

Another strategy to target macrophages is the administration of bisphosphonates contained within liposomes. Bisphosphonates are used extensively to treat osteoporosis. Bisphosphonates accumulate in the bone due to their affinity for calcium, and build up inside osteoclasts following bone ingestion, causing apoptosis. Circulating bisphosphonates have a short half life, however encapsulation within liposomes allows extra medullary phagocytes to ingest them until lethal levels accumulate [310]. In pre-clinical models liposomes containing the bisphosphonate clodronate demonstrate significant and reproducible TAM depletion [298,311,312]. Despite almost complete ablation of macrophages from tumours as well as organs, severe toxicity in mice has been reported following the administration of clodronate liposomes, meaning their clinical application is likely to be limited [313].

4.1.2 CSF-1(R) blockade

Given the increase in CSF-1 levels we observed following radiation, we chose to selectively deplete CSF-1 using a blocking antibody. Anti-CSF, or antibodies targeting it's receptor, have previously been shown to be effective at reducing TAMs [291,309,314,315]. Zhu et al showed that TAMs in a murine pancreatic cancer model TAMs started to decrease as early as 6 hours following administration and, were effectively depleted within 24 hours following the first dose [315]. TAMs were not completely eradicated, and following 8 days of treatment 5% total cells were macrophages (from 20%). In an orthotopic pancreatic cancer model, Seifert et al show a more profound reduction in TAMs. Baseline TAMs represented approximately 20% of the tumour, and were reduced to less than 5% after 18 days of aCSF. In the same study, aCSF was combined with radiation, where it was less effective at depleting TAMs (~10% vs ~30%). A similar approach in a murine breast cancer model demonstrated a ~50% reduction in TAMs [316]. Another study from the same group also examined the changes in other immune populations following CSF-1 blockade [220]. In addition to a reduction in both MHC II^{hi} and MHC II^{lo} TAMs, $Ly6C^{hi}$ monocytes remained unchanged but there was an increase in neutrophils. Interestingly, in another setting CSF-1R blockade has been shown to increase granulocytic myeloid derived suppressor cells (gMDSCs) [317]. Here, it was demonstrated that cancer-associated fibroblasts

expressed CSF1-R, which upon stimulation downregulated the secretion of gMDSC chemoattractants. An exception to the consistent TAM depletion reported in these studies is the refractory population of TAMs in glioma demonstrated by Pyonteck et al. Whilst CSF-1R inhibition was associated with a reduction in microglia, TAMs were unchanged. In this case they were supported by tumour-derived GM-CSF and IFNγ. This highlights that when deciding upon TAM depletion strategies, some consideration should be given to the cytokine landscape of the tumour and possible mechanisms of resistance. Prior knowledge of which factor is likely to be responsible for TAM recruitment is critical when deciding upon the best approach. Of course, one cannot predict how tumours might engage compensatory mechanisms, as was seen in the glioma model. In summary, a number of agents have been shown to be effective at reducing TAMs in the pre-clinical setting. Importantly, this includes some studies combining TAM depletion with radiation. WE CHOSE...

4.2 Aims

1. To determine whether treatment with anti-CSF (aCSF) reduces macrophages after tumour irradiation
2. To determine whether aCSF affects the phenotype of TAMs
3. To determine the effects of macrophage depletion on tumour growth after radiation.

4.3 Results

4.3.1 aCSF treatment reduces TAMs

In order to determine whether the TAMs contributed to the regulation of tumour growth after radiation, we sought to deplete them. Because radiation induced CSF-1 in these tumors, we determined the effect of an anti CSF-1 antibody (aCSF) on TAM numbers in tumours both in the absence and presence of tumour irradiation. As previously discussed, targeting CSF-1 potentially acts to both reduce macrophage numbers and re-polarise them. In addition, as CSF-1 is involved in the migration and survival of macrophages, it may act to both inhibit the migration of macrophages as well as reduce those already present within tumours. Mice were treated intraperitoneally when tumours reached 80mm^3 and continued for a total of 14 days. This allowed a dose to be given 24 hours prior to tumour irradiation, which was delivered when tumours reached 100mm^3 (**Error! Reference source not found.**, A). The same CSF-1 blocking antibody has been previously shown to significantly reduce macrophage numbers within 24 hours of the first dose [305]. In MC38 tumours, aCSF treatment significantly reduced TAM numbers, however a small refractory population remained (5.85% vs 1.95% p=<0.01 **Error! Reference source not found.**, B). On day 5 after radiation, the point of maximal TAM numbers, TAMs were significantly reduced. Again, there was a refractory population. Whilst the magnitude of TAM depletion was comparable with and without radiation, the refractory population in irradiated tumours was higher at 3.21%. This was still significantly lower than numbers in isotype control treated mice (8.91% p=<0.01 **Error! Reference source not found.**, B). A similar pattern was observed in KPC tumours. There was a significant reduction in TAM numbers with and without radiation (11.41 vs 4.43 p=<0.01, 26.35 vs 14.43 p=<0.01, respectively **Error! Reference source not found.**, C). Again there was a resistant population which was higher in the irradiated group.

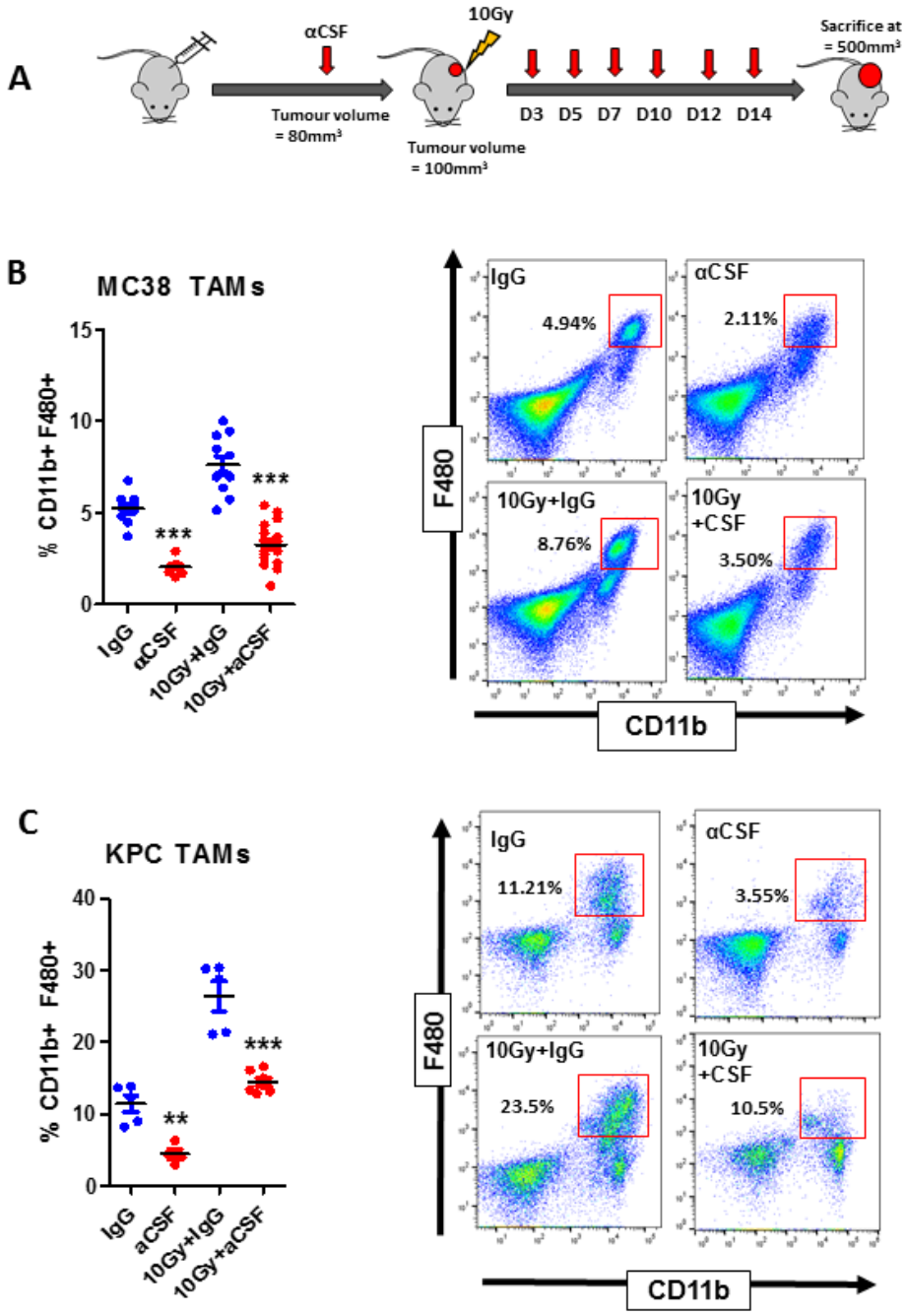


Figure 4.1 – aCSF effectively reduces TAM number in MC38 and KPC tumours with and without irradiation.

A – Schema outlining experimental model. Wild-type C57-BL6 mice were inoculated with MC38 or KPC tumour cells. Tumours were measured daily and randomly assigned sequentially into treatment groups when they reached 80mm3. aCSF was administered when tumours were 80mm^3 and irradiation applied when they reached 100mm^3.
B, C– Macrophage (CD11b+ F480+) numbers were determined by flow cytometry in MC38 (B) and KPC (C) tumours. Non-irradiated tumours were harvested when they reached a volume of 500mm3. Irradiated tumours were harvested 5 days following irradiation (10Gy). Data are presented as mean ± SEM and statistical significance determined by one-way ANOVA. Representative flow cytometry plots are also shown (right panels).

4.3.2 aCSF treatment selectively depletes M2 macrophages

In order to characterise the phenotype of the resistant TAM populations following aCSF we analysed tumours by flow cytometry. In MC38 tumours there was a significant reduction in total CD206+ TAMs both with and without radiation (Figure 4.2, A). The changes in iNOS^{hi} TAMs were more variable. aCSF treatment in the absence of radiation reduced iNOS^{hi} TAMs (Figure 4.2,B). However aCSF in the presence of radiation was associated with an increase in iNOS^{hi} TAMs compared with radiation alone. These results suggest that there is selective depletion of CD206+ TAMs. Also, the iNOS^{hi} TAM population which is diminished after radiation alone is increased to baseline levels with the addition of aCSF (Figure 4.2,B).

In KPC tumours, there was also a consistent reduction in CD206+ TAMs both with and without radiation (Figure 4.2, A). There was no difference in iNOS^{hi} TAMs with aCSF alone (Figure 4.2,B). As previously observed, there was an increase in iNOS^{hi} TAMs in the radiation alone group, and there was a slight reduction with aCSF (not statistically significant). These results suggest that the iNOS^{hi} macrophage population is relatively resistant to aCSF blockade, compared with the CD206+ TAMs. When iNOS^{hi} macrophages are compared with CD206+ macrophages as a ratio, in both MC38 and KPC tumours aCSF was associated with a significant increase in the M1:M2 ratio.

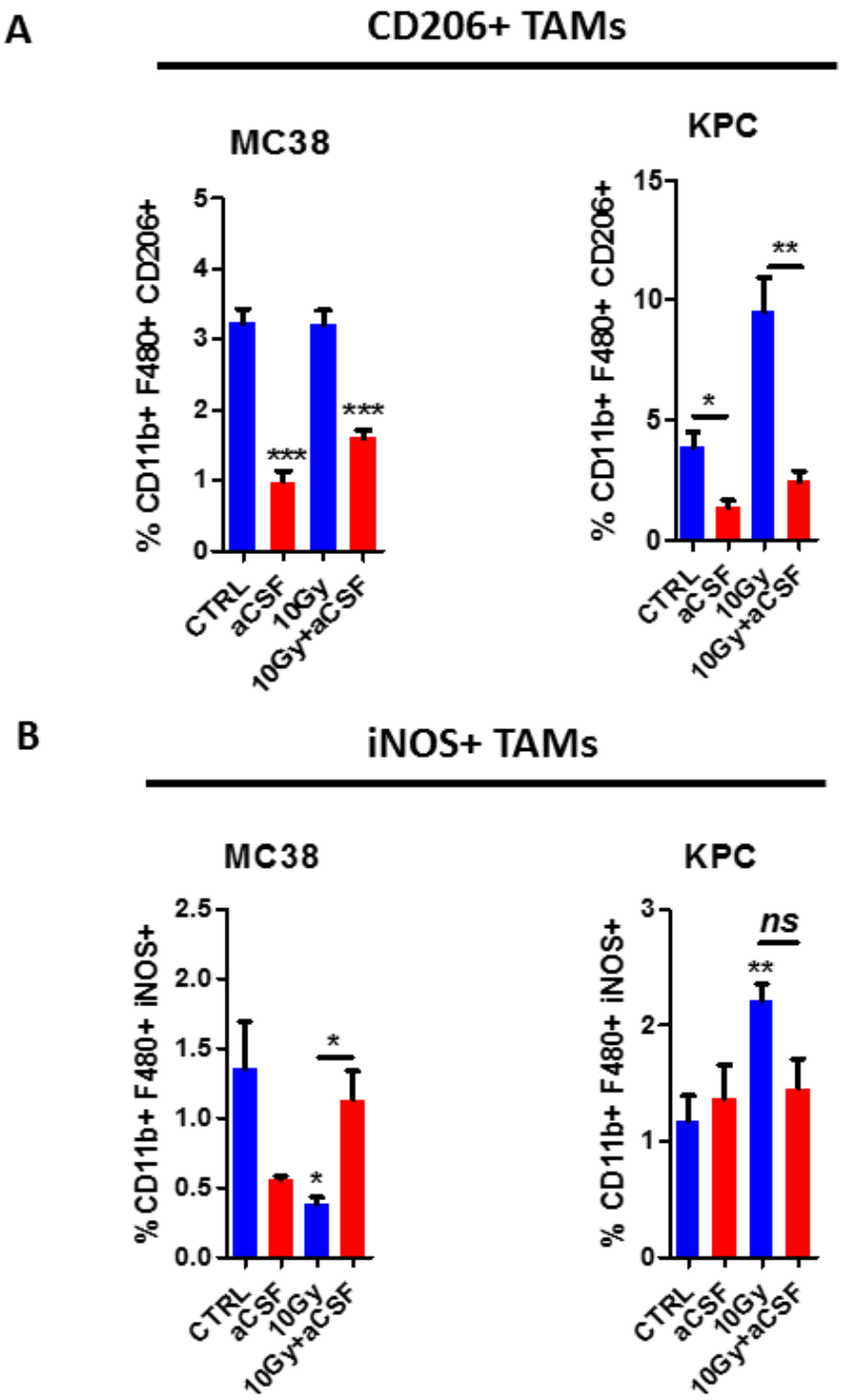


Figure 4.2 – M1 and M2 TAM populations are differentially affected by aCSF

A, B – CD206+ (M2) and iNOS+ (M1) macrophages were analysed by flow cytometry 5 days after 10Gy irradiation (+/-aCSF as indicated, 5 mice/group, pooled samples with technical triplicates). TAMs are quantified as a percentage of the total cells analysed. Data are presented as mean ± SEM and statistical significance determined by one-way ANOVA.

4.3.3 aCSF treatment is associated with macrophage repolarisation

Next, to gain further information on the phenotype of the refractory TAM population we performed gene expression analyses on macrophages isolated from tumours. CD11b+/F480+ macrophages were isolated and RNA was extracted from the raw population. A range of markers associated with immune stimulation and suppression were analysed. In MC38, TAMs from aCSF treated mice showed increased expression of all inflammatory markers (Figure 4.3, A). Strikingly, iNOS showed a substantial upregulation in gene expression. This is starkly different from the down regulation observed in TAMs isolated from tumours receiving radiation alone (Figure 3.5, A). Conversely, there was a significant decrease in the expression of markers associated with immune suppression. Arginase, ccl2 and il10, which were all increased following radiation alone, were all significantly decreased (Figure 4.3, B).

In KPC tumours, the pattern was more variable. There was an increase in some inflammatory markers, including iNOS, il12 and il1a, whereas TNFα was decreased (Figure 4.3, C). Arginase, ccl2 and il10 were all decreased however il6 was increased (Figure 4.3, D). Overall, these data indicate that aCSF treatment is associated with repolarisation of a refractory population of TAMs towards an inflammatory profile.

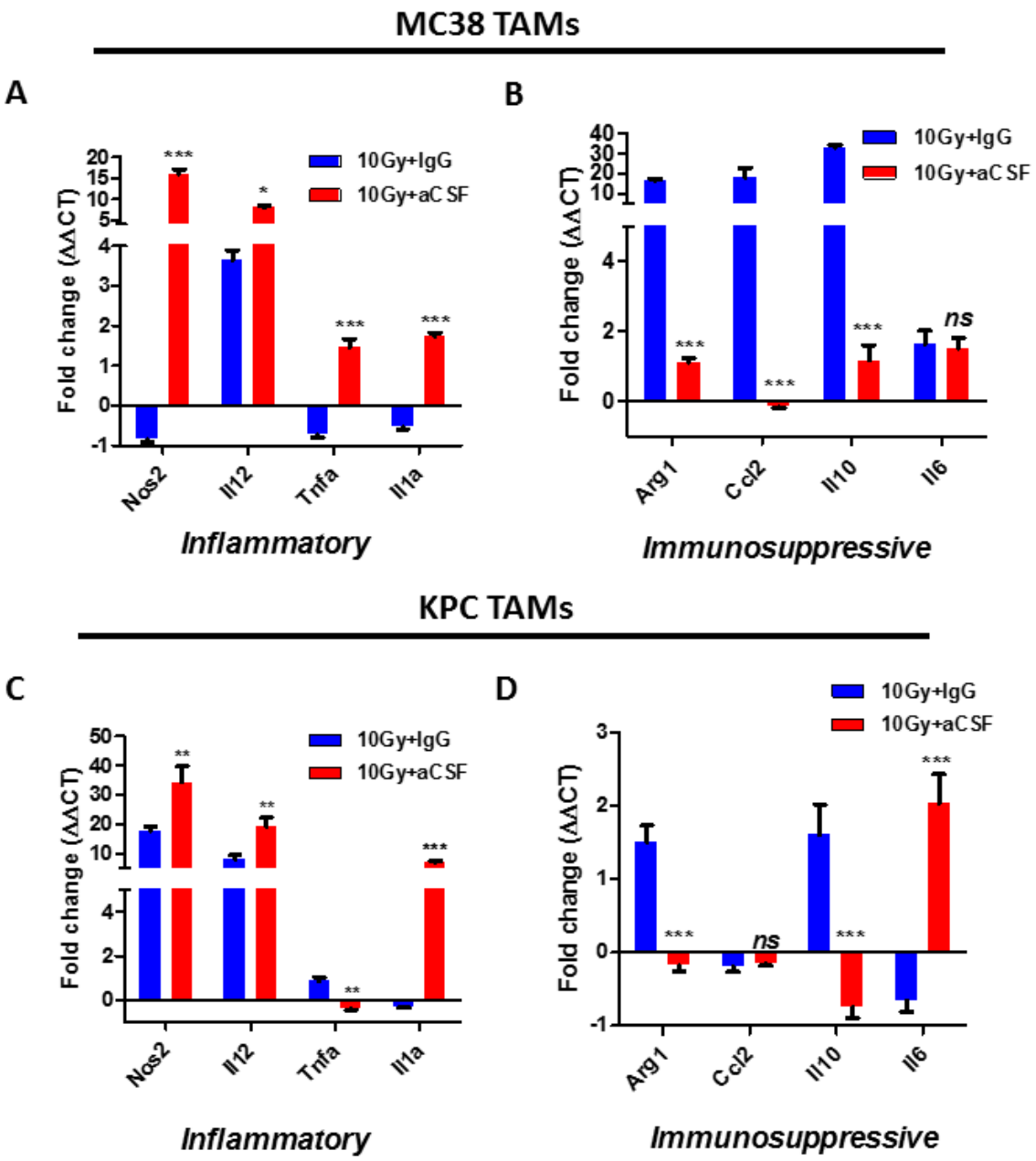


Figure 4.3 – aCSF treatment is associated with TAM repolarisation

A-D – TAMs were isolated from MC38 (A,B) and KPC (C,D) tumours by FACS , RNA extracted and mRNA levels determined by qPCR. A selection of typical immune stimulatory (A,C) and suppressive (B,D) genes were analysed. Data are shown as mean ± SEM and statistical significance determined by unpaired t-test.

4.3.4 aCSF treatment combined with radiation delays tumour growth

After confirming that TAMs are reduced via aCSF we next sought to determine the effect on tumour growth delay. In mice treated with aCSF alone, tumour growth was unaffected and growth rate was identical to mice treated with isotype control antibody (Figure 4.4 – Irradiation combined with aCSF treatment A,B). This was the case in both MC38 and KPC tumours. The rapid growth rate meant that mice were continually treated until tumours reached a volume of 500mm^3. Combined treatment with 10Gy radiation and aCSF led to significantly increased growth delay in both MC38 and KPC tumours. In MC38, 10Gy radiation alone delayed tumour growth by 7 days. The addition of aCSF extended growth delay by a further 14 days, to a total of 30 days following tumour cell injection (Figure 4.4 – Irradiation combined with aCSF treatment A). In KPC, 10Gy radiation alone delayed tumour growth by 6 days. The addition of aCSF extended growth delay by a further 7 days, to a total of 19 days following tumour cell injection (Figure 4.4 – Irradiation combined with aCSF treatment B). These results suggest that TAMs play a role in promoting tumour regrowth following irradiation. Furthermore, this effect was dependent upon co-administration of radiation.

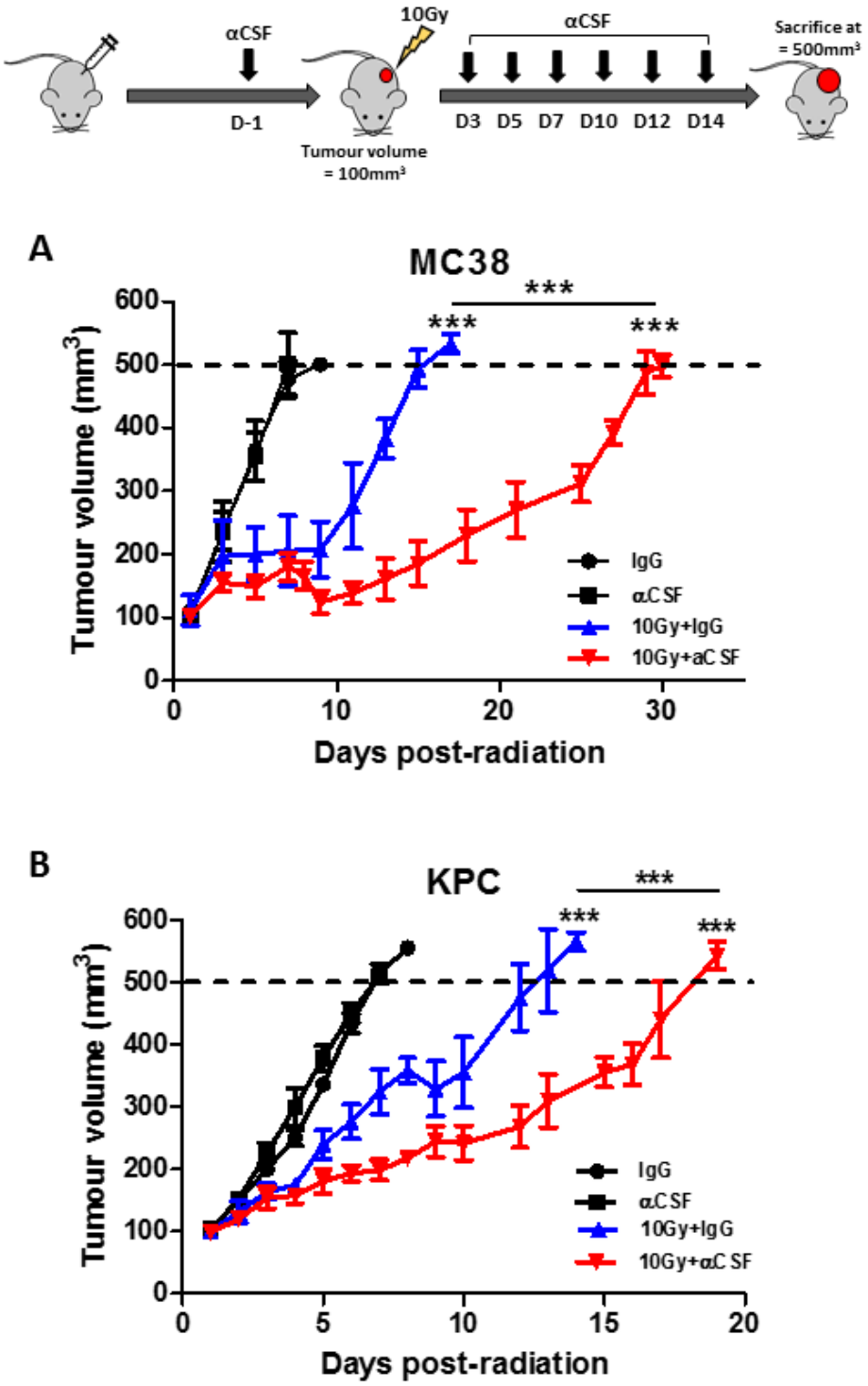


Figure 4.4 – Irradiation combined with aCSF treatment increases tumour growth delay.

A,B – Mice were treated according to the schedule outlined in the schema (top panel). Mice bearing MC38 (A) and KPC (B) tumours were treated with IgG isotype control antibody, aCSF, 10Gy irradiation + IgG isotype control antibody, or 10Gy irradiation + aCSF as indicated. Antibody treatment was initiated when tumours reached 80mm3 and irradiation delivered when tumours reached 100mm^3 (outlined in schema, Figure 4.1, A). Data are presented as mean tumour volume ± SEM. Statistical significance was determined by comparing the number of days to reach end-point by one-way ANOVA. Data are representative of three independent experiments with 8 mice per group.

4.3.5 sCSF does not affect tumour cell radiosensitivity

In order to determine if the effects on tumour growth were due to direct effects of aCSF on intrinsic tumour cell radiosensitivity we performed colony forming assays (clonogenic assays). The addition of anti-CSF to the media of tumour cells treated with varying doses of radiation did not increase radiosensitivity in both cell lines (Figure 4.5, A,B).

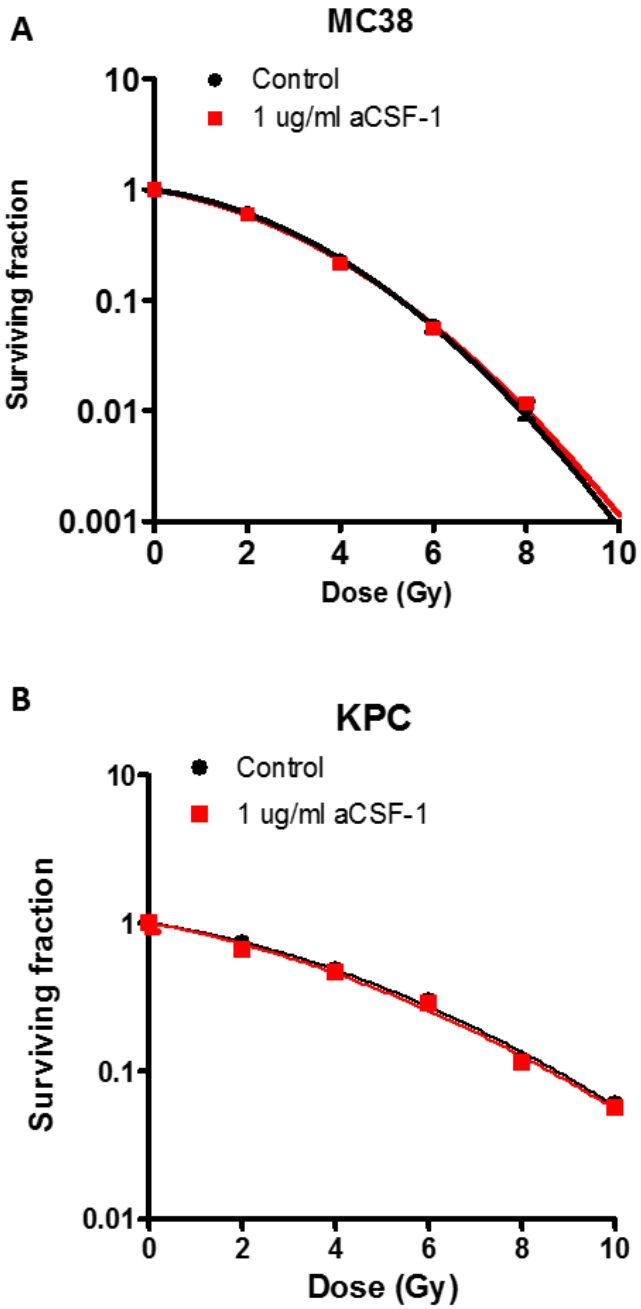


Figure 4.5 – aCSF does not affect tumour cell radiosensitivity

A,B - Clonogenic survival assays in MC38 (A) and KPC (B) tumour cells with the addition of anti-CSF (red line) at the dose indicated. Cells were cultured for 5-8 days following application of the radiation dose indicated. Survival curves were fitted using indirect curve fitting in GraphPad Prism 5.0. Three independent experiments were conducted.

4.3.6 Macrophage depletion is associated with increased CD8+ T cells and penetrance into tumours

Having identified that TAMs contained within irradiated tumours are immunosuppressive, we asked whether TAM depletion was associated with an increase in CD8 T cells. As a reflection of the extent of adaptive anti-tumour immunity, increased CD8 T cells could be one reason for the increased tumour growth delay we observed. In MC38 tumours there was a significant increase in CD8 T cells associated with aCSF, with an approximately two-fold increase (Figure 4.6, A). This increase was present with and without tumour irradiation. In KPC tumours, CD8 T cell numbers were considerably lower, and no changes were observed in association with aCSF treatment. In all treatment groups the total number of CD8 T cells did not exceed 0.5% of the total cell population within the tumour. This is in line with existing reports that describe pancreatic cancer as immunologically 'cold'. This refers to the highly suppressive microenvironment, densely infiltrated with myeloid cells, and very few CD8 T cells [318]. We were thus only able to further characterise the phenotype of CD8 T cells in MC38 tumours, where there were sufficient cells to provide reliable analysis. Firstly, we analysed Ki67 expression to determine whether the increase in T cell numbers was due to proliferation. Interestingly, whilst there was increased Ki67 expression in CD8 T cells in tumours receiving irradiation alone (Figure 4.6, C), those in aCSF treated tumours expressed lower levels of Ki67. In non-irradiated tumours, this was statistically significant. In the irradiated group, there was a trend towards decreases expression in aCSF treated tumours but this did not reach significance. These results suggest that there observed increases in CD8 T cell numbers in MC38 tumours may be due to augmented migration as opposed to in situ proliferation. Next, we measured the expression of programmed death ligand-1 (PD-1), a key marker of an exhausted state. CD8 T cells from irradiated tumours expressed less PD-1 compared with control tumours, and there was a trend towards a further reduction in aCSF treated mice but this was not significant (Figure 4.6, D). Effector CD8 T cells are characterised by their expression of IFN GAMMA and cytolytic granules such as granzyme B. We analysed expression of these markers by flow cytometry. IFN gamma was expressed at significantly higher levels in both groups treated with aCSF (Figure 4.6, E). Granzyme B expression was only significantly increased in tumours treated with radiation and aCSF (Figure 4.6, F). These results suggest that CD8 T cells in aCSF treated tumours are less exhausted, more cytotoxic, and possible present in increased numbers as a result of migration.

In addition to absolute numbers, the spatial distribution of CD8 T cells within tumours has also been shown important [162,319]. T cells need to be in contact with tumour cells to exert their cytotoxic potential, and this can be limited by cells in the ECM present in the stromal compartment [320]. Therefore we checked whether there were differences in the spatial distribution of CD8 T cells within tumours by immunofluorescent staining. In MC38 tumours, CD8 T cells appeared homogenously distributed within tumours, with no discernible areas of T cell exclusion (Figure 4.7, A,C). T cells were also present within the central tumour core (Figure 4.7, B,D). Furthermore, there did not appear to be any gross differences between the expression pattern observed in irradiated tumours and those additionally treated with aCSF (Figure 4.7, A,C). As expected, there were very few CD8 T cells present in KPC tumours. In tumours treated with irradiation alone the few T cells which were present were restricted to the tumour periphery, with very few cells identified in the tumour core (Figure 4.7, E-G). In KPC tumours treated with irradiation and aCSF, there were clusters of CD8 T cells present within the central tumour core (Figure 4.7, H-J). These data suggest that the spatial distribution of CD8 T cells is unaffected by macrophage depletion via aCSF in MC38 tumours. In KPC tumours however, macrophage depletion was associated with penetration of CD8 T cells to the central core of tumours.

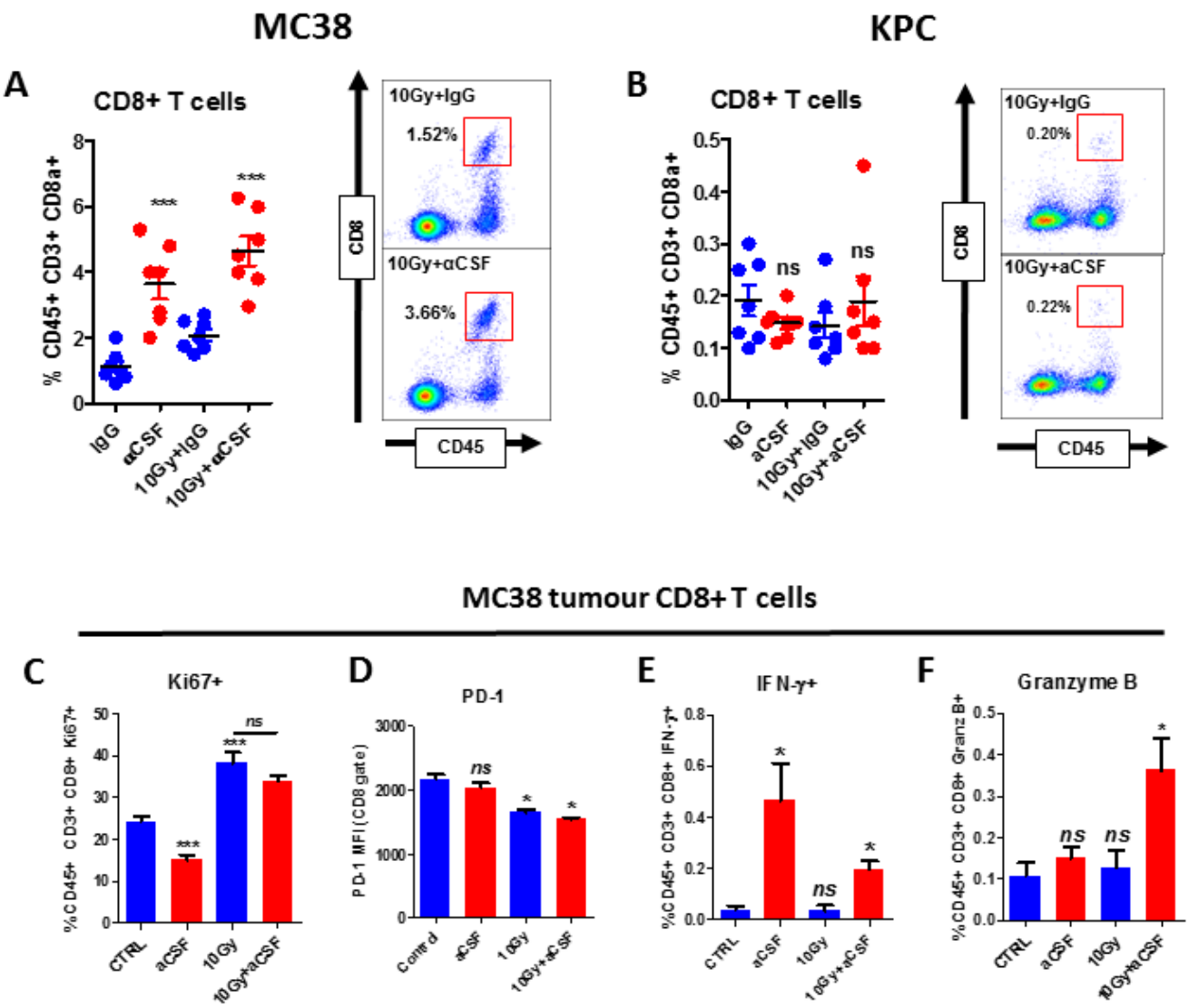


Figure 4.6 – aCSF treatment is associated with increased numbers of CD8+ T cells

A,B – CD8+ T cells (CD45+ CD3+ CD8+) were quantified in MC38 (A) and KPC (B) tumours at end-point (non-irradiated groups) and 5 days following tumour irradiation (10Gy, irradiated groups). Data are presented as mean ± SEM and statistical significance determined by one-way ANOVA. Data are representative of one experiment (8 mice/group, 3 experiments in total/cell line).

C-F – Analysis of Ki67 expression (C), PD-1 expression (D, mean fluorescence intensity), IFNγ and granzyme B (F) expression on pre-gated CD8+ T cells in MC38 tumours receiving treatment as indicated. IFNγ and Granzyme B expression were analysed after simulation with phorbol 12-myristate-13-acetate (PMA) + Ionomycin for 4 hours in the presence of Brefeldin A before intracellular staining was performed.

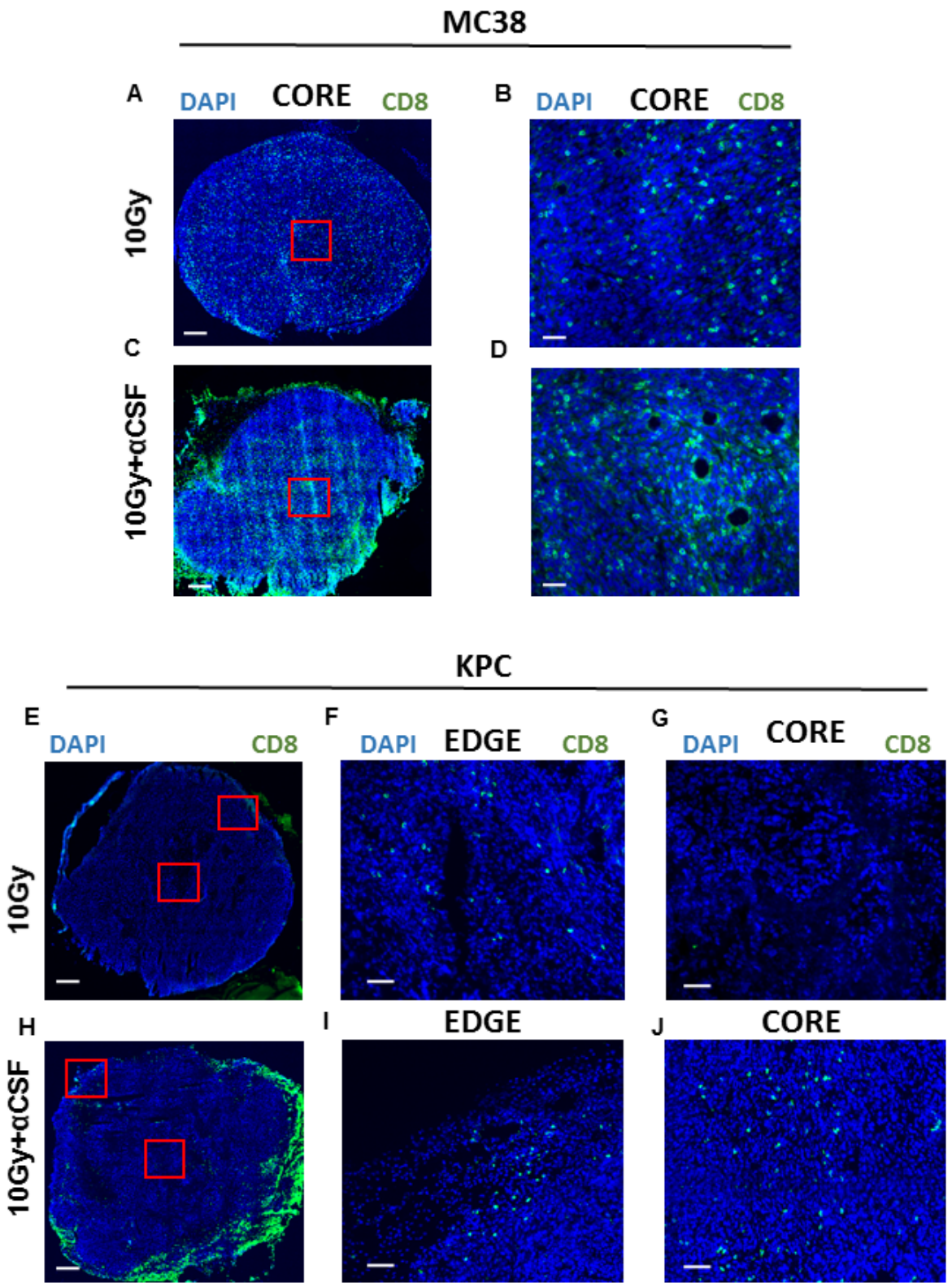


Figure 4.7 – CD8 T cells are homogenously distributed in MC38 tumours, but penetrate the tumour core in KPC tumour treated with irradiation and aCSF.

A-D – Sections from MC38 tumours receiving treatment as indicated were harvested 5 days following radiation and stained for CD8 T cells (green) and nuclei (blue). Images are of the whole tumour (A+C) or a representative image of the central core (B+D).
E-J – Sections from KPC tumours receiving treatment as indicated were harvested 5 days following radiation and stained for CD8 T cells (green) and nuclei (blue). Images are of the whole tumour (E+H) or a representative image tumour edge (F+I) or central core (G+J). Images shown are representative of an experiment with 5 mice/group.

4.3.7 aCSF is associated with variable changes in other immune populations

Previous studies have shown changes in non-macrophage populations in response to aCSF1, therefore measured changes in common myeloid and lymphocytic populations by flow cytometry [220,317]. In MC38 tumours treated with a CSF, there were no significant changes in neutrophil or gMDSC populations (Figure 4.8, A,C). Monocytic MDSCs comprised the majority of the MDSCs detected and these were significantly decreased following aCSF and irradiation (Figure 4.8, D). CD4 T cells were significantly reduced with aCSF with and without radiation (Figure 4.8, E).

In KPC tumours, there were no significant changes in any of the myeloid populations analysed, aside from the monocytic MDSC populations (Figure 4.9, D). There was a reduction in CD4 T cells following aCSF alone, but no difference between tumours treated with irradiation alone or irradiation and aCSF (Figure 4.9, E).

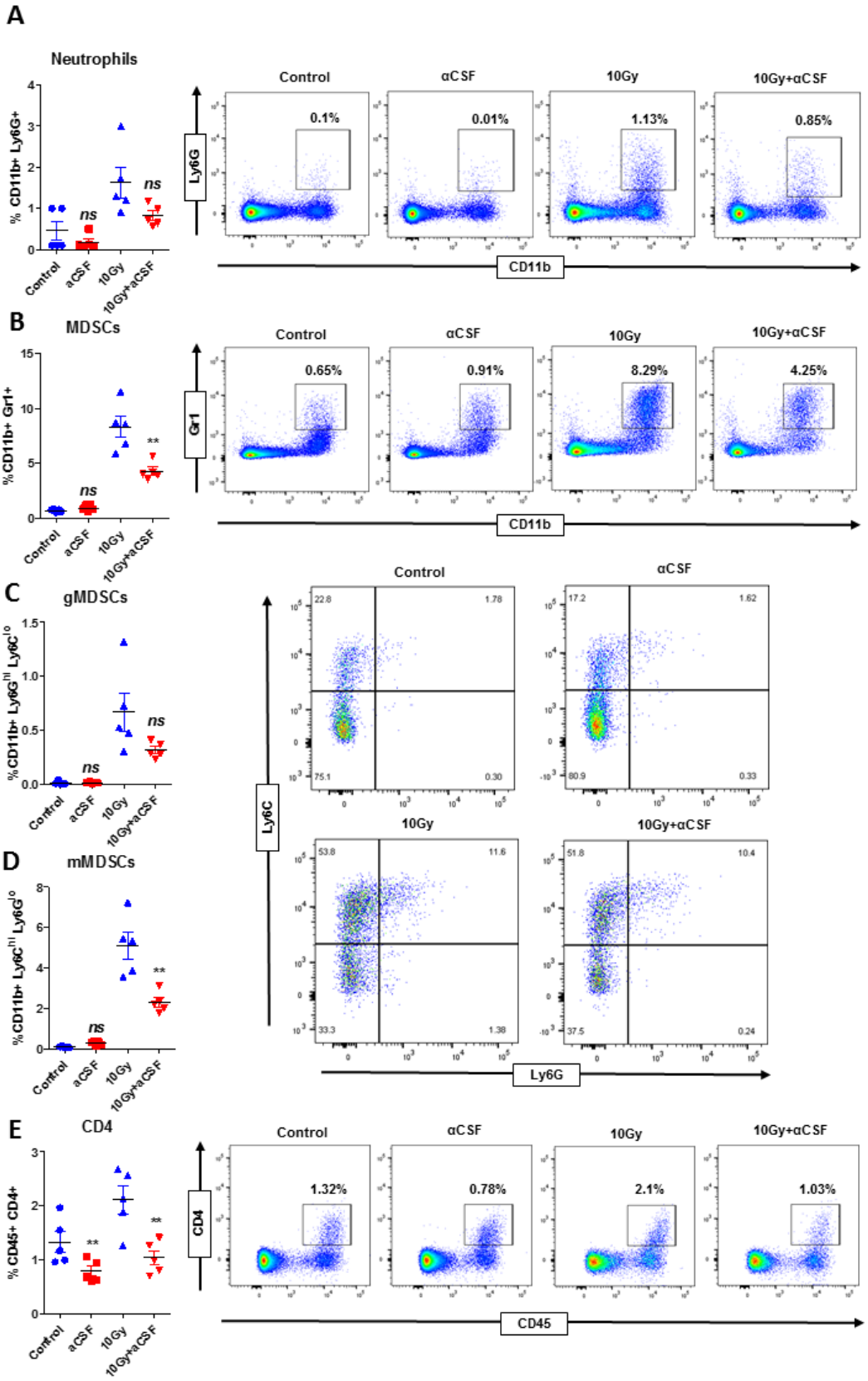


Figure 4.8 - aCSF is associated with changes in other immune populations in MC38 tumours

A-E - Flow cytometric analysis of immune cell populations in MC38 tumours 5 days following 10Gy irradiation, compared with control tumours. Immune populations were gated as indicated in the y axes. Total populations are expressed as a percentage of total cells analysed. Data are presented as mean ± SEM and statistical significance determined by one-way ANOVA.

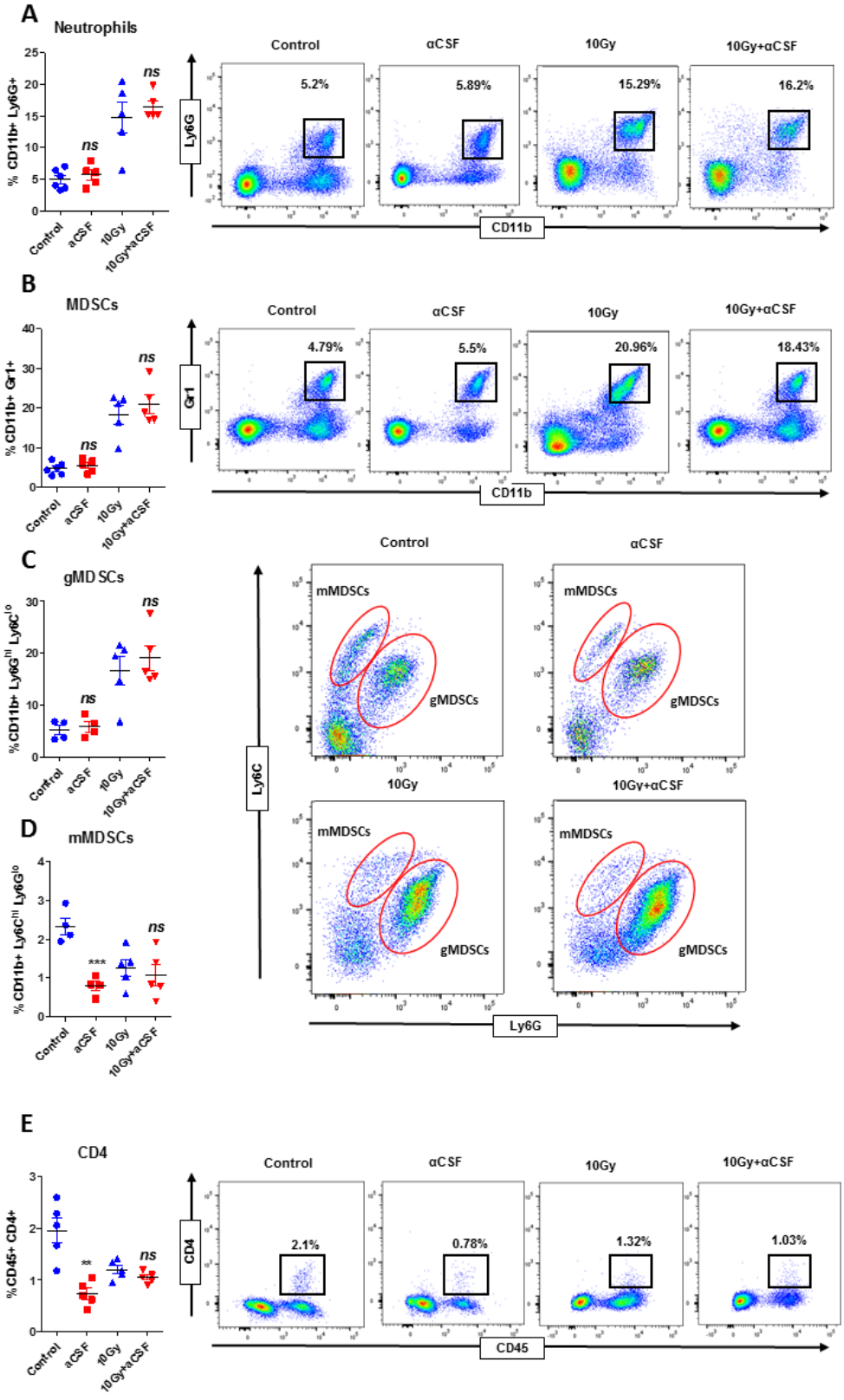


Figure 4.9 - aCSF is associated with changes in other immune populations in KPC tumours

A-E - Flow cytometric analysis of immune cell populations in MC38 tumours 5 days following 10Gy irradiation, compared with control tumours. Immune populations were gated as indicated in the y axes. Total populations are expressed as a percentage of total cells analysed. Data are presented as mean ± SEM and statistical significance determined by one-way ANOVA.

4.3.8 Tumour growth delay is CD8 T cell dependent

Due to the increases in CD8 T cell numbers in MC38 tumours, and central tumour penetrance, we questioned whether CD8 T cells mediated the increased tumour growth delay observed with aCSF treatment. To do this we repeated in vivo xenograft experiments in immune deficient mice (CD1-Nude), which lack T cells. We also repeated the experiments using the same syngeneic model (C57/BL6) with the additional administration of a CD8 blocking antibody. CD8 depletion was confirmed by flow cytometry (Figure 4.10 – Tumour growth delay following aCSF treatment is CD8 T cell dependent A). In both models the growth delay previously observed was completely abrogated. These data confirm that CD8 T cells mediate the tumour growth delay associated with aCSF treatment. Interestingly, increased growth rate was observed in MC38 tumours treated with aCD8 and 10Gy irradiation compared with irradiation alone (9 days vs 14 days). Whilst these were independent experiments and cannot be directly compared or statistically analysed, it does suggest that the effect of radiation on the growth delay in MC38 tumours may be partly CD8 T cell dependent. This was not the case in KPC tumours, which reflects the immunologically cold nature of these tumours [321].

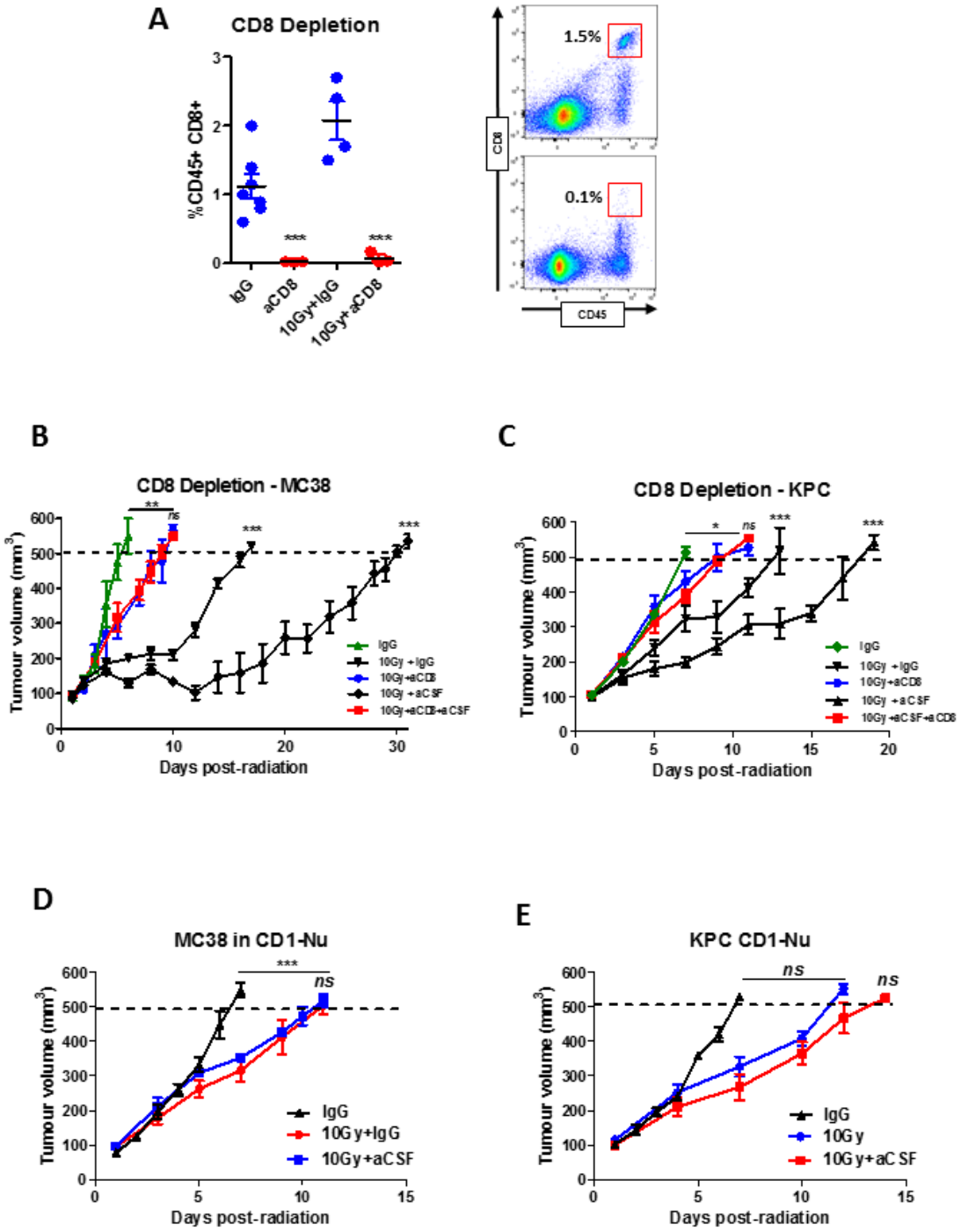


Figure 4.10 – Tumour growth delay following aCSF treatment is CD8 T cell dependent

To test whether tumour growth delay was dependent upon CD8+ T cells, wild-type mice received anti-CD8 antibodies to deplete CD8+ T cells. Mice then received treatment as outlined in Figure 4.4.

A - Confirmation of CD8 T cell depletion. aCD8 antibodies were administered when tumours reached 80mm3 (24 hours before irradiation). After three doses tumours were harvested and analysed by flow cytometry.

B-C, Tumour growth of MC38 (B) and KPC (C) tumours in C57/BL6 mice treated with aCD8 and 10Gy irradiation +/- aCSF. Data are presented as mean tumour volume ± SEM (8 mice/group). Data are presented as mean tumour volume ± SEM and analysed by one-way ANOVA with Tukey post-hoc adjustment. *P <0.05 **P <0.01 ***P <0.001.

D,E – Additional confirmation of CD8 T cell dependency was tested by reproducing the experiments in immunocompromised mice. Tumour growth of MC38 (D) and KPC (E) tumours in CD1-Nude mice treated with 10Gy

irradiation +/- aCSF. Data are presented as mean tumour volume ± SEM (8 mice/group). Data are presented as mean tumour volume ± SEM and analysed by one-way ANOVA with Tukey post-hoc adjustment. *P <0.05 **P <0.01 ***P <0.001.

4.3.9 Radiation stimulates specific adaptive immune priming

Despite significant increases in CD8 T cells in MC38 tumours after treatment with aCSF both with and without irradiation, there was no objective change in tumour growth. Therefore we asked whether radiation elicited tumour specific antigen priming. To determine this we used an ELISPOT assay (Enzyme Linked Immunospot Assay). This method quantifies T cell activity following exposure to antigens, and is widely used in vaccine research [322]. Briefly, systemic CD8 T cells isolated from the spleen of mice can be cultured with tumour cells in vitro and their activation measured by quantifying IFNγ secretion. IFNγ is released by CD8 T cells when they engage with a target antigen and they become activated. By exposing these T cells to naïve or irradiated MC38 tumour cell *ex vivo* it is possible to determine whether systemic T cells have unselected activity against tumour cells, or specifically against irradiated tumour cells. CD8 T cells isolated from mice bearing non-irradiated tumours showed slightly increased activity against irradiated MC38 tumour cells, but this was not statistically significant (Figure 4.11, A). CD8 T cells isolated from mice bearing irradiated tumours also showed slightly higher activity against irradiated tumour cells, but this was also not significant. However they were substantially more active against irradiated tumour cells (Figure 4.11, A). These results confirm that radiation is capable of generating systemic tumour specific immunity. This provides a possible explanation for the absence of any difference between mice treated with aCSF alone, despite having a significant CD8 T cell infiltrate. Therefore we conclude that TAM depletion is associated with increased CD8 T cell numbers present within tumours, however T cell priming is required to generate tumour specific cytolytic activity.

Another key step in the T cell priming cascade is antigen processing and presentation by antigen presenting cells (APCs). These APCs, which include dendritic cells and classically activated macrophages, present antigens via MHC class two (MHCII) molecules. CSF-1 receptors can be present on non-macrophage cells from the CD11b lineage, including dendritic cells (DCs), though they are less dependent upon CSF-1 for survival [323]. As key antigen presenting cells (APCs) we analysed MHCII+ DCs to ensure they were not targeted by CSF-1 blockade. Reassuringly, there was no decrease in MHCII+ DCs following anti-CSF treatment (Figure 4.11, D, E) We did identify a population of MHCII+ TAMs which were significantly reduced following anti-CSF treatment (Figure 4.11, B,C). To determine whether antigen priming was affected by the reduction in this population we performed an ELISPOT using T cells harvested from mice bearing naïve and anti-CSF treated

tumours (+/-radiation). There was no difference between irradiated tumour groups with or without anti-CSF, indicating that the reduction in MHCII TAMs did not appear to affect antigen presentation (Figure 4.11, F,G).

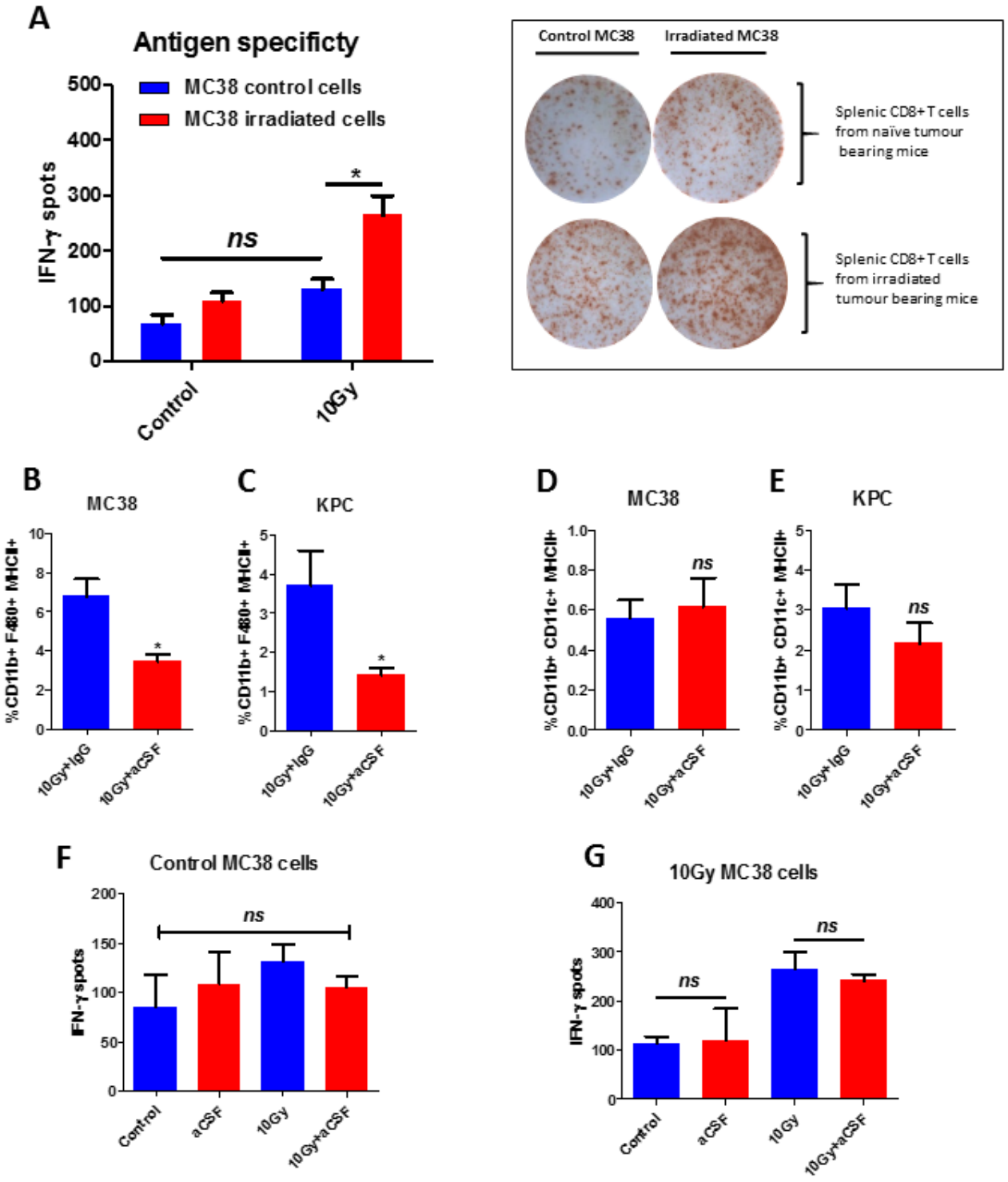


Figure 4.11 – Irradiation stimulates specific anti-tumour immunity

A – Quantification with representative images (right panel) of tumour specific immune response by CD8 T cells by ELISPOT. Splenic CD8 T cells were isolated from tumour bearing mice receiving either 0Gy (control) or 10Gy irradiation. MC38 cells were seeded into a 96-well plate 24 hours prior to CD8 isolation and treated with either 0Gy (control) or 10Gy irradiation. CD8 T cells were then co-cultured with tumour cells for 24 hours and IFNγ spots quantified. Data are presented as mean ± SEM and statistical significance determined by one-way ANOVA.

B,C – Quantification of MHC II+ TAMs present in MC38 (B) and KPC (C) tumours harvested 5 days following radiation. The gating strategy selected CD11b+ F480+ MHC II+ cells, presented as a percentage of the total cell population. Data are presented as mean ± SEM and statistical significance determined by unpaired t-test. D,E = Quantification of MHC II+ dendritic cells (DCs) present in MC38 (D) and KPC (E) tumours harvested 5 days following radiation. The gating strategy included CD11b+ F480- CD11c+ MHC II+ cells, presented as a percentage of the total cell population. Data are presented as mean ± SEM and statistical significance determined by unpaired t-test.

F,G – ELISPOT quantification of tumour specific immune responses with the addition of aCSF treated groups. Data are presented as mean ± SEM and statistical significance determined by one-way ANOVA.

4.3.10 Radiation stimulates the expression of major Histocompatibility Complex I (MHC I) on tumour cells

Having confirmed that radiation generated a T cell response that was specific to irradiated tumour cells, we sought to determine whether this was due to increased expression of MHC I on tumour cells. The presentation of antigens via MHC I antigen complexes is critical for recognition by T cell receptors (TCRs) and subsequent T cell killing. Increased MHC I expression may render tumour cells more recognisable by CD8 T cells, and previous studies with other cell lines show that it is increased following radiation [324–326]. In response to irradiation, MC38 tumour cells had significantly higher MHC I expression (Figure 4.12, A). KPC had much lower baseline MHC I levels (2000 vs 20,000 in MC38), and these did not change in response to irradiation (Figure 4.12, B). MHC I can be augmented by exposure to cytokines, including IFNγ, TNFα, IL-1b, which may be altered in the irradiated tumour microenvironment [327–329]. Thus, to determine if MHC I is differentially altered in response to irradiation *in vivo*, we analysed MHC I expression in MC38 and KPC xenografts 24 hours after 10Gy irradiation. There was a significant increase in MHC I expression in MC38 tumour cells present in xenografts, comparable to the increase observed in vitro (Figure 4.12, C). Interestingly, there was also a significant increase in MHC I expression on KPC cells (Figure 4.12, D). These results suggest that increased MHC I expression in MC38 tumour cells is an intrinsic cellular response. However augmentation of MHC I in KPC cells requires factors present within the irradiated tumour microenvironment.

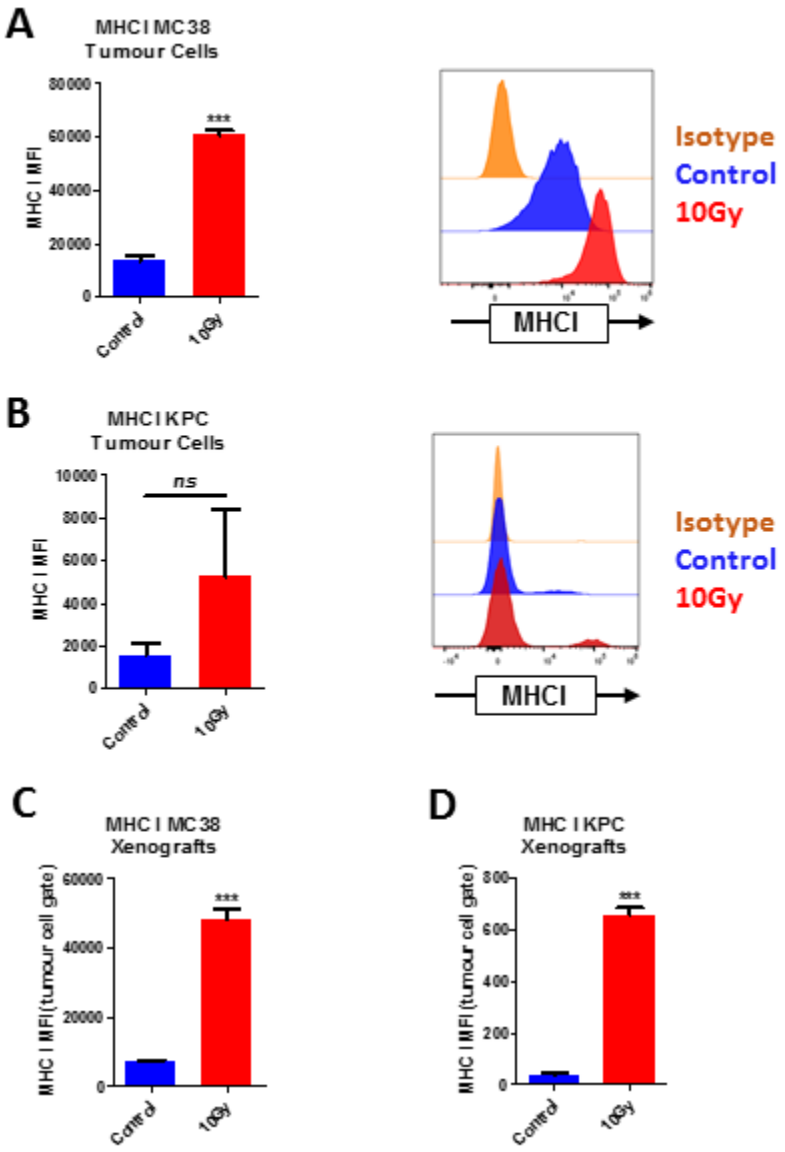


Figure 4.12 - Radiation stimulates the expression of MHC I on tumour cells

A,B - MC38 (A) and KPC (B) cells were treated with 10Gy irradiation and MHC I mean fluorescence intensity analysed by flow cytometry after 24 hours. Data are presented as mean ± SEM and statistical significance determined by unpaired t-test. Representative histograms are shown.

C,D – MHC I expression on tumour cells in MC38 (E) and KPC (F) tumours analysed by flow cytometry 24 hours after tumour irradiation. Tumour cells were determined by excluding CD45+ CD31+ CD140α+ cells. Data are presented as mean ± SEM and statistical significance determined by unpaired t-test.

4.3.11 Radiation induced antigen priming is sufficient to control distant tumours in aCSF treated mice

The results obtained thus far suggest that radiation may be responsible for systemic antigen priming. This raises the possibility the alterations in CD8 T cell numbers and spatial distribution require antigen priming in order to exert their cytotoxic anti-tumour effects. In order to test this *in vivo*, we generated two tumours in individual mice. This allowed targeted radiation treatment to a single lesion, and systemic aCSF treatment (Figure 4.13, A). This therefore allowed us to decipher whether alteration in the T cell infiltrate present in the non-irradiated tumour (as a result of systemic aCSF) could be activated against tumour cells by radiation of the contralateral tumour. This concept has been described in the literature as the so called 'abscopal' effect, referring to objective tumour responses in metastases distant to the irradiated lesion, which is thought to be immune mediated [330].

In mice bearing two MC38 tumours, treatment of the index lesion with 10Gy irradiation resulted in tumour growth stasis. There was no difference in the growth rate of the contralateral tumour compared with mice bearing untreated tumours (Figure 4.13, B). In mice treated with aCSF, radiation of the index lesion was associated with a significant delay in tumour growth of the contralateral, non-irradiated tumour (Figure 4.13, C). This growth delay was also significantly delayed compared with tumours in mice treated with aCSF alone (Figure 4.13, C).

In mice bearing two KPC tumours, treatment of the index lesion with 10Gy was not associated with growth delay in the contralateral tumour, which grew at a rate comparable to mice receiving no treatment (Figure 4.13, C). However in mice treated with irradiation and aCSF, there was a slight but significant reduction in tumour growth delay in the contralateral tumour (Figure 4.13, D).These results show that whilst irradiation is capable of inducing MCH I expression and antigen priming, delayed growth in distant tumours requires additional treatment. In our case, we previously demonstrated that aCSF was associated with augmented CD8 T cell infiltration. Therefore, if there is systemic radiation-mediated CD8 priming, the addition of aCSF may improve anti-tumour responses via improved CD8 infiltration.

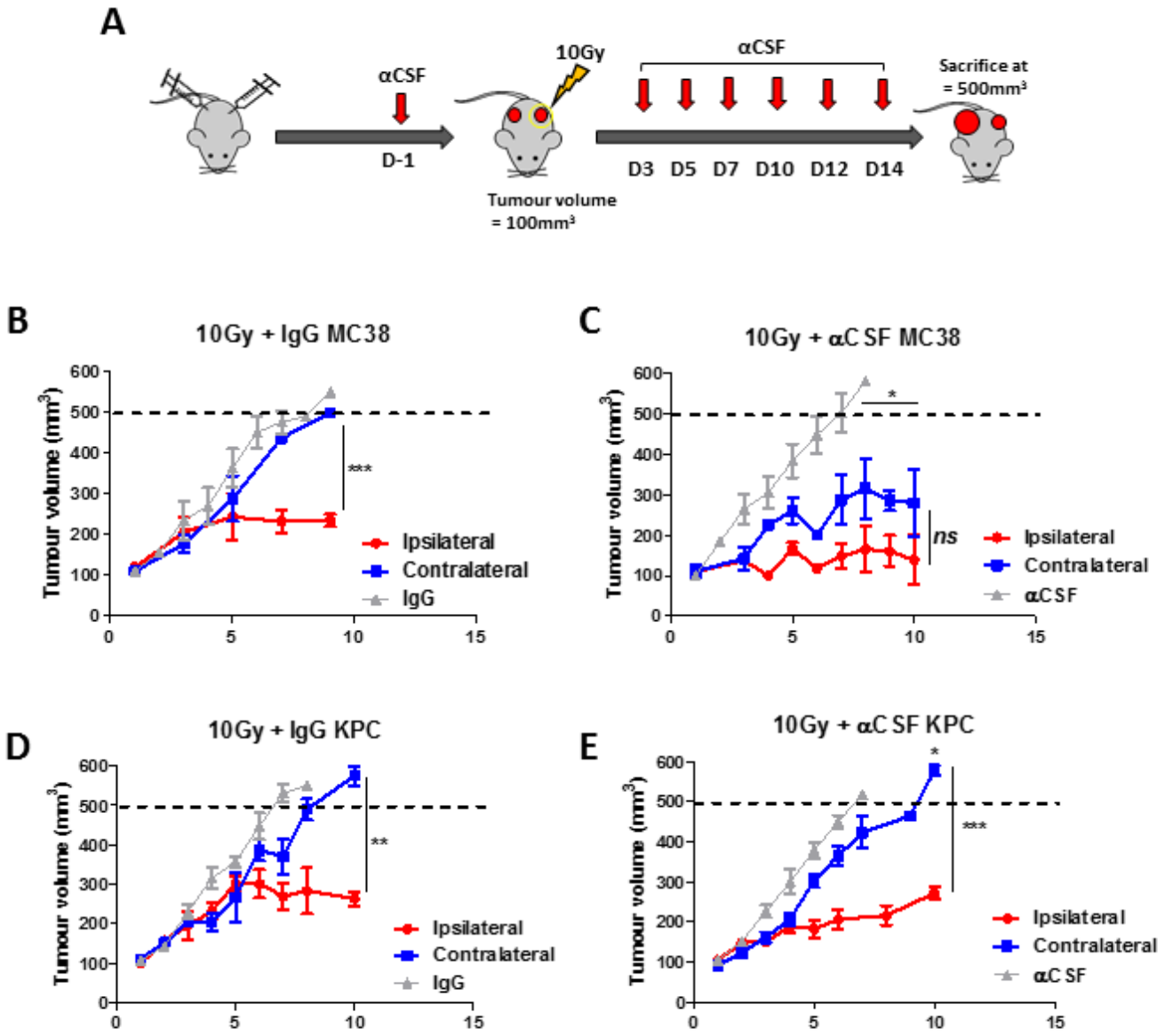


Figure 4.13 – Radiation induced antigen priming is not associated with control of distant tumours unless aCSF is concomitantly administered

A – Schema outlining treatment schedule. Mice were inoculated with tumour cells on both flanks and aCSF treatment initiated when tumours reached 80mm^3, and irradiation administered to a single lesion when tumours reached 100mm^3. Mice were only included if there was less than 20mm^3 size difference between tumours. Mice were culled when either tumour reached 500mm^3.

B, C – MC38 tumours treated with 10Gy irradiation to the index lesion and systemic aCSF as indicated. Data are presented as mean tumour volume ± SEM (8 mice/group). Mean tumour volume on the day that all mice were culled was compared by unpaired t-test.

D,E - KPC tumours treated with 10Gy irradiation to the index lesion and systemic aCSF as indicated. Data are presented as mean tumour volume ± SEM (8 mice/group). Mean tumour volume on the day that all mice were culled was compared by unpaired t-test.

4.4 Discussion

In this chapter, we have shown that aCSF is effective at depleting TAMs. This was the case in naïve tumours as well as those with a CSF-1 driven increase in TAMs. A subset of TAMs was refractory to treatment, and repolarised towards an inflammatory phenotype. We also show that tumour control following combination therapy was CD8 T cell dependent. The lack of any response in non-irradiated tumours, despite increased CD8 T cell numbers, led us to investigate the whether the response was dependent upon radiation induced antigen priming. We subsequently found that irradiation generated systemic T cell priming and combination therapy was able to control distant tumours.

4.4.1 aCSF is associated with a reduced TAM numbers and changes in their phenotype

In our hands treatment of mice with aCSF reduced TAMs by approximately half. Whether aCSF itself is only partially effective, or whether there are redundant mechanisms of recruitment or whether a subset of macrophages are resistant to CSF1 depletion remains to be determined. Given previous observations by Pyonteck et al, it is possible that other factors within the tumour microenvironment support the ongoing survival of some TAMs [169]. Results from the cytokine array do show increases in any of the candidate factors, including GM-CSF and CCL2. However as this was performed in vitro with tumour cells, it does not account for cytokines produced by other stromal cells, or indeed macrophages themselves, in tumours. Alternatively, these macrophages may be more resistant due to reduced CSF-1R expression. We did not measure CSF1R expression on TAM subsets, but a previous report from Zhu et al showed reduced expression on $CD206^{lo}$ TAMs compared with $CD206^{hi}$ TAMs. Nonetheless,TAMs were still significantly reduced. Interestingly, and common amongst previous reports, aCSF did not deplete TAMs to levels seen in non-irradiated tumours [291,292]. It is possible that aCSF is less efficacious in the presence of significantly increased levels of CSF-1 following irradiation. OR...

When we looked at the response of $iNOS^{hi}$ versus CD206+ TAMs, there was variable response compared with the consistent reduction in the CD206+ populations. Interestingly, in MC38 tumours, aCSF led to a decrease in $iNOS^{hi}$ TAMs, but following irradiation and aCSF they were increased. $iNOS^{hi}$ TAMs in KPC tumours were refractory to aCSF blockade both with and without

radiation. It is not possible to determine whether this iNOS^{hi} population is present before aCSF, and is resistant, or if the remaining TAMs following aCSF undergo repolarisation in response to CSF-1 blockade. CSF-1 is capable of inducing M2-like macrophage polarisation. Fleetwood et al show that CSF-1 stimulated cultured macrophages upregulated IL-10 and CCL2, and downregulated inflammatory genes [331]. It is therefore possible that blocking the CSF-1 stimulus reprograms macrophages to an inflammatory phenotype. These results are consistent with a report from Seifert et al where aCSF was combined with radiation in murine pancreatic cancer. Although they used MHC II as a M1 marker, this populations were also resistant to aCSF1 treatment [291]. Similarly, Zhu et al showed preferential targeting of CD206+ TAMs, with higher numbers of dead cells following aCSF [315]. Another interesting feature of their study was the direct comparison between a small molecule inhibitor of CSF-1R (PLX3397) with aCSF monoclonal antibody. There were no significant differences between these agents in terms of TAM depletion, repolarisation or tumour growth.

Analysis of gene expression in TAMs isolated from tumours provided further evidence that TAMs were repolarised in response to aCSF. There was a consistent reduction in most markers of immunosuppression, and an increase in pro-inflammatory genes. It is important to consider the methodological approach when interpreting these data. Due to the low numbers of TAMs following aCSF, raw populations of CD11b+ F480+ gated cells were isolated by FACS and analysed by qPCR. This population will contain a heterogeneous population of both iNOS^{hi} and residual CD206+ TAMs. Therefore it is possible that if we had selectively isolated iNOS^{hi} TAMs, gene expression profiles may be skewed even further towards an inflammatory phenotype. Unfortunately, again due to the low numbers of TAMs isolated by FACS from aCSF tumours, we were unable to perform functional assays to determine whether their suppressive capacity was reversed. To do so would have required a proibitively large number of animals. This was achieved by Zhu et al, who showed that the refractory populations of TAMS in aCSF treated tumours were significantly less suppressive compared with those from untreated tumours [315].

Until recently, most TAM depletion agents did not discriminate between anti-tumour M1 TAMs and pro-tumour M2 TAMS. Results from our work as well as others suggest that retaining a population of pro-inflammatory TAMs may be beneficial for potentiating anti-tumour responses. A landmark paper by Kaneda et al in 2016 demonstrated that phosphoinositide 3-kinase gamma (PI3Kγ) was responsible for the switching of macrophages from an inflammatory to a suppressive

phenotpye [332]. The gamma isoform of PI3K is abundantly and almost uniquely expressed in myeloid cells and promotes recruitment to sites of inflammation [333,334]. PI3Kγ inhibition, via a small molecule inhibitor (IPI-549), led to significant shift towards an inflammatory phenotype in vitro. They showed that PI3Kγ signalling inhibited NFkB activation, but stimulated C/EBP-β. This was reversed following inhibition and led to increased expression of inflammatory genes and reduced immunosuppressive capacity. Importantly, when administered in vivo, total TAM numbers remained unaltered, but were repolarised. This was associated with delayed tumour growth, with an increased CD8 T cell response and augmentation of immune checkpoint blockade. Soon after this, another study showed improved efficacy of immune checkpoint blockade across a range of tumours models, which was dependent upon myeloid cell repolarisation [296].

In summary, we show that aCSF is associated with a significant reduction in TAMS, and repolarisation in a small refractory population. This was in turn associated with a significantly increased tumour growth delay following irradiation.

4.4.2 Tumour growth delay is CD8 dependent

The immunosuppressive function of TAMs was revealed by their depletion. aCSF does not directly target T cells, yet depletion of macrophages led to significant increases in T cell infiltration. In aCSF treated mice bearing MC38 tumours, there was a two-fold increase in $CD8^+$ T cells. Consistent with other reports, we found very few $CD8^+$ T cells in KPC tumors (~0.15%) and no detectable increase following aCSF. Tumour penetration was evident in the central region of the tumors where T cells were absent in untreated KPC tumors. The presence of T cells at the tumor core compared with tumor margins is associated with improved outcomes in patients [319,335]. This is particularly evident in highly stromal tumours where T cells need to reach the tumour colonies to engage with the tumour cells. Others have also reported the surprising ability of very few T cells to mount a potent immune response in KPC tumors [321]. Generally, T cell numbers increase following CSF-1(R) blockade in a variety of tum**ou**r models, but this rarely results in growth inhibition without additional therapies [291,336–339]. For example Zhu et al found that combining CSF1R blockade with anti-CTLA4 or PD-L1 resulted in significant growth inhibition in orthotopic pancreatic tumors [338]. Holmgaard et al used the same

agent in combination with indoleamine 2,3-dioxygenase (IDO) inhibitors [337], and Mok et al found that CSF1R blockade significantly improved CD8 T cell infiltration and activity following adoptive T cell therapy [336]. Other investigators have combined macrophage depletion with conventional chemotherapy regimens to improve tumour control [234,340]. There is consensus amongst these reports that greater T cell activity was due to a reduction in suppressive macrophages, however the exact mechanism remains unclear. Radiation stimulates the expression of T cell chemokines, but the chemoattractant gradient may be limited by the secretion of highly suppressive cytokines by myeloid cells [88,89]. Alternatively, the reprogramming of TAMs in response to depletion therapy may result in macrophage derived T cell chemokine secretion. This was noted to be the case following aCSF-1R treatment in the refractory TAM population [341].

We confirmed the dependency of the response on CD8 T cells by repeating studies in immune deficient mice as well as by CD8 depletion in wild-type mice. In both models there was complete abrogation of he previously observed growth delay, indicating that the anti-tumour response was dependent upon T cells. Therefore we conclude that TAM depletion permits increased T cell penetration into tumours, which is associated with increased tumour growth delay. The exact mechanisms behind the observed increases in T cell numbers and distribution remain unclear.

4.4.3 Combination therapy is required to achieve out-of-field responses

Strikingly, despite increased T cell infiltration resulting from aCSF alone, we did not observe anti-tumor activity unless aCSF was combined with radiation. One possibility which would explain this observation is that radiation is acting to augment the adaptive immune system to become primed towards tumour specific antigens. Therefore, despite being increased in number, the T cells present in aCSF treated tumours may fail to mount effector responses due to a lack of tumour antigen specificity. We demonstrated that radiation was capable of generating systemic immunity, and that T cell activity was specific to irradiated tumour cells. The dependency of radiation on T cell activation via antigen cross-presentation in order to exert its ablative effect has been demonstrated in a limited number of previous studies. Sharabi et al used T cells with a receptor specific to ovalbumin (OT-1 OVA) and demonstrated that irradiation of MC38-OVA cells in vitro resulted in increased T cell activity during co-culture. This suggests that radiation is able to illicit direct antigen presentation in the absence of professional APCs [342]. Using the same T cells (OT-1), they pulsed APCs with conditioned

medium from irradiated B16-OVA cells. This did not elicit a T cell response, which suggested that antigen presentation was the dominant activating mechanism. However to explore this in vivo they injected mice with B16-OVA cells, and following tumour irradiation dendritic cells from tumour-draining lymph nodes were analysed. Expression of SIINFENKL (MHC I OVA peptide complex) was significantly increased on the DCs isolated form irradiated tumours, suggesting that APC cross-presentation also takes place following irradiation. Lee et al adoptively transferred SIY T cells, which recognise B16-SIY tumour cells, to show increased proliferation by CFSE dilution in the tumour draining lymph nodes after irradiation [343]. Lugade et al used B3Z T cells which recognise the $OVA_{257-264}$ peptide to show that DCs isolated from irradiated tumour draining lymph nodes stimulated B3Z T cells to a greater extent than those isolated form control mice [344]. Interestingly, whilst fractionated radiation (5x3Gy) was associated with increased activity, activity following single dose (15Gy) was greater still. The use of foreign antigen expressing cells has its limitations as it may overestimate the extent of the response. However, Lugade also examined responses directed against the endogenous B16 tumour antigen TRP-2. ELISPOT analysis showed activity directed against OVA peptides was equal to that against this endogenous peptide [345]. These observations are consistent with our ELISPOT results, which demonstrated that T cells isolated from mice bearing irradiated tumours showed increased activity against irradiated tumour cells. Together, these data suggest that radiation can elicit antigen specific immune responses, both directly via MHC I, and also indirectly via increased APC cross-presentation.

We also confirmed that radiation significantly increased MHC I expression on the surface of tumour cells, which could result in improved direct antigen presentation and stimulation of primed T cells. The mechanism by which radiation causes increased MHC I expression is still not completely understood. Radiation has been shown to increase the intracellular peptide pool, which coincides with increased MHC I expression. Whether MHC I increases in response to increased intracellular peptide pooling is not known. The specificity of T cells that are primed following irradiation implies that distant, non-irradiated tumours would be unaffected by systemically primed T cells. We tested this by irradiating one of two tumours implanted into mice. As expected, non-irradiated tumours were unaltered and grew at a rate comparable with tumours in naïve mice. This was the case for both MC38 and KPC models. We also tested this following systemic aCSF therapy. Strikingly, in the MC38 model, distant tumours grew at a significantly slower rate, though not to the extent observed in

tumours receiving direct irradiation. A slightly slower, but significant rate was also observed in distant KPC tumours. Because aCSF is administered systemically, the non-irradiated tumour still benefits from macrophage depletion. Conceivably, if this is associated with increased CD8 T cell infiltration, one might expect improved anti-tumour immunity. However, our previous experiments showed that in the absence of tumour irradiation, increased CD8 T cells did not confer any benefit. This suggests that there is an element of priming which involves antigens conserved between naïve and irradiated tumour cells. In support of this, we did observe a relative increase in activity against naïve tumour cells by T cells from irradiated hosts, though this did not reach statistical significance. This would explain the partial response seen in the distant tumours. This phenomenon was explored by Dovedi et al using fractionated radiation with and without anti-PD-1 treatment using a double tumour model. When radiation was delivered alone to the index lesion, there was a limited response in tumours outside of the radiation field. However when combined with radiation, there were significantly more CD8 T cells in the out-of-field tumour, which was also associated with an increased regression rate. Importantly, whilst PD-1 monotherapy increased CD8 T cell numbers, irradiation was required to generate a response. Although the treatment here is different to aCSF, it does highlight the need to facilitate CD8 T cell infiltration in order to unleash immunity in out-of-field tumours.

Alternatively, this phenomenon could potentially be explained by the process of epitope spread. Epitope spread has been observed following vaccination, where clonal expansion occurs with TCRs specific to antigens other than those in the vaccine [346,347]. This phenomenon has been observed in vaccine based oncology trials, where it is thought the initial expansion of a single clone (vaccine driven) initiates a cascade of events characterised by the presentation of previously subdominant antigens [348]. It is possible that, acting as a vaccine, the immunity generated following direct tumour irradiation generates both an antigen specific and generalised anti-tumour immune response. Interestingly, a in the same paper mentioned previously by Dovedi et al, they also analysed the T cell receptor clonal repertoire in lymphocytes present in primary tumours as well as those outside of the radiation field. There was a variable response rate amongst tumours outside of the radiation field, but some tumours did regress. Analysis of the T cell repertoire revealed that clonality was significantly increased in the irradiated tumour, but not in the out-of-field tumour. However when combined with anti-PD-1, there was increased regression in the out-of-field tumours which corresponded with increased clonality conserved from the findings in the irradiated tumour. Using

FTY-720, which inhibits emigration of T cells from lymphoid tissues, they demonstrate that incumbent T cells following combination treatment make a significant contribution. Therefore combination therapy is required to improve CD8 trafficking, which augments the response in non-irradiated tumours. These findings are in keeping with a previous study demonstrating abscopal effects in a pre-clinical model, which was dependent upon Flt33 mediated dendritic cell activation [330]. Taken together, these reports show that abscopal tumour regression may require additional treatments in order to augment T cell infiltration.

In summary, we show that radiation alone is insufficient to generate anti-tumour immunity in distant, non-irradiated tumours. However, in keeping with other reports, additional systemic therapy that increases T cell trafficking may overcome resistance.

5. CHAPTER 5: Immune checkpoint blockade is required for tumour rejection

5.1 Introduction

Our results thus far suggest that radiation may contribute to the generation of adaptive immunity targeted against tumour specific antigens. Effective tumour clearance may be limited by an increase in immunosuppressive macrophages. Depletion of these macrophages permitted increased numbers of CD8 T cells to enter and engage with tumour cells. Despite this, all tumours were eventually refractory to treatment with combination therapy. One of the final steps in immunogenic cell death is effective cytolytic killing by CD8 T cells. For this to happen, CD8 T cells need to engage with tumour cells via MHC I antigen complexes and T cell receptors. At this stage, interaction of immune checkpoint molecules with ligands present on T cells can thwart CD8 killing and cause T cells to be deactivated and anergic. Therefore we questioned whether the expression of immune checkpoints on tumour cells limited effective immunity in our models.

Immune checkpoints belong to a family of molecules (B7) expressed on antigen presenting cells and are involved in immune regulation. These co-stimulatory and co-inhibitory signals help strike the balance between effective immunity, and the prevention of auto-immunity. Fine tuning of T cell responses is essential in order to avoid normal tissue damage during immune responses, and to ensure self-tolerance. The first step in T cell activation is the recognition of MHC I presented peptides on target cells by T cell receptors. In the absence of this first step, co-stimulatory molecules are functionally inactive [349]. One of the most extensively studied signalling pathways is the CD80/CD86 molecules, and their receptors CD28/CTLA-4. CD28 is the prime co-stimulatory pathway, leading to T cell activation. It shares its ligands (CD80/CD86) with CTLA-4, which is a co-inhibitory molecule. CD28 is constitutively expressed by T cells and essential for their activation. CTLA-4 on the other hand is expressed at low levels on naïve T cells but it localised to the plasma membrane following activation [350]. The dynamics of the relationship between CD28 and CTLA-4 are still not fully elucidated. However significance of the suppressive effects of CTLA-4 were shown when mice lacking CTLA-4 developed massive lethal lymphoproliferation [351]. Along with the possibility of inducing autoimmunity, these results produced scepticism at the prospect of therapeutically targeting CTLA-4. However Leach et al demonstrated enhanced anti-tumour immunity in pre-clinical models involving immunogenic cell lines

[352]. CTLA-A targeting antibodies have since demonstrated therapeutic efficacy in clinical trials and Ipilimumab was approved by the Federal Drug Authority for use in melanoma in 2011.

Another widely studies member of the B7 family is the co-inhibitory receptor programmed death 1 (PD-1). It negatively regulates T cell activity following binding to its receptors programmed death-ligand 1 and 2 (PD-L1/PD-L2). PD-1 binding to PD-L1/2 inhibits cytotoxic activation of T cells as well as proliferation [353]. The consequence of CTLA-4 and PD-1 binding overlap, however there are some differences in the pattern and temporality of both molecule and receptor expression. Firstly, unlike CTLA-4, the ligand for PD-1, programmed death-ligand 1 (PD-L1), is present on cells other than professional antigen presenting cells, such as myeloid cells, other stromal cells and epithelial cells [354]. In addition, it is widely expressed on tumour cells [355–357]. CTLA-4 appears to be important during the priming phase of T cell activation, compared with PD-1 which is functional during the effector stage within the target tissue [353]. Engagement with target cells and activation further increases PD-1 expression, giving rise to the so called 'exhausted' phenotype characterised by high PD-1 expression [358]. Also of interest and relevance to our work is the higher affinity PD-1 has for PD-L2, expressed on macrophages and dendritic cells [359]. Whilst many other checkpoint molecules are actively being investigated, CTLA-4 and PD-1 are currently the most widely characterised. We chose to focus on the PD-1 pathway. This is for several reasons. Firstly, TAMs are known to constitutively express PD-L2 and are one of the only sources of PD-L2. Given the significant increase in TAMs after radiation, it is possible that they make a significant contribution to the total pool of PD-L1 present within tumours. Also, it has recently been demonstrated that PD-L1 is upregulated on tumour cells in response to radiation [54,79,360]. Hence, radiation potentially has the dual effect of increasing PD-L1 rich TAMs, in addition to PD-L1 on tumours cells. Therefore we questioned whether blocking PD-L1 could further augment the CD8 T cell response seen following TAM depletion.

5.2 Aims

1. Does radiation increase the expression of immune checkpoint molecules on tumour cells?
2. Does immune checkpoint blockade improve the response to radiation in macrophage depleted tumours?

5.3 Results

5.3.1 Radiation induces upregulation of PD-L1 on tumour cells

Thus far, we have shown that irradiation combined with macrophage depletion via aCSF significantly delays tumour growth beyond what is seen with radiation alone. We have shown that this in part may be due to increased antigen presentation along with improved CD8 penetration into tumours. These results suggest that adaptive immunity via CD8 cytolysis may be responsible for the anti-tumour effects. Despite combination treatment, all tumours eventually recurred and we did not observe regression. Therefore we questioned whether immunity is further limited at the T cell interface by the expression of immune checkpoint molecules on the surface of tumour cells. We first analysed the expression of PD-L1 on tumour cells *in vitro*. 24 hours following 10Gy irradiation PD-L1 expression was significantly elevated on MC38 and KPC cells (Figure 5.1- Radiation stimulates PD-L1 expression on tumour cells A,B). To confirm these findings in vivo, we analysed the expression of PD-L1 on gated tumours cells (CD45- CD31- CD140α) in tumours treated with 10Gy irradiation. 24 hours after irradiation PD-L1 was again significantly elevated on both MC38 and KPC tumour cells.

As macrophages can also be a source of PD-L1 and are one of the only sources of PD-L1 we analysed their expression on the surface of TAMs in MC38 tumours. TAMs abundantly expressed PD-L1 and PD-L2, therefore we analysed mean fluorescent intensity (MFI). Levels of PD-L1 and PD-L2 did not significantly change following irradiation. However due to the substantially increased number of TAMs following radiation, they are still a potentially important source of tumoural PD-L1 and PD-L2.

aCSF has previously been shown to be associated with increased PD-L1 expression on tumour cells, thought to be due to effector T cell interferons [80,341]. Consistent with these reports, we detected increased PD-L1 on MC38 tumour cells following aCSF (Figure 5.1- Radiation stimulates PD-L1 expression on tumour cellsG). Treatment with recombinant IFNγ confirmed the sensitivity of both tumour cells lines (Figure 5.1- Radiation stimulates PD-L1 expression on tumour cells

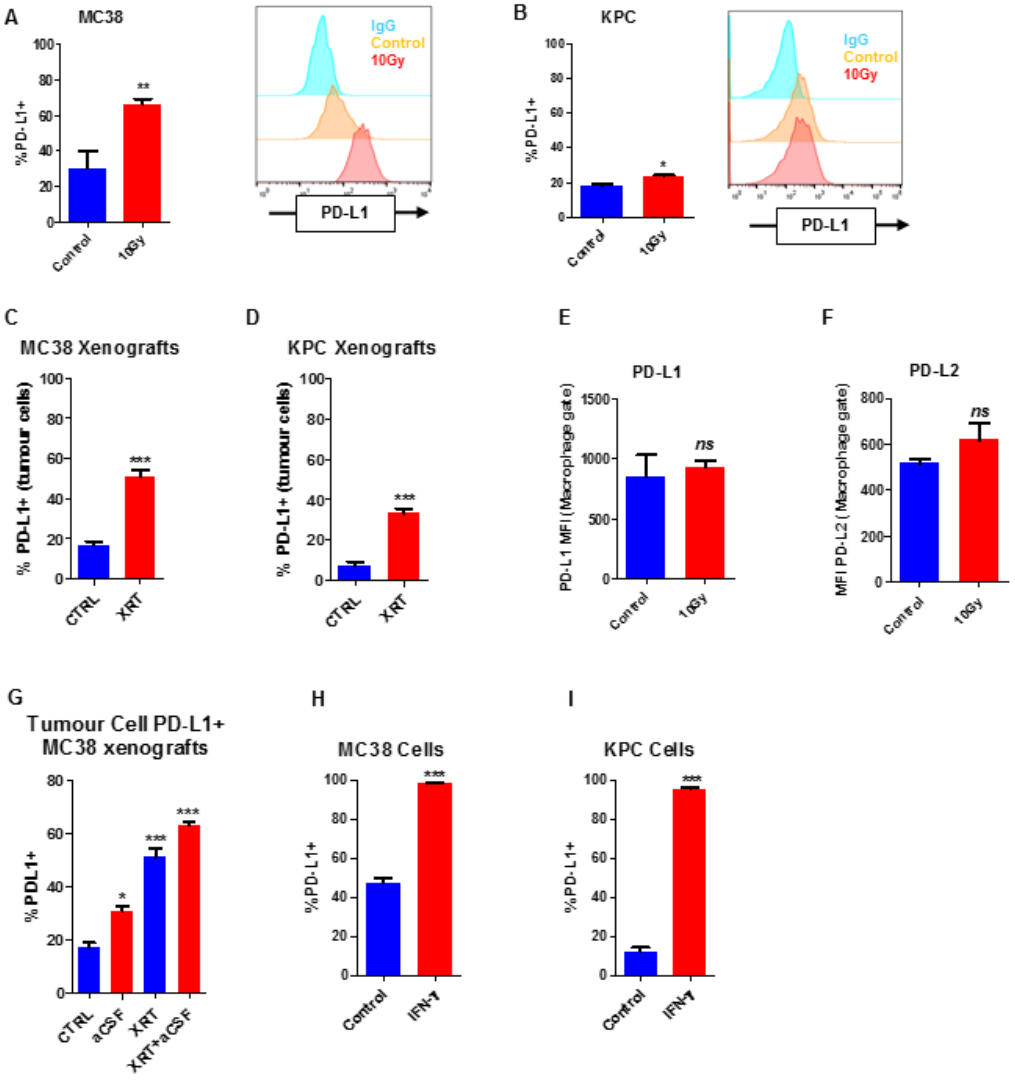


Figure 5.1- Radiation stimulates PD-L1 expression on tumour cells

A, B – PD-L1 expression on the surface of tumour cells was quantified by flow cytometry 24 hours after 10Gy irradiation. Representative histograms are shown. Data are shown as mean ± SEM and statistical significance determine by unpaired t-test.

C,D – PD-L1 expression was analysed on the surface of tumour cells (CD45- CD31- CD140α-) *in vivo.* Tumour were harvested 24 hours after 10Gy irradiation to the tumour. Data are shown as mean ± SEM and statistical significance determine by unpaired t-test (5 mice/group).

E,F – PD-L1 and PD-L2 mean fluorescence intensity was quantified on TAMs in MC38 tumours 24 hours after 10Gy irradiation to the tumours. Data are shown as mean ± SEM and statistical significance determine by unpaired t-test (5 mice/group).

G – PD-L1 expression on gated tumour cells in mice receiving treatment as indicated. Data are shown as mean ± SEM and statistical significance determine by one-way ANOVA (5 mice/group).

H-I – PD-L1 expression on tumour cells after 24 hours treatment with recombinant IFNγ quantified by flow cytometry. Data are shown as mean ± SEM and statistical significance determine by unpaired t-test.

5.3.2 Immune checkpoint blockade combined with radiation shows a variable response in vivo

Before testing a combination strategy combining irradiation, aPD-L1 and aCSF, we first determined whether aPD-L1 alone was sufficient to control tumours. If this was the case, there would be no rationale for triple therapy. In mice bearing MC38 tumours, the addition of aPD-L1 did not significantly slow tumour growth compared to those treated with IgG (Figure 5.2 Radiation combined with immune checkpoint blockade shows a variable response in vivo A). In mice treated with a combination of irradiation and aPD-L1, two divergent groups emerged within a few days. A subset of mice (50%) continued to grow, albeit at a slower rate than the irradiation alone group, reaching end point approximately 3 days later. Tumours in the remaining mice (50%) rapidly regressed and were undetectable one month later (Figure 5.2 Radiation combined with immune checkpoint blockade shows a variable response in vivo A). the mice used in each experiment are derived from the same generation genetically inbred animals. Provided that there is no deviation from the treatment protocol, it was somewhat surprising to see such a heterogeneous response. Clinical trials of immune checkpoint blockade therapy often present their results in a waterfall plot for this very reason. Interestingly, pre-clinical studies investigating checkpoint blockade often use individual growth curves for each animal due to variable responses [361–363]. Furthermore, Twymant-Saint et al used peripheral CD8 phenotyping to predict objective tumour responses in a murine melanoma model [364].

In mice bearing KPC tumours, the addition of aPD-L1 alone or in combination with irradiation did not significantly delay tumours growth. These results demonstrate that MC38 tumours are partially controlled by aPD-L1 checkpoint blockade when combined with radiation, with a subset of tumours completely regressing. However KPC tumours were completely refractory both with and without tumour irradiation.

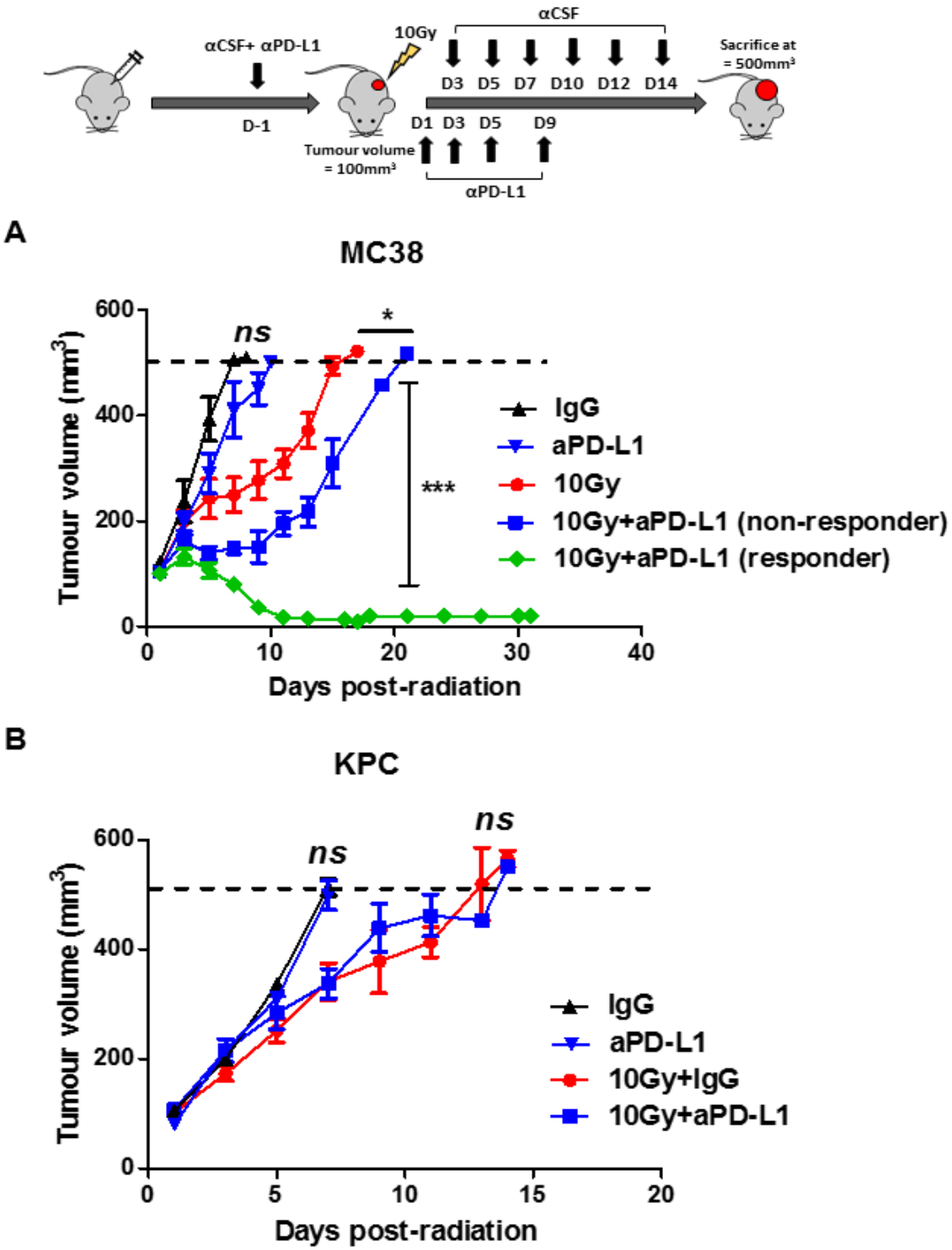


Figure 5.2 Radiation combined with immune checkpoint blockade shows a variable response in vivo.

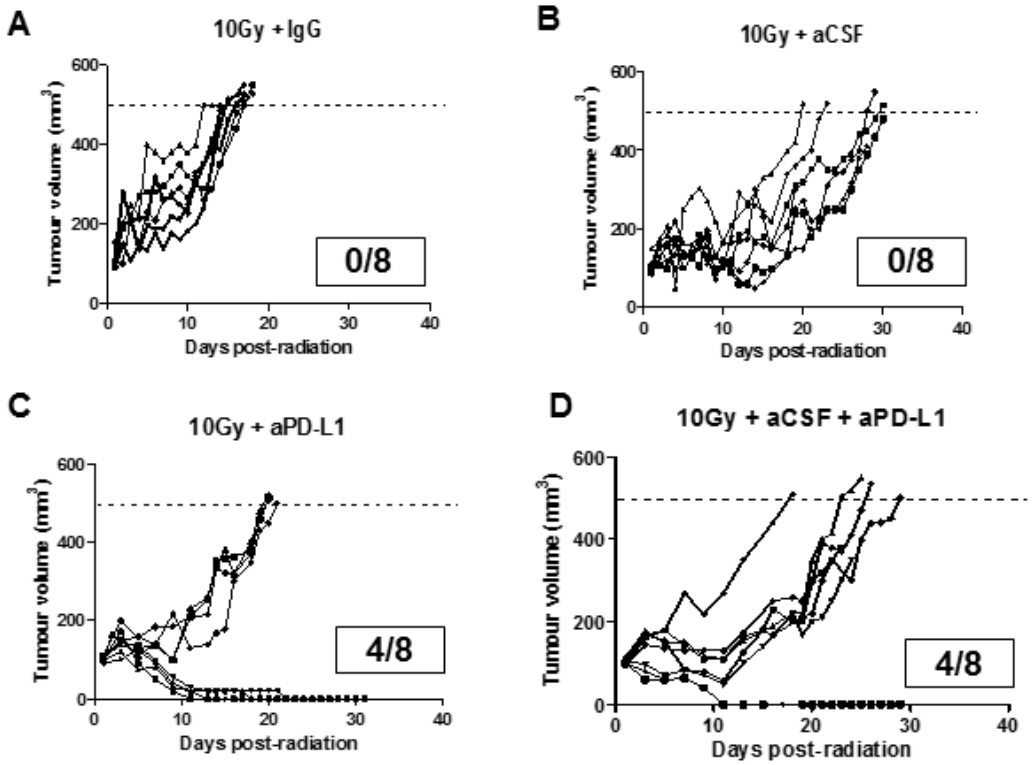
A – Tumour growth of MC38 tumours in wild-type C57/BL6 mice treated with IgG, aPD-L1, 10Gy or 10Gy and aPD-L1. Antibody treatment was initiated when tumours reached 80mm3 and irradiation delivered when tumours reached 100mm^3. Data are presented as mean tumour volume ± SEM. Statistical significance was determined by comparing the number of days to reach end-point by one-way ANOVA. Data are representative of two independent experiments with 8 mice per group. The group receiving 10Gy and aPD-L1 were split into a responder (blue squares) and partial responder (green diamond) group.

B - Tumour growth of KPC tumours in wild-type C57/BL6 mice treated with IgG, aPD-L1, 10Gy or 10Gy and aPD-L1. Antibody treatment was initiated when tumours reached 80mm3 and irradiation delivered when tumours reached 100mm^3. Data are presented as mean tumour volume ± SEM. Statistical significance was determined by comparing the number of days to reach end-point by one-way ANOVA. Data are representative of two independent experiments with 8 mice per group.

5.3.3 Triple combination therapy with radiation, aCSF and aPD-L1 lead to tumour regression in a subset of KPC tumours

Having confirmed that aPD-L1 was only partially effective against MC38 tumours, and ineffective at controlling KPC tumours, we asked whether treatment with irradiation combined with aPD-L1 and aCSF could further improve anti-tumour responses. In MC38 tumours, treatment with aCSF and aPD-L1 did not improve tumour control compared to either agent alone (Figure 5.3, B-D). However in KPC tumours, irradiation combined with aCSF and aPD-L1 led to tumour regression sin 3/8 mice (Figure 5.3, H). This is compared with no regression observed in any of the other groups (Figure 5.3, E-G).

MC38


A
10Gy + IgG
Tumour volume (mm3)
Days post-radiation
0/8
B
10Gy + aCSF
Tumour volume (mm3)
Days post-radiation
0/8
C
10Gy + aPD-L1
Tumour volume (mm3)
Days post-radiation
4/8
D
10Gy + aCSF + aPD-L1
Tumour volume (mm3)
Days post-radiation
4/8

KPC

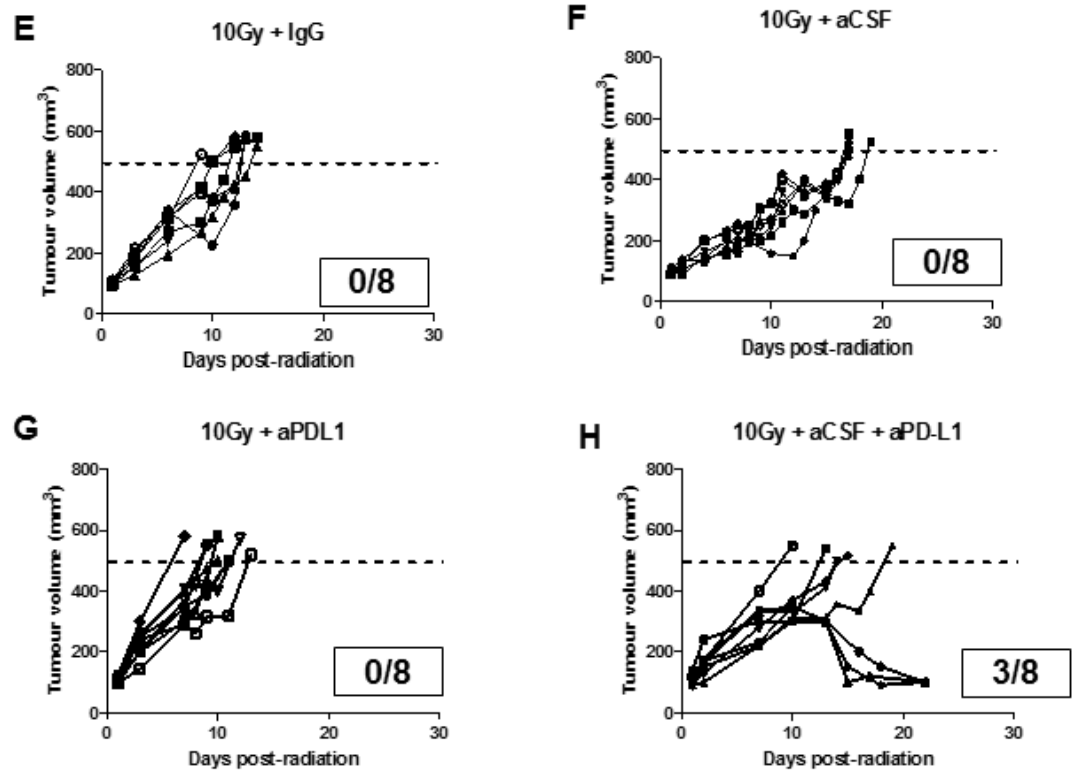

E
10Gy + IgG
Tumour volume (mm3)
Days post-radiation
0/8
F
10Gy + aCSF
Tumour volume (mm3)
Days post-radiation
0/8
G
10Gy + aPDL1
Tumour volume (mm3)
Days post-radiation
0/8
H
10Gy + aCSF + aPD-L1
Tumour volume (mm3)
Days post-radiation
3/8

Figure 5.3 Triple combination therapy with radiation, aCSF and aPD-L1 lead to tumour regression in a subset of KPC tumours

A-D – MC38 tumour growth in mice receiving 10Gy + IgG (A), 10Gy + aCSF (B), 10Gy + aPD-L1 (C) or 10Gy +aPD-L1 + aCSF (D). Data are presented as individual growth curves for each animal. Data are representative of one experiment (two performed in total). E-H – KPC tumour growth in mice receiving 10Gy + IgG (A), 10Gy + aCSF (B), 10Gy + aPD-L1 (C) or 10Gy +aPD-L1 + aCSF (D). Data are presented as individual growth curves for each animal. Data are representative of one experiment (two performed in total).

E-H – KPC tumour growth in mice receiving 10Gy + IgG (A), 10Gy + aCSF (B), 10Gy + aPD-L1 (C) or 10Gy +aPD-L1 + aCSF (D). Data are presented as individual growth curves for each animal. Data are representative of one experiment (two performed in total). E-H – KPC tumour growth in mice receiving 10Gy + IgG (A), 10Gy + aCSF (B), 10Gy + aPD-L1 (C) or 10Gy +aPD-L1 + aCSF (D). Data are presented as individual growth curves for each animal. Data are representative of one experiment (two performed in total).

5.4 Discussion

In this chapter we show that radiation significantly increases the expression of the immune checkpoint molecule PD-L1 on tumour cells both *in vitro* and *in vivo.* The administration of aPD-L1 blocking antibody alone did not affect tumour growth, however in combination with irradiation a subset of mice responded with complete tumour regression. This response was only observed in MC38 tumours, with KPC tumours remaining refractory with or without the addition of radiation.

In line with recently published reports, we show that irradiation of tumour cells stimulates increased PD-L1 surface expression. Responses were variable between MC38 and KPC cell lines, with MC38 having significantly higher basal expression. This is consistent with previous reports showing that MC38 has high baseline expression, and is also responsive to both radiation and IFNγ induced expression[365–367]. Of note, MC38 tumour cells increased PD-L1 expression to a comparable degree both in vitro and in vivo. This suggests that an intrinsic tumour cell mechanism is responsible for the upregulation. Untreated KPC cells expressed little PD-L1 in culture, again in line with previous reports [368,369]. Interestingly, there was a differential response following irradiation *in vitro* versus *in vivo* KPC cells. Although in both settings there was a significant increase in expression, this was significantly greater in vivo. This is possibly due to the presence of cytokines produced by non-tumour cells which can stimulate PD-L1 expression, such as IFNγ [365]. Evidence for an alternative mechanism is presented by Azad et al, who demonstrate a Janus Kinase – STAT1 dependent mechanism in two murine pancreatic cell lines in vivo [369]. In a primary PDAC model, Zhang et al show that tumour cell PD-L1 expression is dependent on the presence of myeloid cells in an epidermal growth factor (EGFR)/mitogen-activated protein kinase (MAPK) dependent manner [368]. In either case, in our models PD-L1 was significantly upregulated on tumour cells following irradiation. Due to the inherent nature of the interaction between PD-L1 and PD-1, it would appear logical that increased expression of PD-L1 on tumour cells would increase resistance to PD-L1/-1 based checkpoint blockade. For this reason there have been a number of clinical studies quantifying the predictive value of baseline tumour PD-L1 expression. Many early reports did correlate tumour cell PD-L1 expression with response to anti-PD-L1 therapy [370–372]. In addition, a clinical trial that prospectively allocated non-small cell lung cancer (NSCLC) patients to treatment groups according to their PD-L1 expression status showed superior outcomes for those with >50% expression [77]. This evidence contributed to the approval of

pembrolizumab for patients with NSCLC and >50% PD-L1 expression by the National Institute for Health and Care Excellence (NCIE) in 2017. However other studies examining tissues from breast and colon cancer patients found that increased PD-L1 correlated with improved outcomes [373,374]. As more nuanced analyses emerge, it has become clear that PD-L1 expression may be transiently altered, and that the host stromal compartment may also contribute to PD-L1 sensitivity [366,367]. As such, the total amount of PD-L1 present in a tumour may have little bearing on its potential response to checkpoint blockade.

Treatment with aPD-L1 antibody alone did not affect tumour growth in mice bearing MC38 and KPC tumours. However, when combined with radiation there was a variable response amongst MC38 tumours and no response in KPC tumours. We therefore questioned whether the increased PD-L1 and TAMs observed after radiation is partly responsible for treatment resistance. Treatment with aPD-L1 and irradiation led to regression in 50% of tumours, and increased growth delay in the remaining tumours (Figure 5.2, A). MC38 is generally a PD-L1 sensitive tumour, with previous reports showing regression in up to 100% of tumours [365,367]. The sensitivity of MC38 to checkpoint blockade is possibly due to its immunogenic profile, as well as its hypermutated state, as discussed in the introduction (Page 20). With this in mind, there is potentially less to be gained by adding additional treatments. However the reported response rate is variable, with other studies demonstrating no regression following aPD-L1 alone [375,376]. Interestingly, in patients with colorectal cancer, only those with microsatellite instability respond to immune checkpoint blockade [377]. Therefore tumours with a checkpoint sensitive phenotype potentially have less to gain from additional combination therapy. We did not see any difference in response between the aPDL1 + irradiation group and the aPD-L1 + aCSF + irradiation group, which suggests that resistance to checkpoint blockade in MC38 tumours is not as a result of increased immunosuppressive TAMs.

In contrast, KPC tumours are robustly resistant to immune checkpoint blockade. This was confirmed in our hands, with no increased tumour growth delay or regressions in mice treated with aPD-L1 alone or in combination with irradiation. Strikingly, depletion of TAMs via aCSF led to tumour regression in 3/8 mice. This suggests that in a more resistant model, TAMs may play an important role in mediating the response. Tumour stroma is a much more significant component of the tumour microenvironment in KPC tumours [378]. The relative contribution to the intra-tumoural PD-L1 of the host stroma and its effect on checkpoint sensitivity remain unclear [211,366,367]. However, our results suggest

that TAMs contribute to the resistance to immune checkpoint blockade observed in murine pancreatic cancer.

6. CHAPTER 6: Concluding remarks

6.1 Synopsis

The aim of this work was to determine the role of macrophages in the tumour response to radiation. We initially demonstrated that CSF-1, one of the key cytokines involved in the recruitment, differentiation and survival of macrophages, was upregulated in tumour cells in response to irradiation. We subsequently characterised the immune response to irradiation in vivo, demonstrating significant alterations in myeloid populations coincident with increases in CSF-1. Phenotypic characterisation of these macrophages revealed that they were highly immunosuppressive, and contributed to resistance to adaptive immunity. Importantly, depletion of these macrophages allowed for a more robust anti-tumour adaptive immune response, which was dependent upon CD8 T lymphocytes. In addition, we demonstrated that radiation generated tumour antigen specific immunity. When radiation was combined with macrophages depletion, this was capable of delaying tumour growth in distant 'out-of-field' tumours. Finally, we are the first to show that resistance to radiation combined with immune checkpoint blockade in a model of pancreatic cancer can be overcome with the addition of macrophage depletion.

Our results indicate that macrophages likely play an important role in orchestrating the immune response to radiation. In light of their immunosuppressive capacity, they may be particularly important in modulating adaptive immunity. There is considerably more evidence available demonstrating some of the possible ways in which macrophages affect non-irradiated compared with irradiated tumours. Our work highlights how potent radiation can be in stimulating an immune response, which with the addition of selected targeted agents, may augment the overall outcome.

6.2 Limitations

There are a number of limitations which need to be accounted for when interpreting the results of this research. Firstly, for all in vivo work we used subcutaenous xenografts to generate tumours. Whilst these facilitate reproducibility and the application of external beam radiation, they are

unlikely to fully recapitulate the tumour microenvironment. In particular, genetically engineered models of spontaneous carcinogenesis would have macrophage contributions from both embryonic and circulating monocyte precursors. In addition, the rate of growth of spontaneous tumours is significantly slower than the growth observed in subcutaenous models. This difference, during which malignant cells are present, allows for a greater time for animals to develop adaptive immunity.

Next, we performed most of our analyses on material harvested from tumours five days following irradiation. We selected this time point as it reflected the point of maximal macrophage numbers, our population of interest. Therefore the comparisons we make with other immune populations must take into account possible alterations at other time points. This is true of the macrophage phenotype we report, which may also change over time following irradiation.

Also, we used a single fraction of 10Gy irradiation for in vitro and in vivo experiments. Therefore it is not possible to draw comparisons between our observations and what might be expected following fractionated radiation. Fractionated radiation is used more frequently in the clinical setting, and has potential differences in the immune response it generates as well as the possible antigen presenting capabilities. Fractionation completely reflective of clinical practise (>20 fractions, 2Gy) is almost impossible to achieve in animal models, however a modest hypofractionated regime could be tested for comparative purposes.

We used flow cytometry and confirmatory immunohistochemical analyses to quantify macrophage numbers in tumours. Based on the literature, macrophages may increase within tumours either due to monocyte recruitment, or proliferation of existing TAMs. Given the speed and magnitude of increase, along with the expression of CSF-1, it is likely that circulating recruitment is responsible for the increase seen in our models. However to definitively address this, an adoptive transfer experiment using labelled macrophages would be required. In addition, an assessment of the proliferative index of existing TAMs would also need to be measured.

We demonstrated that radiation was capable of generating tumour antigen specific immunity, but did not perform any qualitative analysis of the possible antigens involved. Specifically, we did not establish whether any antigens conserved across untreated cells, and if so to what extent. In addition, we did not examine whether any antigens presented following radiation specific to new

mutations. Clearly, if radiation is involved in antigen priming, these are very important questions that need to be addressed before considering the use of radiation as a priming tool.

Finally, we have not extended our findings to any human data. It would have been useful to determine whether macrophages are increased in human tumours following radiotherapy, and also make an assessment of their phenotype. For rectal tumours, obtaining tissue within a realistic time frame from the last dose of radiation is difficult. Resections usually take place months after the cessation of neoadjuvant treatment, and in those who have a complete pathological response there is no tissue to analyse. In pancreatic cancer patients, radiotherapy is used infrequently and obtaining tissue by endoscopy is unpredictable. It is perhaps for these reasons that there is a paucity of clinical evidence reporting the immune effects of tumour radiation in human tumours. Nonetheless, it is imperative that pre-clinical findings are substantiated with reliable clinical data.

6.3 Future directions

Whilst the work thus far completed has answered the research questions originally set out, it has also highlighted some interesting questions which warrant further investigation.

Firstly, our results indicate that a refractory population of TAMs remain following aCSF therapy. These TAMs exhibited features consistent with repolarisation to an inflammatory phenotype. Whilst we cannot determine the functional role these may have within the tumour microenvironment, evidence from the wider field suggests that they may be immune stimulatory and even anti-tumourigenic. For this reason it would be interesting to investigate the effect of macrophage repolarisation, but not depletion, in the irradiated tumour microenvironment. If indeed repolarisation is beneficial, low tumour macrophage numbers may limit any potential benefits. However one could utilise the increased TAMs that are recruited following irradiation. Therefore the effect would be two-fold; increased TAM numbers due to irradiation, and repolarisation using novel agents.

Our data also suggested that radiation was capable of generating antigen specific immunity. These results coincide with emerging reports demonstrating increased T cell receptor clonality following tumour irradiation in pre-clinical models. Together these results provide justification for

further investigation into how radiation might augment antigen priming. The three main existing areas of evidence relate to peptide turnover and MHC presentation, T cell receptor clonality, and the specificity of T cells from irradiated hosts towards irradiated target cells. One area that lacks evidence is the possibility that radiation induced mutagenesis results in tumour specific neopeptides, essentially acting as an in situ tumour vaccine. This would require tumour cell whole exome sequencing combined with mass spectral analysis of peptides associated with MHC molecules. However it would provide definitive evidence that mutated peptides are generated and presented on tumour cells following radiation. The consequence of such neopeptides would also need to be determined. This would require synthetic peptide vaccination in vivo to determine whether the antigen is conserved across tumour cells. It may be that neopeptides are highly heterogeneous and not conserved, meaning antigen specific immunity is limited. However if this is not the case then such results would provide further rational for using radiation to prime the immune system, rendering tumours more susceptible to immunogenic death.

7. References

1. Gordon-Weeks, A. N. *et al.* Neutrophils promote hepatic metastasis growth through fibroblast growth factor 2–dependent angiogenesis in mice. *Hepatology* **65,** (2017).
2. EWING, J. RADIUM THERAPY IN CANCER. *J. Am. Med. Assoc.* **LXVIII,** 1238 (1917).
3. COHEN, A. & COHEN, L. Estimation of the cellular lethal dose and the critical cell number for the C3H mouse mammary carcinoma from radiosensitivity studies in vivo. *Nature* **185,** 262–3 (1960).
4. HADDOW, A. & ALEXANDER, P. AN IMMUNOLOGICAL METHOD OF INCREASING THE SENSITIVITY OF PRIMARY SARCOMAS TO LOCAL IRRADIATION WITH X RAYS. *Lancet (London, England)* **1,** 452–7 (1964).
5. COHEN, A. & COHEN, L. Radiobiology of the C3H mouse mammary carcinoma: increased radiosensitivity of the tumour induced by inoculation of the host with radiation-attenuated isografts. *Br. J. Cancer* **10,** 312–7 (1956).
6. Suit, H. D. & Kastelan, A. Immunologic status of host and response of a methylcholanthrene-induced sarcoma to local x-irradiation. *Cancer* **26,** 232–8 (1970).
7. Slone, H. B., Peters, L. J. & Milas, L. Effect of Host Immune Capability on Radiocurability and Subsequent Transplantability of a Murine Fibrosarcoma<xref ref-type="fn" rid="FN2">2</xref> *JNCI J. Natl. Cancer Inst.* **63,** 1229–1235 (1979).
8. Hewitt, H. B., Blake, E. R. & Walder, A. S. A critique of the evidence for active host defence against cancer, based on personal studies of 27 murine tumours of spontaneous origin. *Br. J. Cancer* **33,** 241–59 (1976).
9. Mole, R. H. Whole Body Irradiation—Radiobiology or Medicine? *Br. J. Radiol.* **26,** 234–241 (1953).
10. Reynders, K., Illidge, T., Siva, S., Chang, J. Y. & De Ruysscher, D. The abscopal effect of local radiotherapy: using immunotherapy to make a rare event clinically relevant. *Cancer Treat. Rev.* **41,** 503–510 (2015).
11. Formenti, S. C. & Demaria, S. Systemic effects of local radiotherapy. *Lancet. Oncol.* **10,** 718–26 (2009).
12. Hodi, F. S. *et al.* Improved Survival with Ipilimumab in Patients with Metastatic Melanoma. *N. Engl. J. Med.* **363,** 711–723 (2010).
13. Hiniker, S. M. *et al.* A systemic complete response of metastatic melanoma to local radiation and immunotherapy. *Transl. Oncol.* **5,** 404–7 (2012).
14. Postow, M. A. *et al.* Immunologic Correlates of the Abscopal Effect in a Patient with Melanoma. *N. Engl. J. Med.* **366,** 925–931 (2012).
15. Dewan, M. Z. *et al.* Fractionated but Not Single-Dose Radiotherapy Induces an Immune-Mediated Abscopal Effect when Combined with Anti-CTLA-4 Antibody. *Clin. Cancer Res.* **15,** 5379–5388 (2009).
16. Demaria, S. *et al.* Immune-mediated inhibition of metastases after treatment with local radiation and CTLA-4 blockade in a mouse model of breast cancer. *Clin. Cancer Res.* **11,** 728–34 (2005).

17. Koo, T. & Kim, I. A. Radiotherapy and immune checkpoint blockades: a snapshot in 2016. *Radiat. Oncol. J.* **34,** 250–259 (2016).

18. Janeway, C. A. Approaching the asymptote? Evolution and revolution in immunology. *Cold Spring Harb. Symp. Quant. Biol.* **54 Pt 1,** 1–13 (1989).

19. Raetz, C. R. H. & Whitfield, C. Lipopolysaccharide Endotoxins. *Annu. Rev. Biochem.* **71,** 635–700 (2002).

20. Silva-Gomes, S., Decout, A. & Nigou, J. Pathogen-Associated Molecular Patterns (PAMPs). doi:10.1007/978-3-0348-0620-6_35-1

21. Tang, D., Kang, R., Coyne, C. B., Zeh, H. J. & Lotze, M. T. PAMPs and DAMPs: signal 0s that spur autophagy and immunity. *Immunol. Rev.* **249,** 158–75 (2012).

22. Land, W. G. The Role of Damage-Associated Molecular Patterns (DAMPs) in Human Diseases: Part II: DAMPs as diagnostics, prognostics and therapeutics in clinical medicine. *Sultan Qaboos Univ. Med. J.* **15,** e157-70 (2015).

23. Gay, N. J. & Gangloff, M. Structure and Function of Toll Receptors and Their Ligands. *Annu. Rev. Biochem.* **76,** 141–165 (2007).

24. Schaefer, L. Complexity of danger: the diverse nature of damage-associated molecular patterns. *J. Biol. Chem.* **289,** 35237–45 (2014).

25. Chen, R. *et al.* Nuclear DAMP complex-mediated RAGE-dependent macrophage cell death. *Biochem. Biophys. Res. Commun.* **458,** 650–655 (2015).

26. Bresnick, A. R., Weber, D. J. & Zimmer, D. B. S100 proteins in cancer. *Nat. Rev. Cancer* **15,** 96–109 (2015).

27. Ahmed, M. M., Guha, C., Hodge, J. W. & Jaffee, E. Immunobiology of Radiotherapy: New Paradigms. *Radiat. Res.* **182,** 123–125 (2014).

28. Hernandez, C., Huebener, P. & Schwabe, R. F. Damage-associated molecular patterns in cancer: a double-edged sword. *Oncogene* **35,** 5931–5941 (2016).

29. Deng, L., Liang, H., Fu, S., Weichselbaum, R. R. & Fu, Y.-X. From DNA Damage to Nucleic Acid Sensing: A Strategy to Enhance Radiation Therapy. *Clin. Cancer Res.* **22,** 20–5 (2016).

30. Diamond, M. S. *et al.* Type I interferon is selectively required by dendritic cells for immune rejection of tumors. *J. Exp. Med.* **208,** 1989–2003 (2011).

31. Fuertes, M. B. *et al.* Host type I IFN signals are required for antitumor CD8+ T cell responses through CD8{alpha}+ dendritic cells. *J. Exp. Med.* **208,** 2005–16 (2011).

32. Xu, J. *et al.* CSF1R signaling blockade stanches tumor-infiltrating myeloid cells and improves the efficacy of radiotherapy in prostate cancer. *Cancer Res.* **73,** 2782–94 (2013).

33. Vilalta, M., Rafat, M., Giaccia, A. J. & Graves, E. E. Recruitment of circulating breast cancer cells is stimulated by radiotherapy. *Cell Rep.* **8,** 402–9 (2014).

34. Desai, S., Kumar, A., Laskar, S. & Pandey, B. N. Cytokine profile of conditioned medium from human tumor cell lines after acute and fractionated doses of gamma radiation and its effect on survival of bystander tumor

cells. *Cytokine* **61,** 54–62 (2013).

35. Dent, P. *et al.* Stress and radiation-induced activation of multiple intracellular signaling pathways. *Radiat. Res.* **159,** 283–300 (2003).

36. Criswell, T., Leskov, K., Miyamoto, S., Luo, G. & Boothman, D. A. Transcription factors activated in mammalian cells after clinically relevant doses of ionizing radiation. *Oncogene* **22,** 5813–5827 (2003).

37. Schaue, D., Kachikwu, E. L. & McBride, W. H. Cytokines in Radiobiological Responses: A Review. *Radiat. Res.* **178,** 505–523 (2012).

38. Hong, J. H. *et al.* Rapid induction of cytokine gene expression in the lung after single and fractionated doses of radiation. *Int. J. Radiat. Biol.* **75,** 1421–7 (1999).

39. Burnette, B. C. *et al.* The Efficacy of Radiotherapy Relies upon Induction of Type I Interferon-Dependent Innate and Adaptive Immunity. *Cancer Res.* **71,** 2488–2496 (2011).

40. Hao, S. & Baltimore, D. The stability of mRNA influences the temporal order of the induction of genes encoding inflammatory molecules. *Nat. Immunol.* **10,** 281–288 (2009).

41. Dancea, H. C., Shareef, M. M. & Ahmed, M. M. Role of Radiation-induced TGF-beta Signaling in Cancer Therapy. *Mol. Cell. Pharmacol.* **1,** 44–56 (2009).

42. Han, S.-K., Song, J.-Y., Yun, Y.-S. & Yi, S.-Y. Effect of gamma radiation on cytokine expression and cytokine-receptor mediated STAT activation. *Int. J. Radiat. Biol.* **82,** 686–697 (2006).

43. Shan, Y.-X., Jin, S.-Z., Liu, X.-D., Liu, Y. & Liu, S.-Z. Ionizing radiation stimulates secretion of pro-inflammatory cytokines: dose–response relationship, mechanisms and implications. *Radiat. Environ. Biophys.* **46,** 21–29 (2007).

44. Chiang, C.-S. *et al.* Functional phenotype of macrophages depends on assay procedures. *Int. Immunol.* **20,** 215–222 (2008).

45. Teresa Pinto, A. *et al.* Ionizing radiation modulates human macrophages towards a pro-inflammatory phenotype preserving their pro-invasive and pro-angiogenic capacities. *Sci. Rep.* **6,** 18765 (2016).

46. Chiang, C.-S. *et al.* Irradiation Promotes an M2 Macrophage Phenotype in Tumor Hypoxia. *Front. Oncol.* **2,** 89 (2012).

47. Vatner, R. E. & Formenti, S. C. Myeloid-Derived Cells in Tumors: Effects of Radiation. *Semin. Radiat. Oncol.* **25,** 18–27 (2015).

48. Liang, H. *et al.* Host STING-dependent MDSC mobilization drives extrinsic radiation resistance. *Nat. Commun.* **8,** 1736 (2017).

49. J., E. *et al.* CSF1 receptor targeting in prostate cancer reverses macrophage-mediated resistance to androgen blockade therapy. *Cancer Research* **75,** 950–962 (2015).

50. Kioi, M. *et al.* Inhibition of vasculogenesis, but not angiogenesis, prevents the recurrence of glioblastoma after irradiation in mice. *J. Clin. Invest.* **120,** 694–705 (2010).

51. Kozin, S. V *et al.* Recruitment of myeloid but not endothelial precursor cells facilitates tumor regrowth after

local irradiation. *Cancer Res.* **70,** 5679–85 (2010).

52. Deng, L. *et al.* Irradiation and anti–PD-L1 treatment synergistically promote antitumor immunity in mice. *J. Clin. Invest.* **124,** 687–695 (2014).

53. Chiang, C.-S. *et al.* Irradiation promotes an M2 macrophage phenotype in tumor hypoxia. (2012). doi:10.3389/fonc.2012.00089

54. Deng, L. *et al.* Irradiation and anti–PD-L1 treatment synergistically promote antitumor immunity in mice. *J. Clin. Invest.* **124,** 687–695 (2014).

55. Takeshima, T. *et al.* Key role for neutrophils in radiation-induced antitumor immune responses: Potentiation with G-CSF. *Proc. Natl. Acad. Sci. U. S. A.* **113,** 11300–11305 (2016).

56. Fridlender, Z. G. *et al.* Polarization of Tumor-Associated Neutrophil Phenotype by TGF-β: 'N1' versus 'N2' TAN. *Cancer Cell* **16,** 183–194 (2009).

57. Teresa Pinto, A. *et al.* Ionizing radiation modulates human macrophages towards a pro-inflammatory phenotype preserving their pro-invasive and pro-angiogenic capacities. *Sci. Rep.* **6,** 18765 (2016).

58. Yuen, G. J., Demissie, E. & Pillai, S. B lymphocytes and cancer: a love-hate relationship. *Trends in cancer* **2,** 747–757 (2016).

59. Joffre, O. P., Segura, E., Savina, A. & Amigorena, S. Cross-presentation by dendritic cells. *Nat. Rev. Immunol.* **12,** 557–569 (2012).

60. Dunn, G. P., Old, L. J. & Schreiber, R. D. The Immunobiology of Cancer Immunosurveillance and Immunoediting. *Immunity* **21,** 137–148 (2004).

61. Shankaran, V. *et al.* IFNγ and lymphocytes prevent primary tumour development and shape tumour immunogenicity. *Nature* **410,** 1107–1111 (2001).

62. Dunn, G. P., Old, L. J. & Schreiber, R. D. The Three Es of Cancer Immunoediting. *Annu. Rev. Immunol.* **22,** 329–360 (2004).

63. Loeb, L. A., Loeb, K. R. & Anderson, J. P. Multiple mutations and cancer. *Proc. Natl. Acad. Sci.* **100,** 776–781 (2003).

64. MacKie, R. M., Reid, R. & Junor, B. Fatal Melanoma Transferred in a Donated Kidney 16 Years after Melanoma Surgery. *N. Engl. J. Med.* **348,** 567–568 (2003).

65. Suranyi, M. G. *et al.* Advanced donor-origin melanoma in a renal transplant recipient: immunotherapy, cure, and retransplantation. *Transplantation* **66,** 655–61 (1998).

66. Marincola, F. M., Jaffee, E. M., Hicklin, D. J. & Ferrone, S. Escape of human solid tumors from T-cell recognition: molecular mechanisms and functional significance. *Adv. Immunol.* **74,** 181–273 (2000).

67. Groh, V., Wu, J., Yee, C. & Spies, T. Tumour-derived soluble MIC ligands impair expression of NKG2D and T-cell activation. *Nature* **419,** 734–738 (2002).

68. Koebel, C. M. *et al.* Adaptive immunity maintains occult cancer in an equilibrium state. *Nature* **450,** 903–907 (2007).

69. Wu, X. *et al.* Immune microenvironment profiles of tumor immune equilibrium and immune escape states of mouse sarcoma. *Cancer Lett.* **340,** 124–133 (2013).

70. Müller-Hermelink, N. *et al.* TNFR1 Signaling and IFN-γ Signaling Determine whether T Cells Induce Tumor Dormancy or Promote Multistage Carcinogenesis. *Cancer Cell* **13,** 507–518 (2008).

71. Hanahan, D. & Weinberg, R. A. Hallmarks of Cancer: The Next Generation. *Cell* **144,** 646–674 (2011).

72. Mittal, D., Gubin, M. M., Schreiber, R. D. & Smyth, M. J. New insights into cancer immunoediting and its three component phases--elimination, equilibrium and escape. *Curr. Opin. Immunol.* **27,** 16–25 (2014).

73. Brunet, J.-F. *et al.* A new member of the immunoglobulin superfamily—CTLA-4. *Nature* **328,** 267–270 (1987).

74. Pardoll, D. M. The blockade of immune checkpoints in cancer immunotherapy. *Nat. Rev. Cancer* **12,** 252–264 (2012).

75. Le, D. T. *et al.* PD-1 Blockade in Tumors with Mismatch-Repair Deficiency. *N. Engl. J. Med.* **372,** 2509–2520 (2015).

76. Schachter, J. *et al.* Pembrolizumab versus ipilimumab for advanced melanoma: final overall survival results of a multicentre, randomised, open-label phase 3 study (KEYNOTE-006). *Lancet (London, England)* **390,** 1853–1862 (2017).

77. Reck, M. *et al.* Pembrolizumab versus Chemotherapy for PD-L1–Positive Non–Small-Cell Lung Cancer. *N. Engl. J. Med.* **375,** 1823–1833 (2016).

78. Dovedi, S. J. *et al.* Acquired Resistance to Fractionated Radiotherapy Can Be Overcome by Concurrent PD-L1 Blockade. *Cancer Res.* **74,** (2014).

79. Azad, A. *et al.* PD-L1 blockade enhances response of pancreatic ductal adenocarcinoma to radiotherapy. *EMBO Mol. Med.* **62,** 1249–1260 (2016).

80. Oweida, A. *et al.* Ionizing radiation sensitizes tumors to PD-L1 immune checkpoint blockade in orthotopic murine head and neck squamous cell carcinoma. *Oncoimmunology* **6,** e1356153 (2017).

81. Escorcia, F. E., Postow, M. A. & Barker, C. A. Radiotherapy and Immune Checkpoint Blockade for Melanoma: A Promising Combinatorial Strategy in Need of Further Investigation. *Cancer J.* **23,** 32–39 (2017).

82. Reits, E. A. *et al.* Radiation modulates the peptide repertoire, enhances MHC class I expression, and induces successful antitumor immunotherapy. *J. Exp. Med.* **203,** 1259–71 (2006).

83. Rudqvist, N.-P. *et al.* Radiotherapy and CTLA-4 Blockade Shape the TCR Repertoire of Tumor-Infiltrating T Cells. *Cancer Immunol. Res.* **6,** 139–150 (2018).

84. Dovedi, S. J. *et al.* Fractionated Radiation Therapy Stimulates Antitumor Immunity Mediated by Both Resident and Infiltrating Polyclonal T-cell Populations when Combined with PD-1 Blockade. *Clin. Cancer Res.* **23,** 5514–5526 (2017).

85. Golden, E. B. *et al.* Radiation fosters dose-dependent and chemotherapy-induced immunogenic cell death. *Oncoimmunology* **3,** e28518 (2014).

86. Gameiro, S. R. *et al.* Radiation-induced immunogenic modulation of tumor enhances antigen processing and

calreticulin exposure, resulting in enhanced T-cell killing. *Oncotarget* **5,** 403–16 (2014).

87. Kulzer, L. *et al.* Norm- and hypo-fractionated radiotherapy is capable of activating human dendritic cells. *J. Immunotoxicol.* **11,** 328–336 (2014).

88. Matsumura, S. *et al.* Radiation-induced CXCL16 release by breast cancer cells attracts effector T cells. *J. Immunol.* **181,** 3099–107 (2008).

89. Lim, J. Y. H., Gerber, S. A., Murphy, S. P. & Lord, E. M. Type I interferons induced by radiation therapy mediate recruitment and effector function of CD8+ T cells. *Cancer Immunol. Immunother.* **63,** 259–271 (2014).

90. Tauber, A. I. Metchnikoff and the phagocytosis theory. *Nat. Rev. Mol. Cell Biol.* **4,** 897–901 (2003).

91. HARRIS, H. Role of chemotaxis in inflammation. *Physiol. Rev.* **34,** 529–62 (1954).

92. Wynn, T. A., Chawla, A. & Pollard, J. W. Macrophage biology in development, homeostasis and disease. *Nature* **496,** 445–455 (2013).

93. van Furth, R. & Cohn, Z. A. The origin and kinetics of mononuclear phagocytes. *J. Exp. Med.* **128,** 415–35 (1968).

94. Richards, D. M., Hettinger, J. & Feuerer, M. Monocytes and macrophages in cancer: development and functions. *Cancer Microenviron.* **6,** 179–191 (2013).

95. Ginhoux, F. *et al.* Fate Mapping Analysis Reveals That Adult Microglia Derive from Primitive Macrophages. *Science (80-.).* **330,** 841–845 (2010).

96. Yona, S. *et al.* Fate Mapping Reveals Origins and Dynamics of Monocytes and Tissue Macrophages under Homeostasis. *Immunity* **38,** 79–91 (2013).

97. Hoeffel, G. *et al.* Adult Langerhans cells derive predominantly from embryonic fetal liver monocytes with a minor contribution of yolk sac–derived macrophages. *J. Exp. Med.* **209,** 1167–1181 (2012).

98. Tushinski, R. J. *et al.* Survival of mononuclear phagocytes depends on a lineage-specific growth factor that the differentiated cells selectively destroy. *Cell* **28,** 71–81 (1982).

99. Sherr, C. J., Roussel, M. F. & Rettenmier, C. W. Colony-stimulating factor-1 receptor (c-fms). *J. Cell. Biochem.* **38,** 179–187 (1988).

100. Erblich, B., Zhu, L., Etgen, A. M., Dobrenis, K. & Pollard, J. W. Absence of Colony Stimulation Factor-1 Receptor Results in Loss of Microglia, Disrupted Brain Development and Olfactory Deficits. *PLoS One* **6,** e26317 (2011).

101. Boulakirba, S. *et al.* IL-34 and CSF-1 display an equivalent macrophage differentiation ability but a different polarization potential. *Sci. Rep.* **8,** 256 (2018).

102. Pollard, J. W. & Stanley, E. R. Pleiotropic Roles for CSF-1 in Development Defined by the Mouse Mutation Osteopetrotic. *Adv. Dev. Biochem.* **4,** 153–193 (1996).

103. Gordy, C., Pua, H., Sempowski, G. D. & He, Y.-W. Regulation of steady-state neutrophil homeostasis by macrophages. *Blood* **117,** 618–629 (2011).

104. Feng, M. *et al.* Macrophages eat cancer cells using their own calreticulin as a guide: roles of TLR and Btk.

Proc. Natl. Acad. Sci. U. S. A. **112,** 2145–50 (2015).

105. Munn, D. H. & Cheung, N. K. Phagocytosis of tumor cells by human monocytes cultured in recombinant macrophage colony-stimulating factor. *J. Exp. Med.* **172,** 231–7 (1990).

106. Gouon-Evans, V., Rothenberg, M. E. & Pollard, J. W. Postnatal mammary gland development requires macrophages and eosinophils. *Development* **127,** 2269–82 (2000).

107. Van Nguyen, A. & Pollard, J. W. Colony Stimulating Factor-1 Is Required to Recruit Macrophages into the Mammary Gland to Facilitate Mammary Ductal Outgrowth. *Dev. Biol.* **247,** 11–25 (2002).

108. Rae, F. *et al.* Characterisation and trophic functions of murine embryonic macrophages based upon the use of a Csf1r–EGFP transgene reporter. *Dev. Biol.* **308,** 232–246 (2007).

109. Stefater III, J. A. *et al.* Regulation of angiogenesis by a non-canonical Wnt–Flt1 pathway in myeloid cells. *Nature* **474,** 511–515 (2011).

110. Fantin, A. *et al.* Tissue macrophages act as cellular chaperones for vascular anastomosis downstream of VEGF-mediated endothelial tip cell induction. *Blood* **116,** 829–840 (2010).

111. Lobov, I. B. *et al.* WNT7b mediates macrophage-induced programmed cell death in patterning of the vasculature. *Nature* **437,** 417–421 (2005).

112. Grunewald, M. *et al.* VEGF-Induced Adult Neovascularization: Recruitment, Retention, and Role of Accessory Cells. *Cell* **124,** 175–189 (2006).

113. Rao, S. *et al.* Obligatory participation of macrophages in an angiopoietin 2-mediated cell death switch. *Development* **134,** 4449–4458 (2007).

114. Gautier, E. L. *et al.* Gene-expression profiles and transcriptional regulatory pathways that underlie the identity and diversity of mouse tissue macrophages. *Nat. Immunol.* **13,** 1118–28 (2012).

115. Bain, C. C. *et al.* Constant replenishment from circulating monocytes maintains the macrophage pool in the intestine of adult mice. *Nat. Immunol.* **15,** 929–937 (2014).

116. Movahedi, K. *et al.* Different Tumor Microenvironments Contain Functionally Distinct Subsets of Macrophages Derived from Ly6C(high) Monocytes. *Cancer Res.* **70,** 5728–5739 (2010).

117. De Palma, M. *et al.* Tie2 identifies a hematopoietic lineage of proangiogenic monocytes required for tumor vessel formation and a mesenchymal population of pericyte progenitors. *Cancer Cell* **8,** 211–226 (2005).

118. De Palma, M., Venneri, M. A., Roca, C. & Naldini, L. Targeting exogenous genes to tumor angiogenesis by transplantation of genetically modified hematopoietic stem cells. *Nat. Med.* **9,** 789–795 (2003).

119. Franklin, R. A. *et al.* The cellular and molecular origin of tumor-associated macrophages. *Science (80-.).* **344,** 921–925 (2014).

120. Zhu, Y. *et al.* Tissue-Resident Macrophages in Pancreatic Ductal Adenocarcinoma Originate from Embryonic Hematopoiesis and Promote Tumor Progression. *Immunity* **47,** 323–338.e6 (2017).

121. Grivennikov, S. I., Greten, F. R. & Karin, M. Immunity, Inflammation, and Cancer. *Cell* **140,** 883–899 (2010).

122. Burd, E. M. Human papillomavirus and cervical cancer. *Clin. Microbiol. Rev.* **16,** 1–17 (2003).

123. de Oliveria Andrade, L. J. *et al.* Association between hepatitis C and hepatocellular carcinoma. *J. Glob. Infect. Dis.* **1,** 33–7 (2009).

124. Brown, E. R. *et al.* A clinical study assessing the tolerability and biological effects of infliximab, a TNF-α inhibitor, in patients with advanced cancer. *Ann. Oncol.* **19,** 1340–1346 (2008).

125. Oguma, K. *et al.* Activated macrophages promote Wnt signalling through tumour necrosis factor-α in gastric tumour cells. *EMBO J.* **27,** 1671–1681 (2008).

126. Lin, E. Y., Nguyen, A. V, Russell, R. G. & Pollard, J. W. Colony-stimulating factor 1 promotes progression of mammary tumors to malignancy. *J. Exp. Med.* **193,** 727–40 (2001).

127. Colotta, F., Allavena, P., Sica, A., Garlanda, C. & Mantovani, A. Cancer-related inflammation, the seventh hallmark of cancer: links to genetic instability. *Carcinogenesis* **30,** 1073–1081 (2009).

128. Meira, L. B. *et al.* DNA damage induced by chronic inflammation contributes to colon carcinogenesis in mice. *J. Clin. Invest.* **118,** 2516–25 (2008).

129. Pang, B. *et al.* Lipid peroxidation dominates the chemistry of DNA adduct formation in a mouse model of inflammation. *Carcinogenesis* **28,** 1807–1813 (2007).

130. Modi, B. G. *et al.* Langerhans Cells Facilitate Epithelial DNA Damage and Squamous Cell Carcinoma. *Science (80-.).* **335,** 104–108 (2012).

131. Murray, P. J. *et al.* Macrophage activation and polarization: nomenclature and experimental guidelines. *Immunity* **41,** 14–20 (2014).

132. Stein, M., Keshav, S., Harris, N. & Gordon, S. Interleukin 4 potently enhances murine macrophage mannose receptor activity: a marker of alternative immunologic macrophage activation. *J. Exp. Med.* **176,** 287–92 (1992).

133. Mills, C. D., Kincaid, K., Alt, J. M., Heilman, M. J. & Hill, A. M. M-1/M-2 macrophages and the Th1/Th2 paradigm. *J. Immunol.* **164,** 6166–73 (2000).

134. Stout, R. D. & Suttles, J. Functional plasticity of macrophages: reversible adaptation to changing microenvironments. *J. Leukoc. Biol.* **76,** 509–513 (2004).

135. Biswas, S. K. & Mantovani, A. Macrophage plasticity and interaction with lymphocyte subsets: cancer as a paradigm. *Nat. Immunol.* **11,** 889–896 (2010).

136. Alexander, C. & Rietschel, E. T. Bacterial lipopolysaccharides and innate immunity. *J. Endotoxin Res.* **7,** 167–202 (2001).

137. Zanoni, I. *et al.* CD14 controls the LPS-induced endocytosis of Toll-like receptor 4. *Cell* **147,** 868–80 (2011).

138. Zajac, E. *et al.* Angiogenic capacity of M1- and M2-polarized macrophages is determined by the levels of TIMP-1 complexed with their secreted proMMP-9. *Blood* **122,** 4054–67 (2013).

139. Hayes, E. M. *et al.* Classical and Alternative Activation and Metalloproteinase Expression Occurs in Foam Cell Macrophages in Male and Female ApoE Null Mice in the Absence of T and B Lymphocytes. *Front. Immunol.* **5,** 537 (2014).

140. Ly, L. V. *et al.* In Aged Mice, Outgrowth of Intraocular Melanoma Depends on Proangiogenic M2-Type Macrophages. *J. Immunol.* **185,** 3481–3488 (2010).

141. Tarique, A. A. *et al.* Phenotypic, Functional, and Plasticity Features of Classical and Alternatively Activated Human Macrophages. *Am. J. Respir. Cell Mol. Biol.* **53,** 676–688 (2015).

142. Martinez, F. O., Gordon, S., Locati, M. & Mantovani, A. Transcriptional profiling of the human monocyte-to-macrophage differentiation and polarization: new molecules and patterns of gene expression. *J. Immunol.* **177,** 7303–11 (2006).

143. Jablonski, K. A. *et al.* Novel Markers to Delineate Murine M1 and M2 Macrophages. *PLoS One* **10,** e0145342 (2015).

144. Spiller, K. L. *et al.* Sequential delivery of immunomodulatory cytokines to facilitate the M1-to-M2 transition of macrophages and enhance vascularization of bone scaffolds. *Biomaterials* **37,** 194–207 (2015).

145. Zhang, W. *et al.* Polarization of macrophages in the tumor microenvironment is influenced by EGFR signaling within colon cancer cells. *Oncotarget* (2016).

146. Colegio, O. R. *et al.* Functional polarization of tumour-associated macrophages by tumour-derived lactic acid. *Nature* **513,** 559–563 (2014).

147. Pyonteck, S. M. *et al.* Deficiency of the macrophage growth factor CSF-1 disrupts pancreatic neuroendocrine tumor development. *Oncogene* **31,** 1459–1467 (2012).

148. Qian, B.-Z. *et al.* CCL2 recruits inflammatory monocytes to facilitate breast-tumour metastasis. *Nature* **475,** 222–225 (2011).

149. Wang, T. *et al.* Melanoma-derived conditioned media efficiently induce the differentiation of monocytes to macrophages that display a highly invasive gene signature. *Pigment Cell Melanoma Res.* **25,** 493–505 (2012).

150. Al-Rayahi, I. A. M., Browning, M. J. & Stover, C. Tumour cell conditioned medium reveals greater M2 skewing of macrophages in the absence of properdin. *Immunity, Inflamm. Dis.* **5,** 68–77 (2017).

151. L., S. *et al.* Radiation Therapy Induces Macrophages to Suppress T-Cell Responses Against Pancreatic Tumors in Mice. *Gastroenterology* **150,** 1659 (2016).

152. Hamilton, T. A., Zhao, C., Pavicic, P. G. & Datta, S. Myeloid Colony-Stimulating Factors as Regulators of Macrophage Polarization. *Front. Immunol.* **5,** 554 (2014).

153. Joyce, J. A. & Pollard, J. W. Microenvironmental regulation of metastasis. *Nat. Rev. Cancer* **9,** 239–52 (2009).

154. Qian, B.-Z. & Pollard, J. W. Macrophage diversity enhances tumor progression and metastasis. *Cell* **141,** 39–51 (2010).

155. R., N. Tumor-Associated Macrophages: From Mechanisms to Therapy. *Immunity* **41,** 49–61 (2014).

156. Y., Z. *et al.* High-Infiltration of Tumor-Associated Macrophages Predicts Unfavorable Clinical Outcome for Node-Negative Breast Cancer. *PLoS ONE* **8,** no pagination (2013).

157. Zhao, X. *et al.* Prognostic significance of tumor-associated macrophages in breast cancer: a meta-analysis of the literature. *Oncotarget* **8,** 30576–30586 (2017).

158. Cavnar, M. J. *et al.* Tumor-Associated Macrophage Infiltration in Colorectal Cancer Liver Metastases is Associated With Better Outcome. *Ann. Surg. Oncol.* **24,** 1835–1842 (2017).

159. Kim, D.-W. *et al.* High tumour islet macrophage infiltration correlates with improved patient survival but not with EGFR mutations, gene copy number or protein expression in resected non-small cell lung cancer. *Br. J. Cancer* **98,** 1118–1124 (2008).

160. Welsh, T. J. *et al.* Macrophage and Mast-Cell Invasion of Tumor Cell Islets Confers a Marked Survival Advantage in Non–Small-Cell Lung Cancer. *J. Clin. Oncol.* **23,** 8959–8967 (2005).

161. Ruffell, B. & Coussens, L. M. Macrophages and therapeutic resistance in cancer. *Cancer Cell* **27,** 462–472 (2015).

162. Galon, J. *et al.* Type, density, and location of immune cells within human colorectal tumors predict clinical outcome. *Science* **313,** 1960–4 (2006).

163. Dong, J. *et al.* Prognostic potential of an immune score based on the density of CD8+ T cells, CD20+ B cells, and CD33+/p-STAT1+ double-positive cells and HMGB1 expression within cancer nests in stage IIIA gastric cancer patients. *Chin. J. Cancer Res.* **28,** 543–552 (2016).

164. Mlecnik, B. *et al.* Comprehensive Intrametastatic Immune Quantification and Major Impact of Immunoscore on Survival. *JNCI J. Natl. Cancer Inst.* **110,** 97–108 (2018).

165. Varn, F. S., Wang, Y., Mullins, D. W., Fiering, S. & Cheng, C. Systematic Pan-Cancer Analysis Reveals Immune Cell Interactions in the Tumor Microenvironment. doi:10.1158/0008-5472.CAN-16-2490

166. Lyons, Y. A., Wu, S. Y., Overwijk, W. W., Baggerly, K. A. & Sood, A. K. Immune cell profiling in cancer: molecular approaches to cell-specific identification. *npj Precis. Oncol.* **1,** 26 (2017).

167. Quail, D. F. *et al.* The tumor microenvironment underlies acquired resistance to CSF-1R inhibition in gliomas. *Science* **352,** aad3018 (2016).

168. van de Laar, L. *et al.* Yolk Sac Macrophages, Fetal Liver, and Adult Monocytes Can Colonize an Empty Niche and Develop into Functional Tissue-Resident Macrophages. *Immunity* **44,** 755–768 (2016).

169. Pyonteck, S. M. *et al.* CSF-1R inhibition alters macrophage polarization and blocks glioma progression. *Nat. Med.* **19,** 1264–1272 (2013).

170. Mantovani, A., Bottazzi, B., Colotta, F., Sozzani, S. & Ruco, L. The origin and function of tumor-associated macrophages. *Immunol. Today* **13,** 265–270 (1992).

171. Biswas, S. K. & Mantovani, A. Macrophage plasticity and interaction with lymphocyte subsets: cancer as a paradigm. *Nat. Immunol.* **11,** 889–896 (2010).

172. Bottazzi, B. *et al.* Regulation of the macrophage content of neoplasms by chemoattractants. *Science* **220,** 210–2 (1983).

173. Hambardzumyan, D., Gutmann, D. H. & Kettenmann, H. The role of microglia and macrophages in glioma maintenance and progression. *Nat. Neurosci.* **19,** 20–27 (2016).

174. M., R. *et al.* Genetic and Pharmacological Targeting of CSF-1/CSF-1R Inhibits Tumor-Associated Macrophages and Impairs BRAF-Induced Thyroid Cancer Progression. *PLoS ONE* **8,** no pagination (2013).

175. D.F., Q. *et al.* The tumor microenvironment underlies acquired resistance to CSF-1R inhibition in gliomas. *Science* **352,** no pagination (2016).

176. Wyckoff, J. B. *et al.* Direct Visualization of Macrophage-Assisted Tumor Cell Intravasation in Mammary Tumors. *Cancer Res.* **67,** 2649–2656 (2007).

177. Zhu, X.-D. *et al.* High Expression of Macrophage Colony-Stimulating Factor in Peritumoral Liver Tissue Is Associated With Poor Survival After Curative Resection of Hepatocellular Carcinoma. *J. Clin. Oncol.* **26,** 2707–2716 (2008).

178. Groblewska, M. *et al.* Serum levels of granulocyte colony-stimulating factor (G-CSF) and macrophage colony-stimulating factor (M-CSF) in pancreatic cancer patients. *Clin. Chem. Lab. Med.* **45,** 30–4 (2007).

179. Zhao, L. *et al.* Recruitment of a myeloid cell subset (CD11b/Gr1 ^{mid}) via CCL2/CCR2 promotes the development of colorectal cancer liver metastasis*. *Hepatology* **57,** 829–839 (2013).

180. Pahler, J. C. *et al.* Plasticity in tumor-promoting inflammation: impairment of macrophage recruitment evokes a compensatory neutrophil response. *Neoplasia* **10,** 329–40 (2008).

181. Li, X. *et al.* Targeting of tumour-infiltrating macrophages via CCL2/CCR2 signalling as a therapeutic strategy against hepatocellular carcinoma. *Gut* **66,** 157–167 (2017).

182. Serbina, N. V & Pamer, E. G. Monocyte emigration from bone marrow during bacterial infection requires signals mediated by chemokine receptor CCR2. *Nat. Immunol.* **7,** 311–317 (2006).

183. Lebrecht, A. *et al.* Monocyte Chemoattractant Protein-1 Serum Levels in Patients with Breast Cancer. *Tumor Biol.* **25,** 14–17 (2004).

184. Lan, C. *et al.* Expression of M2-polarized macrophages is associated with poor prognosis for advanced epithelial ovarian cancer. *Technol. Cancer Res. Treat.* **12,** 259–267 (2013).

185. Mahadevan, D. & Von Hoff, D. D. Tumor-stroma interactions in pancreatic ductal adenocarcinoma. *Mol. Cancer Ther.* **6,** 1186–1197 (2007).

186. Kryczek, I., Wei, S., Keller, E., Liu, R. & Zou, W. Stroma-derived factor (SDF-1/CXCL12) and human tumor pathogenesis. *Am. J. Physiol. Physiol.* **292,** C987–C995 (2007).

187. Meng, W., Xue, S. & Chen, Y. The role of CXCL12 in tumor microenvironment. *Gene* **641,** 105–110 (2018).

188. Leek, R. D., Landers, R. J., Harris, A. L. & Lewis, C. E. Necrosis correlates with high vascular density and focal macrophage infiltration in invasive carcinoma of the breast. *Br. J. Cancer* **79,** 991–995 (1999).

189. Leek, R. D. *et al.* Association of macrophage infiltration with angiogenesis and prognosis in invasive breast carcinoma. *Cancer Res.* **56,** 4625–9 (1996).

190. Lewis, J. S., Landers, R. J., Underwood, J. C. E., Harris, A. L. & Lewis, C. E. Expression of vascular endothelial growth factor by macrophages is up-regulated in poorly vascularized areas of breast carcinomas. *J. Pathol.* **192,** 150–158 (2000).

191. Lin, E. Y. *et al.* Vascular endothelial growth factor restores delayed tumor progression in tumors depleted of macrophages. *Mol. Oncol.* **1,** 288–302 (2007).

192. Linde, N. *et al.* Vascular endothelial growth factor-induced skin carcinogenesis depends on recruitment and alternative activation of macrophages. *J. Pathol.* **227,** 17–28 (2012).

193. Barbay, V. *et al.* Role of M2-like macrophage recruitment during angiogenic growth factor therapy. *Angiogenesis* **18,** 191–200 (2015).

194. Lindsten, T. *et al.* Effect of macrophages on breast cancer cell proliferation, and on expression of hormone receptors, uPAR and HER-2. *Int. J. Oncol.* **51,** 104–114 (2017).

195. Carroll, M. J., Kapur, A., Felder, M., Patankar, M. S. & Kreeger, P. K. M2 macrophages induce ovarian cancer cell proliferation via a heparin binding epidermal growth factor/matrix metalloproteinase 9 intercellular feedback loop. *Oncotarget* (2016).

196. Li, C., Shintani, S., Terakado, N., Nakashiro, K. I. & Hamakawa, H. Infiltration of tumor-associated macrophages in human oral squamous cell carcinoma. **9,** 1219–1223 (2002).

197. Onita, T. *et al.* Hypoxia-induced, perinecrotic expression of endothelial Per-ARNT-Sim domain protein-1/hypoxia-inducible factor-2α correlates with tumor progression, vascularization, and focal macrophage infiltration in bladder cancer. **8,** 471–480 (2002).

198. Willenborg, S. *et al.* CCR2 recruits an inflammatory macrophage subpopulation critical for angiogenesis in tissue repair. *Blood* **120,** 613–625 (2012).

199. Coffelt, S. B. *et al.* Angiopoietin-2 Regulates Gene Expression in TIE2-Expressing Monocytes and Augments Their Inherent Proangiogenic Functions. *Cancer Res.* **70,** 5270–5280 (2010).

200. Kubota, Y. *et al.* M-CSF inhibition selectively targets pathological angiogenesis and lymphangiogenesis. *J. Exp. Med.* **206,** 1089–1102 (2009).

201. Rego, S. L., Helms, R. S. & Dreau, D. Breast tumor cell TACE-shed MCSF promotes pro-angiogenic macrophages through NF-kappaB signaling. *Angiogenesis* **17,** 573–585 (2014).

202. Imtiyaz, H. Z. *et al.* Hypoxia-inducible factor 2α regulates macrophage function in mouse models of acute and tumor inflammation. *J. Clin. Invest.* **120,** 2699–2714 (2010).

203. Giraudo, E., Inoue, M. & Hanahan, D. An amino-bisphosphonate targets MMP-9–expressing macrophages and angiogenesis to impair cervical carcinogenesis. *J. Clin. Invest.* **114,** 623–633 (2004).

204. Mazzieri, R. *et al.* Targeting the ANG2/TIE2 Axis Inhibits Tumor Growth and Metastasis by Impairing Angiogenesis and Disabling Rebounds of Proangiogenic Myeloid Cells. *Cancer Cell* **19,** 512–526 (2011).

205. Chen, L. *et al.* Tie2 Expression on Macrophages Is Required for Blood Vessel Reconstruction and Tumor Relapse after Chemotherapy. *Cancer Res.* **76,** 6828–6838 (2016).

206. Forget, M. A. *et al.* Macrophage colony-stimulating factor augments Tie2-expressing monocyte differentiation, angiogenic function, and recruitment in a mouse model of breast cancer. *PLoS One* **9,** e98623 (2014).

207. Loke, P. & Allison, J. P. PD-L1 and PD-L2 are differentially regulated by Th1 and Th2 cells. *Proc. Natl. Acad. Sci.* **100,** 5336–5341 (2003).

208. Winograd, R. *et al.* Induction of T-cell Immunity Overcomes Complete Resistance to PD-1 and CTLA-4 Blockade and Improves Survival in Pancreatic Carcinoma. *Cancer Immunol. Res.* **3,** 399–411 (2015).

209. Bloch, O. *et al.* Gliomas Promote Immunosuppression through Induction of B7-H1 Expression in Tumor-Associated Macrophages. *Clin. Cancer Res.* **19,** 3165–3175 (2013).

210. Kuang, D.-M. *et al.* Activated monocytes in peritumoral stroma of hepatocellular carcinoma foster immune privilege and disease progression through PD-L1. *J. Exp. Med.* **206,** 1327–1337 (2009).

211. Juneja, V. R. *et al.* PD-L1 on tumor cells is sufficient for immune evasion in immunogenic tumors and inhibits CD8 T cell cytotoxicity. *J. Exp. Med.* **214,** 895–904 (2017).

212. Lau, J. *et al.* Tumour and host cell PD-L1 is required to mediate suppression of anti-tumour immunity in mice. *Nat. Commun.* **8,** 14572 (2017).

213. Rodriguez, P. C. *et al.* Arginase I Production in the Tumor Microenvironment by Mature Myeloid Cells Inhibits T-Cell Receptor Expression and Antigen-Specific T-Cell Responses. *Cancer Res.* **64,** 5839–5849 (2004).

214. Briken, V. & Mosser, D. M. Editorial: switching on arginase in M2 macrophages. *J. Leukoc. Biol.* **90,** 839–41 (2011).

215. Pegg, A. E. & McCann, P. P. Polyamine metabolism and function. *Am. J. Physiol. Physiol.* **243,** C212–C221 (1982).

216. Förstermann, U. & Sessa, W. C. Nitric oxide synthases: regulation and function. *Eur. Heart J.* **33,** 829–37, 837a–837d (2012).

217. Trinchieri, G. Interleukin-12: a cytokine produced by antigen-presenting cells with immunoregulatory functions in the generation of T-helper cells type 1 and cytotoxic lymphocytes. *Blood* **84,** 4008–27 (1994).

218. Ng, T. H. S. *et al.* Regulation of Adaptive Immunity; The Role of Interleukin-10. *Front. Immunol.* **4,** 129 (2013).

219. Daurkin, I. *et al.* Tumor-associated macrophages mediate immunosuppression in the renal cancer microenvironment by activating the 15-lipoxygenase-2 pathway. *Cancer Res.* **71,** 6400–6409 (2011).

220. Ruffell, B. *et al.* Macrophage IL-10 Blocks CD8+ T Cell-Dependent Responses to Chemotherapy by Suppressing IL-12 Expression in Intratumoral Dendritic Cells. *Cancer Cell* **26,** 623–637 (2014).

221. Oh, S. A. & Li, M. O. TGF- : Guardian of T Cell Function. *J. Immunol.* **191,** 3973–3979 (2013).

222. Denning, T. L., Wang, Y., Patel, S. R., Williams, I. R. & Pulendran, B. Lamina propria macrophages and dendritic cells differentially induce regulatory and interleukin 17–producing T cell responses. *Nat. Immunol.* **8,** 1086–1094 (2007).

223. Liou, G.-Y. *et al.* Macrophage-secreted cytokines drive pancreatic acinar-to-ductal metaplasia through NF-κB and MMPs. *J. Cell Biol.* **202,** 563–577 (2013).

224. E., S. *et al.* Tumor-infiltrating monocytic myeloid-derived suppressor cells mediate CCR5-dependent recruitment of regulatory T cells favoring tumor growth. *Journal of Immunology* **189,** 5602–5611 (2012).

225. Liu, J. *et al.* Tumor-Associated Macrophages Recruit CCR6+ Regulatory T Cells and Promote the Development of Colorectal Cancer via Enhancing CCL20 Production in Mice. *PLoS One* **6,** e19495 (2011).

226. Curiel, T. J. *et al.* Specific recruitment of regulatory T cells in ovarian carcinoma fosters immune privilege and predicts reduced survival. *Nat. Med.* **10,** 942–949 (2004).

227. Condeelis, J. & Pollard, J. W. Macrophages: Obligate Partners for Tumor Cell Migration, Invasion, and Metastasis. *Cell* **124,** 263–266 (2006).

228. Psaila, B. & Lyden, D. The metastatic niche: adapting the foreign soil. *Nat. Rev. Cancer* **9,** 285–293 (2009).

229. B.-Z., Q. *et al.* CCL2 recruits inflammatory monocytes to facilitate breast-tumour metastasis. *Nature* **475,** 222–225 (2011).

230. Qian, B. *et al.* A Distinct Macrophage Population Mediates Metastatic Breast Cancer Cell Extravasation, Establishment and Growth. *PLoS One* **4,** e6562 (2009).

231. Gao, D. *et al.* Myeloid Progenitor Cells in the Premetastatic Lung Promote Metastases by Inducing Mesenchymal to Epithelial Transition. *Cancer Res.* **72,** 1384–1394 (2012).

232. Batlle, E. & Clevers, H. Cancer stem cells revisited. *Nat. Med.* **23,** 1124–1134 (2017).

233. Iliopoulos, D., Hirsch, H. A. & Struhl, K. An Epigenetic Switch Involving NF-κB, Lin28, Let-7 MicroRNA, and IL6 Links Inflammation to Cell Transformation. *Cell* **139,** 693–706 (2009).

234. Mitchem, J. B. *et al.* Targeting tumor-infiltrating macrophages decreases tumor-initiating cells, relieves immunosuppression, and improves chemotherapeutic responses. *Cancer Res.* **73,** 1128–1141 (2013).

235. S., W. *et al.* Tumor-associated macrophages produce interleukin 6 and signal via STAT3 to promote expansion of human hepatocellular carcinoma stem cells. *Gastroenterology* **147,** 1393–1404 (2014).

236. Watanabe, H., Numata, K., Ito, T., Takagi, K. & Matsukawa, A. Innate immune response in Th1- and Th2-dominant mouse strains. *Shock* **22,** 460–6 (2004).

237. Mosely, S. I. S. *et al.* Rational Selection of Syngeneic Preclinical Tumor Models for Immunotherapeutic Drug Discovery. (2017). doi:10.1158/2326-6066.CIR-16-0114

238. Le, D. T. *et al.* KEYNOTE-164: Pembrolizumab for patients with advanced microsatellite instability high (MSI-H) colorectal cancer. *J. Clin. Oncol.* **36,** 3514–3514 (2018).

239. vom Berg, J. & Kobold, S. The need for speed: how PD1-blockade only works if T cells are properly activated. *Transl. Cancer Res.* **6,** S1018–S1021 (2017).

240. Hollmen, M. *et al.* G-CSF regulates macrophage phenotype and associates with poor overall survival in human triple-negative breast cancer. *Oncoimmunology* **5,** e1115177 (2016).

241. D., L. *et al.* Tumor-associated macrophages in breast cancer: Distinct subsets, distinct functions. *International Journal of Developmental Biology* **55,** 861–867 (2011).

242. Qian, B.-Z. & Pollard, J. W. Macrophage Diversity Enhances Tumor Progression and Metastasis. *Cell* **141,** 39–51 (2010).

243. Smith, H. O. *et al.* The clinical significance of inflammatory cytokines in primary cell culture in endometrial carcinoma. *Mol. Oncol.* **7,** 41–54 (2013).

244. Cortez-Retamozo, V. *et al.* Origins of tumor-associated macrophages and neutrophils. *Proc. Natl. Acad. Sci. U. S. A.* **109,** 2491–2496 (2012).

245. Bujko, K. *et al.* Sphincter preservation following preoperative radiotherapy for rectal cancer: report of a

randomised trial comparing short-term radiotherapy vs. conventionally fractionated radiochemotherapy. *Radiother. Oncol.* **72,** 15–24 (2004).

246. Xiao, L. *et al.* Pathological Assessment of Rectal Cancer after Neoadjuvant Chemoradiotherapy: Distribution of Residual Cancer Cells and Accuracy of Biopsy. *Sci. Rep.* **6,** 34923 (2016).

247. Johnke, R. M. *et al.* Circulating cytokine levels in prostate cancer patients undergoing radiation therapy: influence of neoadjuvant total androgen suppression. *In Vivo* **23,** 827–33 (2009).

248. Siva, S. *et al.* A Pattern of Early Radiation-Induced Inflammatory Cytokine Expression Is Associated with Lung Toxicity in Patients with Non-Small Cell Lung Cancer. *PLoS One* **9,** e109560 (2014).

249. Fenig, E., Sulkes, A., Rescigno, J. & Shohat, B. Interleukin-I p Plasma Levels Decrease Following - Local Radiation Therapy for Breast Cancer. *Radiat. Oncol. Investig.* **2,** 224–229

250. Eide, H. A. *et al.* Serum cytokine profiles and metabolic tumour burden in patients with non-small cell lung cancer undergoing palliative thoracic radiotherapy. *Adv. Radiat. Oncol.* (2018). doi:10.1016/J.ADRO.2017.12.007

251. Bower, J. E. *et al.* Inflammatory Biomarkers and Fatigue during Radiation Therapy for Breast and Prostate Cancer There is considerable interest in the identification of clinical. *Imaging Diagnosis, Progn. (Clin Cancer Res* **15,** 5534–40 (2009).

252. Ashamalla, H. *et al.* Correlation of cytokine levels and response to radiation therapy and/or brachytherapy in low/intermediate risk prostate cancer. *J. Clin. Oncol.* **23,** 2600–2600 (2005).

253. Reers, S. *et al.* Cytokine changes in response to radio-/chemotherapeutic treatment in head and neck cancer. *Anticancer Res.* **33,** 2481–9 (2013).

254. Kalbasi, A. *et al.* Cancer Therapy: Preclinical Tumor-Derived CCL2 Mediates Resistance to Radiotherapy in Pancreatic Ductal Adenocarcinoma. *Clin Cancer Res* 1–12 doi:10.1158/1078-0432.CCR-16-0870

255. Ramirez-Carrozzi, V. R. *et al.* A Unifying Model for the Selective Regulation of Inducible Transcription by CpG Islands and Nucleosome Remodeling. *Cell* **138,** 114–128 (2009).

256. Dent, P. *et al.* Stress and radiation-induced activation of multiple intracellular signaling pathways. *Radiat. Res.* **159,** 283–300 (2003).

257. Janus, P. *et al.* Pro-inflammatory cytokine and high doses of ionizing radiation have similar effects on the expression of NF-kappaB-dependent genes. *Cell. Signal.* **46,** 23–31 (2018).

258. Aravindan, S. *et al.* Abscopal effect of low-LET γ-radiation mediated through Rel protein signal transduction in a mouse model of nontargeted radiation response. *Cancer Gene Ther.* **21,** 54–59 (2014).

259. Panta, G. R. *et al.* ATM and the catalytic subunit of DNA-dependent protein kinase activate NF-kappaB through a common MEK/extracellular signal-regulated kinase/p90(rsk) signaling pathway in response to distinct forms of DNA damage. *Mol. Cell. Biol.* **24,** 1823–35 (2004).

260. Hernandez, C., Huebener, P. & Schwabe, R. F. Damage-associated molecular patterns in cancer: a double-edged sword. *Oncogene* **35,** 5931–5941 (2016).

261. Gribar, S., Richardson, W., Sodhi, C. P. & Hackam, D. J. No longer an innocent bystander: epithelial toll-like

receptor signalling in the development of mucosal inflammation. *Mol. Med.* **14,** 1 (2008).

262. Neal, M. D. *et al.* Enterocyte TLR4 mediates phagocytosis and translocation of bacteria across the intestinal barrier. *J. Immunol.* **176,** 3070–9 (2006).

263. Schaue, D. & McBride, W. H. Links between Innate Immunity and Normal Tissue Radiobiology. *Radiat. Res.* **173,** 406–417 (2010).

264. Hong, J.-H. *et al.* Induction of acute phase gene expression by brain irradiation. *Int. J. Radiat. Oncol.* **33,** 619–626 (1995).

265. Mills, C. D., Kincaid, K., Alt, J. M., Heilman, M. J. & Hill, A. M. M-1/M-2 macrophages and the Th1/Th2 paradigm. *J. Immunol.* **164,** 6166–73 (2000).

266. Coussens, L. M. & Pollard, J. W. Leukocytes in Mammary Development and Cancer. *Cold Spring Harb. Perspect. Biol.* **3,** a003285–a003285 (2011).

267. U.C., M.-Q., L., P. & J., M.-Q. Tumor-cell co-culture induced alternative activation of macrophages is modulated by interferons in vitro. *Journal of Interferon and Cytokine Research* **32,** 169–177 (2012).

268. Hollmen, M., Roudnicky, F., Karaman, S. & Detmar, M. Characterization of macrophage--cancer cell crosstalk in estrogen receptor positive and triple-negative breast cancer. *Sci. Rep.* **5,** 9188 (2015).

269. Roudnicky, F. & Hollmen, M. Transcriptional profiling of macrophage and tumor cell interactions in vitro. *Genomics data* **8,** 1–3 (2016).

270. Kuen, J., Darowski, D., Kluge, T. & Majety, M. Pancreatic cancer cell/fibroblast co-culture induces M2 like macrophages that influence therapeutic response in a 3D model. *PLoS One* **12,** e0182039 (2017).

271. Jeong, H., Bok, S., Hong, B.-J., Choi, H.-S. & Ahn, G.-O. Radiation-induced immune responses: mechanisms and therapeutic perspectives. *Blood Res.* **51,** 157–163 (2016).

272. Ladner, M. B. *et al.* Human CSF-1: gene structure and alternative splicing of mRNA precursors. *EMBO J.* **6,** 2693–8 (1987).

273. Kawasaki, E. S. *et al.* Molecular cloning of a complementary DNA encoding human macrophage-specific colony-stimulating factor (CSF-1). *Science* **230,** 291–6 (1985).

274. Nandi, S., Akhter, M. P., Seifert, M. F., Dai, X.-M. & Stanley, E. R. Developmental and functional significance of the CSF-1 proteoglycan chondroitin sulfate chain. *Blood* **107,** 786–95 (2006).

275. Yao, G.-Q. *et al.* The Cell Surface Form of Colony-Stimulating Factor-1 Is Biologically Active in Bone *in Vivo*. *Endocrinology* **144,** 3677–3682 (2003).

276. Dai, X.-M., Zong, X.-H., Sylvestre, V. & Stanley, E. R. Incomplete restoration of colony-stimulating factor 1 (CSF-1) function in CSF-1-deficient Csf1op/Csf1op mice by transgenic expression of cell surface CSF-1. *Blood* **103,** 1114–1123 (2003).

277. Wittrant, Y. *et al.* PDGF Up-regulates CSF-1 Gene Transcription in Ameloblast-like Cells. *J. Dent. Res.* **87,** 33–38 (2008).

278. Chen, C. *et al.* L-selectin ligation-induced CSF-1 gene transcription is regulated by AP-1 in a c-Abl kinase-

dependent manner. *Hum. Immunol.* **69,** 501–509 (2008).

279. Harrington, M., Konicek, B. W., Xia, X.-L. & Song, A. Transcriptional regulation of the mouse CSF-1 gene. *Mol. Reprod. Dev.* **46,** 39–45 (1997).

280. Song, Z. *et al.* Nuclear actin is involved in the regulation of CSF1 gene transcription in a chromatin required, BRG1 independent manner. *J. Cell. Biochem.* **102,** 403–411 (2007).

281. Bsoul, S., Terezhalmy, G., Abboud, H., Woodruff, K. & Abboud, S. . PDGF BB and bFGF stimulate DNA synthesis and upregulate CSF-1 and MCP-1 gene expression in dental follicle cells. *Arch. Oral Biol.* **48,** 459–465 (2003).

282. J., X. *et al.* CSF1R signaling blockade stanches tumor-infiltrating myeloid cells and improves the efficacy of radiotherapy in prostate cancer. *Cancer Research* **73,** 2782–2794 (2013).

283. Hamer, G., Gademan, I. S., Kal, H. B. & de Rooij, D. G. Role for c-Abl and p73 in the radiation response of male germ cells. *Oncogene* **20,** 4298–304 (2001).

284. Baskaran, R. *et al.* Ataxia telangiectasia mutant protein activates c-Abl tyrosine kinase in response to ionizing radiation. *Nature* **387,** 516–519 (1997).

285. Kharbanda, S. *et al.* The stress response to ionizing radiation involoves c-Abl-dependent phosphorylation of SHPTP1. *Proc. Natl. Acad. Sci. U. S. A.* **93,** 6898–901 (1996).

286. Xu, J. *et al.* CSF1R Signaling Blockade Stanches Tumor-Infiltrating Myeloid Cells and Improves the Efficacy of Radiotherapy in Prostate Cancer. *Cancer Res.* **73,** 2782–2794 (2013).

287. Seifert, L. *et al.* Radiation Therapy Induces Macrophages to Suppress T-Cell Responses Against Pancreatic Tumors in Mice. *Gastroenterology* **150,** 1659–1672.e5 (2016).

288. Crittenden, M. R. *et al.* Expression of NF-κB p50 in Tumor Stroma Limits the Control of Tumors by Radiation Therapy. *PLoS One* **7,** e39295 (2012).

289. K., Z., K., B., M., B. & D., Z. Tumour-infiltrating CD11b+ myelomonocytes and response to fractionated irradiation of human squamous cell carcinoma (hSCC) xenografts. *Radiotherapy and Oncology* **101,** 80–85 (2011).

290. Deng, L., Liang, H., Burnette, B., Weicheslbaum, R. R. & Fu, Y.-X. Radiation and anti-PD-L1 antibody combinatorial therapy induces T cell-mediated depletion of myeloid-derived suppressor cells and tumor regression. *Oncoimmunology* **3,** e28499 (2014).

291. Seifert, L. *et al.* Radiation Therapy Induces Macrophages to Suppress T-Cell Responses Against Pancreatic Tumors in Mice. *Gastroenterology* **150,** 1659–1672.e5 (2016).

292. Shiao, S. L. *et al.* Limit Efficacy of Radiotherapy. *Cancer Immunol Res* **3,** 518–25

293. Liu, C. *et al.* Targeting the shift from M1 to M2 macrophages in experimental autoimmune encephalomyelitis mice treated with fasudil. *PLoS One* **8,** e54841 (2013).

294. Geiger, R. *et al.* L-Arginine Modulates T Cell Metabolism and Enhances Survival and Anti-tumor Activity. *Cell* **167,** 829–842.e13 (2016).

295. Kubota, K. *et al.* CD163+CD204+ tumor-associated macrophages contribute to T cell regulation via interleukin-10 and PD-L1 production in oral squamous cell carcinoma. *Sci. Rep.* **7,** 1755 (2017).

296. De Henau, O. *et al.* Overcoming resistance to checkpoint blockade therapy by targeting PI3Kγ in myeloid cells. *Nature* **539,** 443–447 (2016).

297. Fridlender, Z. G. *et al.* Monocyte Chemoattractant Protein–1 Blockade Inhibits Lung Cancer Tumor Growth by Altering Macrophage Phenotype and Activating CD8 $^{+}$ Cells. *Am. J. Respir. Cell Mol. Biol.* **44,** 230–237 (2011).

298. J.M., F. *et al.* Depletion of tumor-associated macrophages slows the growth of chemically induced mouse lung adenocarcinomas. *Frontiers in Immunology* **5,** no pagination (2014).

299. Lim, S. Y., Yuzhalin, A. E., Gordon-Weeks, A. N. & Muschel, R. J. Targeting the CCL2-CCR2 signaling axis in cancer metastasis. *Oncotarget* **7,** 28697–710 (2016).

300. Bonapace, L. *et al.* Cessation of CCL2 inhibition accelerates breast cancer metastasis by promoting angiogenesis. *Nature* **515,** 130–133 (2014).

301. K.J., P. *et al.* Phase 2 study of carlumab (CNTO 888), a human monoclonal antibody against CC-chemokine ligand 2 (CCL2), in metastatic castration-resistant prostate cancer. *Investigational New Drugs* **31,** 760–768 (2013).

302. Brana, I. *et al.* Carlumab, an anti-C-C chemokine ligand 2 monoclonal antibody, in combination with four chemotherapy regimens for the treatment of patients with solid tumors: an open-label, multicenter phase 1b study. *Target. Oncol.* **10,** 111–123 (2015).

303. Sandhu, S. K. *et al.* A first-in-human, first-in-class, phase I study of carlumab (CNTO 888), a human monoclonal antibody against CC-chemokine ligand 2 in patients with solid tumors. *Cancer Chemother. Pharmacol.* **71,** 1041–1050 (2013).

304. Cannarile, M. A. *et al.* Colony-stimulating factor 1 receptor (CSF1R) inhibitors in cancer therapy. *J. Immunother. Cancer* **5,** 53 (2017).

305. Zhu, Y. *et al.* CSF1/CSF1R Blockade Reprograms Tumor-Infiltrating Macrophages and Improves Response to T-cell Checkpoint Immunotherapy in Pancreatic Cancer Models. *Cancer Res.* **74,** 5057–5069 (2014).

306. Strachan, D. C. *et al.* CSF1R inhibition delays cervical and mammary tumor growth in murine models by attenuating the turnover of tumor-associated macrophages and enhancing infiltration by CD8 $^{+}$ T cells. *Oncoimmunology* **2,** e26968 (2013).

307. Escamilla, J. *et al.* CSF1 receptor targeting in prostate cancer reverses macrophage-mediated resistance to androgen blockade therapy. *Cancer Res.* **75,** 950–962 (2015).

308. Mitchem, J. B. *et al.* Targeting Tumor-Infiltrating Macrophages Decreases Tumor-Initiating Cells, Relieves Immunosuppression, and Improves Chemotherapeutic Responses. *Cancer Res.* **73,** 1128–1141 (2013).

309. Wiehagen, K. R. *et al.* Combination of CD40 Agonism and CSF-1R Blockade Reconditions Tumor-Associated Macrophages and Drives Potent Antitumor Immunity. *Cancer Immunol. Res.* **5,** 1109–1121 (2017).

310. van Rooijen, N. & Hendrikx, E. in *Methods in molecular biology (Clifton, N.J.)* **605,** 189–203 (2010).

311. X., W. *et al.* Depletion of M2-like tumor-associated macrophages delays cutaneous T-cell lymphoma

development in vivo. *Journal of Investigative Dermatology* **134,** 2814–2822 (2014).

312. Griesmann, H. *et al.* Pharmacological macrophage inhibition decreases metastasis formation in a genetic model of pancreatic cancer. *Gut* **66,** 1278–1285 (2017).

313. Li, Z., Xu, X., Feng, X. & Murphy, P. M. The Macrophage-depleting Agent Clodronate Promotes Durable Hematopoietic Chimerism and Donor-specific Skin Allograft Tolerance in Mice. *Sci. Rep.* **6,** 22143 (2016).

314. Ries, C. H. *et al.* Targeting tumor-associated macrophages with anti-CSF-1R antibody reveals a strategy for cancer therapy. *Cancer Cell* **25,** 846–859 (2014).

315. Zhu, Y. *et al.* CSF1/CSF1R blockade reprograms tumor-infiltrating macrophages and improves response to T-cell checkpoint immunotherapy in pancreatic cancer models. *Cancer Res.* **74,** 5057–69 (2014).

316. Shiao, S. L. *et al.* Limit Efficacy of Radiotherapy. *Cancer Immunol Res* **3,** 518–25 (2015).

317. Kumar, V. *et al.* Cancer-Associated Fibroblasts Neutralize the Anti-tumor Effect of CSF1 Receptor Blockade by Inducing PMN-MDSC Infiltration of Tumors. *Cancer Cell* **32,** 654–668.e5 (2017).

318. Beatty, G. L. *et al.* Exclusion of T Cells From Pancreatic Carcinomas in Mice Is Regulated by Ly6C(low) F4/80(+) Extratumoral Macrophages. *Gastroenterology* **149,** 201–210 (2015).

319. Berthel, A. *et al.* Detailed resolution analysis reveals spatial T cell heterogeneity in the invasive margin of colorectal cancer liver metastases associated with improved survival. (2017). doi:10.1080/2162402X.2017.1286436

320. Joyce, J. A. & Fearon, D. T. T cell exclusion, immune privilege, and the tumor microenvironment. *Science* **348,** 74–80 (2015).

321. Evans, R. A. *et al.* Lack of immunoediting in murine pancreatic cancer reversed with neoantigen. *JCI insight* **1,** (2016).

322. Ranieri, E., Popescu, I. & Gigante, M. in *Methods in molecular biology (Clifton, N.J.)* **1186,** 75–86 (2014).

323. MacDonald, K. P. A. *et al.* The colony-stimulating factor 1 receptor is expressed on dendritic cells during differentiation and regulates their expansion. *J. Immunol.* **175,** 1399–405 (2005).

324. CHIRIVA-INTERNATI, M. *et al.* GAMMA-RADIATION UPREGULATES MHC CLASS I/II AND ICAM-I MOLECULES IN MULTIPLE MYELOMA CELL LINES AND PRIMARY TUMORS. *Vitr. Cell. Dev. Biol. - Anim.* **42,** 89 (2006).

325. Sharma, A. *et al.* γ-Radiation Promotes Immunological Recognition of Cancer Cells through Increased Expression of Cancer-Testis Antigens In Vitro and In Vivo. *PLoS One* **6,** e28217 (2011).

326. Sharma, A. *et al.* Radiotherapy of Human Sarcoma Promotes an Intratumoral Immune Effector Signature. *Clin. Cancer Res.* **19,** 4843–4853 (2013).

327. Svane, I. M., Engel, A. M., Nielsen, M. & Werdelin, O. Interferon-gamma-induced MHC class I expression and defects in Jak/Stat signalling in methylcholanthrene-induced sarcomas. *Scand. J. Immunol.* **46,** 379–87 (1997).

328. Propper, D. J. *et al.* Low-dose IFN-gamma induces tumor MHC expression in metastatic malignant melanoma. *Clin. Cancer Res.* **9,** 84–92 (2003).

329. Raval, A., Puri, N., Rath, P. C. & Saxena, R. K. Cytokine regulation of expression of class I MHC antigens. *Exp. Mol. Med.* **30,** 1–13 (1998).

330. Demaria, S. *et al.* Ionizing radiation inhibition of distant untreated tumors (abscopal effect) is immune mediated. *Int. J. Radiat. Oncol.* **58,** 862–870 (2004).

331. Fleetwood, A. J., Lawrence, T., Hamilton, J. A. & Cook, A. D. Granulocyte-macrophage colony-stimulating factor (CSF) and macrophage CSF-dependent macrophage phenotypes display differences in cytokine profiles and transcription factor activities: implications for CSF blockade in inflammation. *J. Immunol.* **178,** 5245–52 (2007).

332. Kaneda, M. M. *et al.* PI3Kγ is a molecular switch that controls immune suppression. *Nature* **539,** 437–442 (2016).

333. Schmid, M. C. *et al.* PI3-Kinase γ Promotes Rap1a-Mediated Activation of Myeloid Cell Integrin α4β1, Leading to Tumor Inflammation and Growth. *PLoS One* **8,** e60226 (2013).

334. Schmid, M. C. *et al.* Receptor Tyrosine Kinases and TLR/IL1Rs Unexpectedly Activate Myeloid Cell PI3Kγ, A Single Convergent Point Promoting Tumor Inflammation and Progression. *Cancer Cell* **19,** 715–727 (2011).

335. Galon, J. *et al.* Type, Density, and Location of Immune Cells Within Human Colorectal Tumors Predict Clinical Outcome. *Science (80-.).* **313,** (2006).

336. Mok, S. *et al.* Inhibition of CSF-1 receptor improves the antitumor efficacy of adoptive cell transfer immunotherapy. *Cancer Res.* **74,** 153–161 (2014).

337. Holmgaard, R. B., Zamarin, D., Lesokhin, A., Merghoub, T. & Wolchok, J. D. Targeting myeloid-derived suppressor cells with colony stimulating factor-1 receptor blockade can reverse immune resistance to immunotherapy in indoleamine 2,3-dioxygenase-expressing tumors. *EBioMedicine* **6,** 50–8 (2016).

338. Zhu, Y. *et al.* CSF1/CSF1R blockade reprograms tumor-infiltrating macrophages and improves response to T-cell checkpoint immunotherapy in pancreatic cancer models. *Cancer Res.* **74,** 5057–69 (2014).

339. D.C., S. *et al.* CSF1R inhibition delays cervical and mammary tumor growth in murine models by attenuating the turnover of tumor-associated macrophages and enhancing infiltration by CD8+ T cells. *OncoImmunology* **2,** no pagination (2013).

340. DeNardo, D. G. *et al.* Leukocyte complexity predicts breast cancer survival and functionally regulates response to chemotherapy. *Cancer Discov.* **1,** 54–67 (2011).

341. Zhu, Y. *et al.* CSF1/CSF1R Blockade Reprograms Tumor-Infiltrating Macrophages and Improves Response to T Cell Checkpoint Immunotherapy in Pancreatic Cancer Models. *Cancer Res* **74,** 5057–5069 (2014).

342. Sharabi, A. B. *et al.* Stereotactic Radiation Therapy Augments Antigen-Specific PD-1-Mediated Antitumor Immune Responses via Cross-Presentation of Tumor Antigen. *Cancer Immunol. Res.* **3,** 345–355 (2015).

343. Lee, Y. *et al.* Therapeutic effects of ablative radiation on local tumor require CD8+ T cells: changing strategies for cancer treatment. *Blood* **114,** 589–595 (2009).

344. Lugade, A. A. *et al.* Local radiation therapy of B16 melanoma tumors increases the generation of tumor antigen-specific effector cells that traffic to the tumor. *J. Immunol.* **174,** 7516–23 (2005).

345. Lugade, A. A. *et al.* Local radiation therapy of B16 melanoma tumors increases the generation of tumor antigen-specific effector cells that traffic to the tumor. *J. Immunol.* **174,** 7516–23 (2005).

346. Karyampudi, L. *et al.* Accumulation of Memory Precursor CD8 T Cells in Regressing Tumors following Combination Therapy with Vaccine and Anti-PD-1 Antibody. *Cancer Res.* **74,** 2974–2985 (2014).

347. Ribas, A., Timmerman, J. M., Butterfield, L. H. & Economou, J. S. Determinant spreading and tumor responses after peptide-based cancer immunotherapy. *Trends Immunol.* **24,** 58–61 (2003).

348. Vanderlugt, C. L. & Miller, S. D. EPITOPE SPREADING IN IMMUNE-MEDIATED DISEASES: IMPLICATIONS FOR IMMUNOTHERAPY. *Nat. Rev. Immunol.* **2,** 85–95 (2002).

349. Schwartz, R. H. T C ELL A NERGY. *Annu. Rev. Immunol.* **21,** 305–334 (2003).

350. Chambers, C. A., Kuhns, M. S., Egen, J. G. & Allison, J. P. C TLA -4-M EDIATED I NHIBITION IN R EGULATION OF T C ELL R ESPONSES : Mechanisms and Manipulation in Tumor Immunotherapy. *Annu. Rev. Immunol.* **19,** 565–594 (2001).

351. Tivol, E. A. *et al.* Loss of CTLA-4 leads to massive lymphoproliferation and fatal multiorgan tissue destruction, revealing a critical negative regulatory role of CTLA-4. *Immunity* **3,** 541–7 (1995).

352. Leach, D. R., Krummel, M. F. & Allison, J. P. Enhancement of antitumor immunity by CTLA-4 blockade. *Science* **271,** 1734–6 (1996).

353. Keir, M. E., Butte, M. J., Freeman, G. J. & Sharpe, A. H. PD-1 and Its Ligands in Tolerance and Immunity. *Annu. Rev. Immunol.* **26,** 677–704 (2008).

354. Zou, W. & Chen, L. Inhibitory B7-family molecules in the tumour microenvironment. *Nat. Rev. Immunol.* **8,** 467–477 (2008).

355. Hino, R. *et al.* Tumor cell expression of programmed cell death-1 ligand 1 is a prognostic factor for malignant melanoma. *Cancer* **116,** 1757–1766 (2010).

356. Taube, J. M. *et al.* Association of PD-1, PD-1 Ligands, and Other Features of the Tumor Immune Microenvironment with Response to Anti-PD-1 Therapy. *Clin. Cancer Res.* **20,** 5064–5074 (2014).

357. Wang, X., Teng, F., Kong, L. & Yu, J. PD-L1 expression in human cancers and its association with clinical outcomes. *Onco. Targets. Ther.* **9,** 5023–39 (2016).

358. Catakovic, K., Klieser, E., Neureiter, D. & Geisberger, R. T cell exhaustion: from pathophysiological basics to tumor immunotherapy. *Cell Commun. Signal.* **15,** 1 (2017).

359. Rozali, E. N., Hato, S. V., Robinson, B. W., Lake, R. A. & Lesterhuis, W. J. Programmed Death Ligand 2 in Cancer-Induced Immune Suppression. *Clin. Dev. Immunol.* **2012,** 1–8 (2012).

360. Derer, A. *et al.* Chemoradiation Increases PD-L1 Expression in Certain Melanoma and Glioblastoma Cells. *Front. Immunol.* **7,** 610 (2016).

361. Noguchi, T. *et al.* Temporally Distinct PD-L1 Expression by Tumor and Host Cells Contributes to Immune Escape. *Cancer Immunol. Res.* **5,** 106–117 (2017).

362. Lau, J. *et al.* Tumour and host cell PD-L1 is required to mediate suppression of anti-tumour immunity in mice.

Nat. Commun. **8,** 14572 (2017).

363. Woo, S.-R. *et al.* Immune Inhibitory Molecules LAG-3 and PD-1 Synergistically Regulate T-cell Function to Promote Tumoral Immune Escape. *Cancer Res.* **72,** 917–927 (2012).

364. Twyman-Saint Victor, C. *et al.* Radiation and dual checkpoint blockade activate non-redundant immune mechanisms in cancer. *Nature* **520,** 373–377 (2015).

365. Juneja, V. R. *et al.* PD-L1 on tumor cells is sufficient for immune evasion in immunogenic tumors and inhibits CD8 T cell cytotoxicity. *J. Exp. Med.* **214,** 895–904 (2017).

366. Kleinovink, J. W. *et al.* PD-L1 expression on malignant cells is no prerequisite for checkpoint therapy. *Oncoimmunology* **6,** e1294299 (2017).

367. Lau, J. *et al.* Tumour and host cell PD-L1 is required to mediate suppression of anti-tumour immunity in mice. *Nat. Commun.* **8,** 14572 (2017).

368. Zhang, Y. *et al.* Myeloid cells are required for PD-1/PD-L1 checkpoint activation and the establishment of an immunosuppressive environment in pancreatic cancer. *Gut* gutjnl-2016-312078 (2016). doi:10.1136/gutjnl-2016-312078

369. Azad, A. *et al.* PD-L1 blockade enhances response of pancreatic ductal adenocarcinoma to radiotherapy. *EMBO Mol. Med.* **9,** 167–180 (2017).

370. Patel, S. P. & Kurzrock, R. PD-L1 Expression as a Predictive Biomarker in Cancer Immunotherapy. *Mol. Cancer Ther.* **14,** 847–56 (2015).

371. Blank, C., Gajewski, T. F. & Mackensen, A. Interaction of PD-L1 on tumor cells with PD-1 on tumor-specific T cells as a mechanism of immune evasion: implications for tumor immunotherapy. *Cancer Immunol. Immunother.* **54,** 307–314 (2005).

372. Meng, X., Huang, Z., Teng, F., Xing, L. & Yu, J. Predictive biomarkers in PD-1/PD-L1 checkpoint blockade immunotherapy. *Cancer Treat. Rev.* **41,** 868–876 (2015).

373. Li, Y. *et al.* Prognostic impact of programed cell death-1 (PD-1) and PD-ligand 1 (PD-L1) expression in cancer cells and tumor infiltrating lymphocytes in colorectal cancer. *Mol. Cancer* **15,** 55 (2016).

374. Sabatier, R. *et al.* Prognostic and predictive value of PDL1 expression in breast cancer. *Oncotarget* **6,** 5449–5464 (2015).

375. Chen, S. *et al.* Combination of 4-1BB Agonist and PD-1 Antagonist Promotes Antitumor Effector/Memory CD8 T Cells in a Poorly Immunogenic Tumor Model. *Cancer Immunol. Res.* **3,** 149–160 (2015).

376. Woo, S.-R. *et al.* Immune Inhibitory Molecules LAG-3 and PD-1 Synergistically Regulate T-cell Function to Promote Tumoral Immune Escape. *Cancer Res.* **72,** 917–927 (2012).

377. Overman, M. J. *et al.* Nivolumab in patients with metastatic DNA mismatch repair-deficient or microsatellite instability-high colorectal cancer (CheckMate 142): an open-label, multicentre, phase 2 study. *Lancet. Oncol.* **18,** 1182–1191 (2017).

378. Feng, M. *et al.* PD-1/PD-L1 and immunotherapy for pancreatic cancer. *Cancer Lett.* **407,** 57–65 (2017).